PITHA 08/09

Top quark physics at the LHC

Werner Bernreuther*

Institut für Theoretische Physik, RWTH Aachen University, 52056 Aachen, Germany

Abstract

The physics perspectives of the production and decay of single top quarks and top quark pairs at the CERN Large Hadron Collider (LHC) are reviewed from a phenomenological point of view.

PACS number(s): 13.85.t, 13.90.i, 14.65.Ha

*Email: breuther@physik.rwth-aachen.de

1. Introduction

The top quark, the heaviest known fundamental particle, was discovered thirteen years ago [1,2] at the Tevatron proton antiproton collider. At a hadron collider like the Tevatron, top quarks are predominantly produced together with their antiquarks. Quite recently, the D0 [3] and the CDF [4] experiment reported also evidence for the observation of singly produced t and $\bar{t}$ quarks. To date the Tevatron is the only source of these quarks. However, this should change soon when the CERN Large Hadron Collider (LHC) will start operation. Millions of top quarks will be produced already in the low luminosity phase $L \sim 10\,\mathrm{fb}^{-1}$ of this collider – see table 1. This will open up the possibility to explore this quark with hitherto unprecedented precision.

What is interesting about the physics of top quarks? Although it is almost as heavy as a gold atom it seems to behave as a pointlike particle, at least at length scales $\gtrsim 10^{-18}$ m, according to experimental findings. So far the Tevatron results are in accord with expectations and predictions within the standard model (SM) of particle physics. While the mass of this particle has already been precisely measured, other properties and its production and decay dynamics could, however, not be investigated in great detail so far. Hopefully this will change in the years to come. There are exciting physics topics to be explored – we mention here only a few of them. In view of its large mass the top quark is an excellent probe of the mechanism that breaks the electroweak gauge symmetry and should therefore play a key role in clarifying the nature of the force(s)/particle(s) responsible for this phenomenon. The top quark is also good probe for possible new parity-violating and/or non-SM *CP* violating interactions which could be induced, for instance, by non-standard Higgs bosons. Are there new top-quark decay modes, for instance to supersymmetric particles? So far, experimental data are consistent with the SM prediction that $t \to W^+ b$ is the dominant mode – but its branching ratio and the structure of the tbW vertex is not yet measured directly with high accuracy. Does the pointlike behaviour of the top quark continue once it can be probed at distance scales significantly below 10^{-18} m? These and other topics, while being addressed also at the Tevatron, will be in the focus of the future experiments at the LHC.

The top quark is unique among the known quarks in that it decays before it can form hadronic bound states. This has important consequences, as will be discussed in the following sections. Above all, it offers the possibility to explore the interactions of a *bare* quark at energies of a few hundred GeV to several TeV. Furthermore, it is an important asset of top quark physics that not only the effects of the electroweak interactions, but also of the strong interactions of these particles can, in most situations, be reliably predicted. Needless to say, this is necessary for the analysis and interpretation of present and future experimental data.

There are already a number of excellent reviews of hadronic top-quark production and decay [5–8]. In this exposition the top-quark physics perspectives at the LHC are discussed from a phenomenological point of view, of course taking the results and insights gained at the Tevatron into account. We shall first sketch the profile of this quark in section 2. In sections 3, 4, and 5 we discuss top-quark decay, $t\bar{t}$ pair production, and finally single-top-

quark production. In each section, we first review the presently available standard model predictions and discuss then possible new physics effects. Moreover, experimental results from the Tevatron and measurement perspectives at the LHC will be briefly outlined. As usual in particle phenomenology, values of particles masses and decay widths are given in natural units putting $\hbar = c = 1$.

Table 1: Upper part: number of $t\bar{t}$ events produced at the Tevatron and expected $t\bar{t}$ production rates at the LHC and at a future e^+e^- linear collider (ILC), where L is the integrated luminosity of the respective collider in units of fb^{-1}. Lower part: Number of t and $\bar{t}$ events at the Tevatron and expected number at the LHC produced in single top reactions.

$t\bar{t}$ pairs	dominant reaction	$N_{t\bar{t}}$
Tevatron: $p\bar{p}$ (1.96 TeV)	$q\bar{q} \to t\bar{t}$	$\sim 7 \cdot 10^4 \times L$
LHC: pp (14 TeV)	$gg \to t\bar{t}$	$\sim 9 \cdot 10^5 \times L$
ILC: e^+e^- (400 GeV)	$e^+e^- \to t\bar{t}$	$\sim 800 \times L$
single top	dominant reaction	$(N_t + N_{\bar{t}})$
Tevatron:	$u + b \xrightarrow{W} d + t$	$\sim 3 \cdot 10^3 \times L$
LHC:	$u + b \xrightarrow{W} d + t$	$\sim 3.3 \cdot 10^5 \times L$

2. The profile of the top quark

The top quark couples to all known fundamental interactions. Because of its large mass, it is expected to couple strongly to the forces that break the electroweak gauge symmetry. While the interactions of the top quark have not been explored in great detail so far, its mass has been experimentally determined very precisely. In this section we briefly describe what is known about the properties of the top quark, i.e., its mass, lifetime, spin, and its charges. Because its mass plays a central role in the physics of this quark, we shall first discuss the meaning of this parameter.

2.1. Mass

The top mass is a convention-dependent parameter, like the other parameters of the SM. As the top quark does not hadronize (see section 2.2), it seems natural to exploit the picture of the top quark being a highly unstable bare fermion. This suggests to use the concept of on-shell or pole mass, which is defined to be the real part of the complex-valued pole of the quark propagator $S_t(p)$. This is a purely perturbative concept. A quark is unobservable due to colour confinement, so its full propagator has no pole. In finite-order perturbation theory the propagator of the top quark has a pole at the complex value $\sqrt{p^2} = m_t - \mathrm{i}\Gamma_t/2$, where m_t is the pole or on-shell mass and Γ_t is the decay width of the

top quark. However, the all-order resummation of a class of diagrams, associated with so-called infrared renormalons, implies that the pole mass has an intrinsic, non-perturbative ambiguity of order $\Lambda_{QCD} \sim$ a few hundred MeV [9–12]. So-called short distance masses, for instance the quark mass $\overline{m}_q(\mu)$ defined in the $\overline{\rm MS}$ renormalization scheme, are free from such ambiguities. Here μ denotes the renormalization scale. The relation between the pole mass and the $\overline{\rm MS}$ mass is known in QCD to $O(\alpha_s^3)$ [13–15]. Evaluating this relation for the top quark at $\mu = \overline{m}_t$ it reads

$$\overline{m}_t(\overline{m}_t) = m_t \left(1 + \frac{4}{3}\frac{\alpha_s}{\pi} + 8.2364\,(\frac{\alpha_s}{\pi})^2 + 73.638\,(\frac{\alpha_s}{\pi})^3 + O(\alpha_s^4)\right)^{-1}, \qquad (2.1)$$

where $\alpha_s(\mu = \overline{m}_t)$ is the $\overline{\rm MS}$ coupling of 6-flavour QCD. One should remember that the relation (2.1) has an additional uncertainty of $O(\Lambda_{QCD})$. Using $\alpha_s = 0.109$ we get $m_t/\overline{m}_t = 1.06$. Thus, the $\overline{\rm MS}$ mass is 10 GeV lower than the pole mass; $m_t = 171$ GeV (see below) corresponds to $\overline{m}_t = 161$ GeV.

The present experimental determinations of the top mass at the Tevatron use global fits to data which involve a number of top-mass dependent (kinematical) variables. The modeling involved uses lowest-order matrix elements and parton showering (see section 4.3). Recently, the value

$$m_t^{exp} = 172.6 \pm 1.4\,\text{GeV} \qquad (2.2)$$

was obtained from the combined measurements of the CDF and D0 collaborations [16]. The relative error of 0.8% is smaller than that of any other quark mass. In view of this precision the question arises how (2.2) is to be interpreted. How is it related to a well-defined Lagrangian mass parameter? As most of the measurements use kinematic variables, it seems natural to identify (2.2) with the pole mass. However, one should be aware that the present experimental determinations of the top mass cannot be related to observables which have been calculated in higher-order perturbative QCD in terms of a Lagrangian mass parameter.

As is well known, the value of the top-quark mass plays a key role in SM fits to electroweak precision data which yield constraints on the SM Higgs mass[1]. The common practice is to interpret (2.2) as the on-shell mass m_t. With the world average of last year, $m_t^{exp} = 170.9 \pm 1.4$ GeV [17], the upper limit $m_H < 182$ GeV (95% C.L.) was obtained [18]. With (2.2) the upper limit on m_H increases by about 18 GeV. This limit should be taken with a grain of salt in view of the uncertainty in interpreting (2.2).

In the following sections, m_t always refers to the pole mass. With no better alternative at present, we shall stick to interpreting (2.2) in terms of this mass parameter[2].

2.2. Lifetime

The top quark is an extremely elusive object. Because its mass is so large, it can decay into on-shell W bosons, i.e., the two-particle decay mode $t \to bW^+$ is kinematically possible.

[1] For a discussion of the role of the top-quark mass in electroweak precision physics, see, e.g. [5].

[2] Below we shall mostly use $m_t = 171$ GeV – the world-average value at the time when this article was written – when theoretical results are evaluated for a definite top mass.

The SM predicts the top quark to decay almost exclusively into this mode (see section 3). This process is CKM-allowed[3], leading to the prediction that the average proper lifetime of the t quark is extremely short, $\tau_t = 1/\Gamma_t \simeq 5 \times 10^{-25}$ s. For comparison, the mean lifetime of b hadrons, which involve the next heaviest quark, is almost 13 orders of magnitude larger, $\tau_{b\,hadron} \simeq 1.5 \times 10^{-12}$ s. The lifetime τ_t is an order of magnitude smaller the hadronization time $\tau_{had} \simeq 1/\Lambda_{QCD} \approx 3 \times 10^{-24}$ s, which characterizes the time it takes for an (anti)quark produced in some reaction to combine with other produced (anti)quarks and form a colour-neutral hadron due to confinement. Thus, top quarks are unable to form top mesons $t\bar{q}$ or baryons tqq'. In particular there will be no spectroscopy of toponium $t\bar{t}$ bound states [20]. To illustrate this central feature further, we consider the production of a $t\bar{t}$ pair at the Tevatron or at the LHC, $p\bar{p}$, $pp \to t\bar{t}X$. The distance the t and $\bar{t}$ quarks are able to move away from their production vertex before they decay is on average 0.1 fm, a length scale much smaller than the typical hadron size of 1 fm. At distances not more than about 0.1 fm even the strong interactions of t and $\bar{t}$ quarks are still weak owing to the asymptotic freedom property of QCD. Therefore the top quark behaves like a highly unstable particle which couples only weakly to the other known quanta.

The decay width of the top quark manifests itself in the Breit-Wigner line-shape, i.e., the width of the invariant mass distribution of the top-decay products, $\mathrm{d}\sigma/\mathrm{d}M_t$, $M_t^2 = (\sum p_f)^2$. Unfortunately, the top width $\Gamma_t \simeq 1.3$ GeV is much smaller than the experimental resolution at the Tevatron or at the LHC. At present, no sensible method is known how to directly determine Γ_t at a hadron collider. In conjuction with some assumptions, an indirect determination is possible from the measurement of the $t\bar{t}$ and the single-top production cross sections [6].

An important consequence of the distinctive property of the top quark not forming hadrons pertains top-spin effects. The spin polarization and/or spin-spin correlations which are imprinted upon an ensemble of single top quarks or $t\bar{t}$ pairs by the production dynamics are not diluted by hadronization, but result in characteristic angular distributions and correlations of the final state particles/jets into which the top quarks decay [21] (see sections 3.1.3, 4.5, and 5.3). Gluon radiation off a top quark may flip its spin, but such a chromomagnetic $M1$ transition is suppressed by the large mass m_t. The spin-flip transition rate of an off-shell t quark decaying into an on-shell gluon with energy E_g and a t quark may be estimated as $\Gamma(M1) \sim \alpha_s E_g^3/m_t^2$, where $\alpha_s(m_t) = 0.1$. Thus the spin-flip time $\tau_{flip} = 1/\Gamma(M1)$ is on average much larger than the top-lifetime τ_t. In any case, top-spin effects can be computed reliably in perturbation theory because the QCD coupling α_s is small at energies of the order of m_t. This is in contrast to the case of lighter quarks, for instance b quarks, where the transition of b quarks to b hadrons is governed by non-perturbative strong interaction dynamics, and such transitions cannot be computed so far with ab initio methods. A large fraction of quark hadronization results in spin-zero mesons. Thus there will be no information left in the meson decay products on the quark spin at production. In this respect top quarks offer a richer phenomenology than lighter

[3]CKM is the acronym for the Cabibbo-Kobayashi-Maskawa matrix $(V_{qq'})$, the 3×3 unitary matrix that parameterizes the strength of the interactions of quarks with $W^{\pm}$ bosons. The unitarity of this matrix implies that the modulus of the matrix element V_{tb} is close to one, $|V_{tb}| \simeq 0.999$ [19].

quarks: "good observables" – i.e., observables that are both measurable and reliably predictable – are not only quantities like production cross sections, decay rates, transverse momentum and rapidity distributions, but also final-state angular distributions and correlations that are caused by top-spin polarization and $t\bar{t}$ spin correlations.

2.3. Spin

There is no doubt that the top quark, as observed at the Tevatron, is a spin $1/2$ fermion – although a dedicated experimental verification has so far not been made. The observed decay $t \to bW$, the known spins of W and b, and the conservation of total angular momentum imply that the top quark is a fermion. If the spin of the top quark were $3/2$, the $t\bar{t}$ cross section at the Tevatron would be much larger than the measured one. A direct experimental evidence for the top quark having spin $1/2$ would be the observation of the resulting polarization and spin-correlation effects (see sections 4.5 and 5.3). Definite measurements are expected to be feasible at the LHC [22, 23]. Another possibility is the measurement of the differential cross section $\mathrm{d}\sigma/\mathrm{d}M_{t\bar{t}}$ near the $t\bar{t}$ production threshold [24] ($M_{t\bar{t}}$ denotes the invariant mass of the $t\bar{t}$ pair). As is well-known the behaviour of the near-threshold cross section as a function of the particle velocity is characteristic of the spin of the produced particle and antiparticle.

2.4. Colour and electric charge

Top quarks, like the other quarks, carry colour charge – they transform as a colour triplet under the $SU(3)_c$ gauge group of the strong interactions. Colour-confinement precludes the direct measurement of this quantum number; but indeed, measurements of the $t\bar{t}$ production cross section are consistent with the SM predictions for a colour-triplet and antitriplet quark-antiquark pair.

The top quark is the $I_3 = 1/2$ weak-isospin partner of the b quark, assuring the consistency of the SM at the quantum level. The electric charge of the top quark, which is therefore $Q_t = 2/3$ in units of the positron charge $e > 0$ according to the SM, has so far not been measured. The observed channel $t\bar{t} \to bbW^+W^-$ does a priori not preclude the possibility that the observed top resonance is an exotic heavy quark with charge $Q = -4/3$ decaying into bW^- [25]. However, this has been excluded in the meantime by the D0 and CDF experiments at the Tevatron [26, 27]. The top-quark charge can be directly determined by measuring the production rate of $t\bar{t}$ plus a hard photon and taking the ratio $\sigma(t\bar{t}\gamma)/\sigma(t\bar{t})$. At the LHC this ratio is approximately proportional to Q_t^2 because $t\bar{t}$ and $t\bar{t}\gamma$ production is dominated by gluon fusion. This will be discussed in more detail in section 4.6.

3. Top-quark decays

Because the top quark is an extremely short-lived resonance, only its decay products can be detected by experiments. Thus for comparison with data, theoretical predictions must entail, in general, top-production and decay. However, this resonance is narrow, as

$\Gamma_t/m_t \simeq 0.008$. Thus one can factorize, to good approximation, the theoretical description of these reactions into the production of on-shell single top quarks or $t\bar{t}$ pairs (being produced in a certain spin configuration) and the decay of t and/or $\bar{t}$. We treat top-quark decays first while the survey of hadronic production of these quarks is postponed to the following sections. We shall review (polarized) top-quark decays in the SM, then discuss effects of possible anomalous couplings in the tbW vertex, and finally consider several new decay modes which are possible in various SM extensions.

3.1. SM decays

In the SM, which involves three generations of quarks and leptons, the only two-particle decays of the top quark[4] which are possible to lowest order in the (gauge) couplings are $t \to bW^+$, $t \to sW^+$, and $t \to dW^+$. Their rates are proportional to the squares of the CKM matrix elements $|V_{tq}|^2$, $q = b,s,d$, respectively. The rate of $t \to X$, i.e. the total decay width Γ_t of the top quark, is given by the sum of the widths of these three decay modes, as the branching ratios of the loop-induced flavour-changing neutral current decays are negligibly small in the SM (see section 3.2.4). The analysis of data from weak decays of hadrons yields $0.9990 < |V_{tb}| < 0.9992$ at 95% C.L. [19], using the unitarity of the CKM matrix. From the recent observation of the oscillation of $B_s \leftrightarrow \bar{B}_s$ mesons by the D0 and CDF experiments at the Tevatron and from analogous data on $B_d \leftrightarrow \bar{B}_d$ oscillations one can extract the ratio $0.20 < |V_{td}/V_{ts}| < 0.22$ [19]. The unitarity relation $|V_{tb}|^2 + |V_{ts}|^2 + |V_{td}|^2 = 1$ implies that the total decay rate is completely dominated by $t \to bW^+$, and one gets for the branching ratios

$$B(t \to bW^+) = 0.998, \qquad B(t \to sW^+) \simeq 1.9 \times 10^{-3}, \qquad B(t \to dW^+) \simeq 10^{-4}. \quad (3.1)$$

There is direct information from the Tevatron which implies that $|V_{tb}| \gg |V_{td}|, |V_{td}|$, without using the unitarity constraint. The CDF and D0 collaborations measured

$$R \equiv \frac{B(t \to bW)}{\sum_{q=b,s,d} B(t \to qW)} = \frac{|V_{tb}|^2}{|V_{tb}|^2 + |V_{ts}|^2 + |V_{td}|^2} \quad (3.2)$$

by comparing the number of $t\bar{t}$ candidates with 0, 1, and 2 tagged b jets. The right-hand side of (3.2) is the standard-model interpretation of this ratio. A collection of CDF and D0 results on R is given in [28,29]; the recent D0 result is $R = 0.97^{+0.09}_{-0.08}$ [29]. The D0 [3] and the CDF [4] experiments reported evidence for single top quark production. The agreement of the measured production cross section with the SM expectation was used by these experiments for a direct determination of the CKM matrix element V_{tb} with the result $0.68 < |V_{tb}| \leq 1$ [3] and $|V_{tb}| = 0.88 \pm 0.14 \pm 0.07$ [4]. (See also section 5).

3.1.1. The total decay width:

As just discussed, the total decay width of the top quark is given in the SM, to the precision required for interpreting the Tevatron or forthcoming LHC experiments, by the

[4] Unless stated otherwise, the discussion of this section applies analogously also to $\bar{t}$ decays.

partial width of the decay $t \to bW^+$ – more precisely, of the sum of the widths of the decays

$$t \to bW^+ \to b\ell^+\nu_\ell, \quad bu\bar{d}, \quad bc\bar{s}, \quad \cdots \tag{3.3}$$

where $\ell = e, \mu, \tau$ and the ellipses indicate CKM-suppressed decays of the W boson. Taking the intermediate W boson to be on-shell, one gets to Born approximation:

$$\Gamma_t^B \equiv \Gamma_t^B(t \to bW) = \frac{G_F}{8\pi\sqrt{2}} m_t^3 |V_{tb}|^2 \left(1 - \frac{m_W^2}{m_t^2}\right)^2 \left(1 + 2\frac{m_W^2}{m_t^2}\right) = 1.44\,\text{GeV}, \tag{3.4}$$

where G_F is the Fermi constant, $m_t = 171$ GeV and $m_W = 80.40$ GeV has been used, and the mass of the b quark ($m_b \simeq 4.9$ GeV) has been neglected. The order α_s QCD corrections [30], the order α weak and electromagnetic[5] corrections [31, 32], and the corrections due to the width of off-shell W bosons [33] and to $m_b \neq 0$ were determined quite some time ago. Moreover, the order α_s^2 QCD corrections were computed as an expansion in $(m_W/m_t)^2$ [34, 35]. While the $O(\alpha)$ corrections are positive and rather small (+2%) and are almost compensated by the finite W-width corrections, the $O(\alpha_s)$ and $O(\alpha_s^2)$ corrections are negative. Thus, essentially only the QCD corrections matter, and the SM prediction for the radiatively corrected width may be represented by the following expression [34, 35]:

$$\Gamma_t = \Gamma_t^B (1 - 0.81\alpha_s - 1.81\alpha_s^2), \tag{3.5}$$

where $\alpha_s = \alpha_s(m_t)$ is the QCD coupling in the $\overline{\text{MS}}$ renormalization scheme. With $\alpha_s(m_t) = 0.108$ the correction factor (3.5) to the lowest-order width is 0.89. Thus for $m_t = 171$ GeV we have[6] $\Gamma_t = 1.28$ GeV.

It should be noted that gluon radiation, $t \to bWg$, can make up a fair fraction of the total rate if the cut on the minimal gluon energy E_g is relatively low. For gluon energies $E_g \gtrsim 10$ GeV the branching ratio $B(t \to bWg) \simeq 0.3$.

For the dominant semileptonic and nonleptonic decay modes (3.3) the branching ratios are, for $\Gamma_W, m_b \neq 0$ and including the $O(\alpha_s)$ QCD corrections:

$$B(t \to b\ell^+\nu_\ell) = 0.108 \quad (\ell = e, \mu, \tau), \qquad B(t \to bq\bar{q}') = 0.337 \times |V_{q\bar{q}'}|^2. \tag{3.6}$$

Using the central values of the respective CKM matrix elements [19] we have then $B(t \to bu\bar{d}) = B(t \to bc\bar{s}) = 0.328$, $B(t \to bu\bar{s}) = 0.017$, and $B(t \to bc\bar{b}) = 6 \times 10^{-4}$.

3.1.2. W-boson helicity:

In the SM the strength and structure of the tbW vertex is determined (up to V_{tb}) by the universal $V-A$ charged-current interaction. A basic test of the structure of this vertex is the measurement of the decay fractions $F_0 = B(t \to bW(\lambda_W = 0))$, $F_\mp = B(t \to bW(\lambda_W = \mp 1))$ into W^+ bosons of helicity $\lambda_W = 0, \mp 1$. By definition $F_0 + F_- + F_+ = 1$. The

[5] As usual, $\alpha = e^2/4\pi$. Recall that the weak and electromagnetic couplings are related by $g_w = e/\sin\theta_w$.

[6] The higher-order QCD corrections to the top-decay width should be evaluated using $\overline{m}_t$ rather than the pole mass m_t, in order to avoid renormalon ambiguities.

$V-A$ structure and angular momentum conservation allow the decay into a zero-helicity and negative helicity W boson, but the decay amplitude into $W(\lambda_W = +1)$ is suppressed by a factor m_b^2/m_W^2. This is due to the fact that the $V-A$ law forces the b quark, if it were massless, to have negative helicity – but this is in conflict with angular momentum conservation. The three cases are illustrated in figure 1. For the decay fractions one

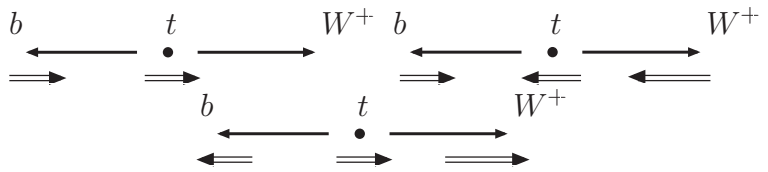

Figure 1: Illustration of top-quark decay into a b quark and a W^+ boson with $\lambda_W = 0, \mp 1$. For $W^+(\lambda_W = +1)$ the b quark must have positive helicity (to lowest order), which has vanishing probability for $m_b \to 0$.

obtains at tree level, putting $m_b = 0$, and using $m_W = 80.40$ GeV:

$$F_0^B = \frac{m_t^2}{m_t^2 + 2m_W^2} = 0.6934 - 0.0025 \times (171 - m_t\,[\text{GeV}])\,,$$
$$F_-^B = \frac{2m_W^2}{m_t^2 + 2m_W^2} = 0.3066 + 0.0025 \times (171 - m_t\,[\text{GeV}])\,, \qquad F_+^B = 0\,. \tag{3.7}$$

Once gluon (and photon) radiation is taken into account, $F_+ \neq 0$ even in the limit $m_b = 0$. The W-helicity fractions $F_{0,\mp}$ were computed in [36, 46], taking the $O(\alpha_s)$ QCD and $O(\alpha)$ electroweak corrections, and the corrections due to the finite W width and $m_b \neq 0$ into account. These corrections are very small; in particular they generate a small fraction F_+. The result of [36] is

$$F_0 = 0.99 \times F_0^B\,, \qquad F_- = 1.02 \times F_-^B\,, \qquad F_+ = 0.001\,. \tag{3.8}$$

For $\bar{t} \to \bar{b}W^-$ we have $\bar{F}_0 = F_0$, $\bar{F}_- = F_+$, and $\bar{F}_+ = F_-$ in the SM. Violations of these relations due to the CP-violating KM phase δ_{KM} are negligibly small.

The large fraction $F_0 \simeq 0.7$ signifies that top-quark decay is a source of longitudinally polarized W bosons – in fact, the only significant one at the LHC. (Almost all W bosons produced in QCD reactions are transversely polarized.) Recall that, in the SM, the longitudinally polarized state of the W boson is generated by the charged component of the $SU(2)$ Higgs doublet field. If the dynamics of electroweak symmetry breaking is different from the SM Higgs mechanism, one may expect deviations of the tbW vertex from its SM structure, and F_0 should be sensitive to it. The fraction F_+ is obviously sensitive to a possible $V+A$ admixture in the charged weak current involving the top quark. These issues will be addressed in sections 3.1.3 and 3.2.1.

Information about the polarization of the W boson is obtained from the angular distributions of one of its decay products, $W^+ \to \ell^+\nu_\ell, q\bar{q}'$. As a u-type jet cannot be distinguished experimentally from a d-type jet, the best choice is to consider a charged lepton

$\ell^+ = e^+, \mu^+$. Consider the decay $t \to bW^+ \to b\ell^+\nu_\ell$ and define ψ^* to be the angle between the direction of ℓ^+ in the W^+ rest frame and the W^+ direction in the t rest frame. Then one obtains for the distribution of this angle:

$$\frac{1}{\Gamma}\frac{d\Gamma}{d\cos\psi^*} = \frac{3}{4}F_0 \sin^2\psi^* + \frac{3}{8}F_-(1-\cos\psi^*)^2 + \frac{3}{8}F_+(1+\cos\psi^*)^2, \qquad (3.9)$$

Thus, in the one-dimensional distribution (3.9), interference terms due to different polarization states of the intermediate W boson do not contribute[7]. The helicity fractions can be obtained from a fit of (3.9) to the measured $\cos\psi^*$ distribution and from the constraint $F_0 + F_- + F_+ = 1$. In addition one may employ the forward-backward asymmetry A_{FB} with respect to $\cos\psi^*$, $A_{FB} = 3(F_+ - F_-)/4$. A generalization of this asymmetry has been suggested in [38]:

$$A_z = \frac{N(\cos\psi^* > z) - N(\cos\psi^* < z)}{N(\cos\psi^* > z) + N(\cos\psi^* < z)}, \qquad (3.10)$$

with $-1 < z < 1$. The fractions $F_{0,\mp}$ can be obtained from appropriate combinations of A_z. The use of these asymmetries helps to reduce measurement uncertainties.
At the Tevatron the CDF and D0 experiments measured the W-boson helicity fractions in semileptonic [39–41] and recently also in nonleptonic [42] top-quark decays[8]. The results given in Table 2 for F_0 and F_+ were obtained by putting F_+ and F_0 to their SM values, respectively. Recently, these assumptions were dropped in a simultaneous measurement of F_0 and F_+ by the D0 collaboration [42], with the result: $F_0 = 0.425 \pm 0.166 \pm 0.102$ and $F_+ = 0.119 \pm 0.090 \pm 0.053$.
For comparison, table 2 contains also the expected systematic measurement uncertainties for $F_{0,\pm}$ at the LHC, as estimated in the study of [22]. Statistical errors should not be a problem at the LHC once a sufficiently large sample of top quark events will have been recorded. After selection of $\sim 10^6$ $t\bar{t}$ events in the dileptonic and lepton + jets decay channels the statistical error on the helicity fractions will be an order of magnitude below the systematic one [22]. The analysis [43] arrived at similar results. Thus $F_{0,\pm}$ should be measurable at the LHC with a precision of about 2%. This will allow a precise determination of the structure of the the tbW vertex, as will be discussed in section 3.2.1.

3.1.3. Distributions for semileptonic and nonleptonic decays:

Apart from (3.9) there are other energy and angular distributions that are useful for studying the structure of the top-decay vertex in semi- and nonleptonic decays of top quarks, $t \to b\ell\nu_\ell$, $bq\bar{q}'$ ($q\bar{q}' = u\bar{d}$, $c\bar{s}, \ldots$). A number of distributions were calculated for these decays, including radiative corrections. Here we discuss in detail only angular

[7] Higher dimensional distributions, which are sensitive to such interferences, that is, to non-diagonal terms in the W-boson spin density matrix $(\rho^W)_{ij}$, can also be considered [37].

[8] Because in $W \to q\bar{q}'$ the flavour of the jets cannot be tagged, a W daughter jet was chosen at random in [42]. The sign ambiguity in the calculated $\cos\psi^*$ was avoided by considering the distribution of $|\cos\psi^*|$.

Table 2: First and second row: Tevatron results for the W helicity fractions in t quark decay. Third row: estimated systematic error in future LHC measurements.

		F_0		F_+		F_-
Tevatron:	CDF	$0.85^{+0.16}_{-0.23}$	[39]	-0.02 ± 0.08	[40]	
	D0	0.62 ± 0.10	[42]	-0.002 ± 0.07	[42]	
LHC ($\Delta_{\rm syst}$) [22]		± 0.015		± 0.012		± 0.024

distributions for polarized top-quark decays. They are important for determining top-spin effects – see below and sections 4.5 and 5.3.

An ensemble of top quarks self-analyzes its spin polarization via its weak decays. Consider the decay $t \to f + \cdots$ of a polarized top in the top quark rest frame. Information about the top spin vector is encoded in the distribution of $\cos\theta_f$, where θ_f is the angle between the direction of the particle/jet f (used as t spin analyzer) in the t rest frame and the polarization vector of the top quark. It has the a priori form

$$\frac{1}{\Gamma_f}\frac{{\rm d}\Gamma_f}{{\rm d}\cos\theta_f} = \frac{1}{2}(1 + p\, c_f \cos\theta_f)\,, \tag{3.11}$$

where Γ_f denotes the partial decay width, p is the polarization degree of the ensemble, and c_f is the t spin-analyzing power of f. Obviously, $|c_f| \leq 1$. In the SM the charged lepton or the d-type quark from W-boson decay are the best t spin analyzers. We have $c_{\ell^+} = c_{\bar{d}} = 1$ at tree level, while $c_{\nu_\ell} = c_u = -0.30$ and $c_b = [2(m_b/m_t)^2 - 1]/[2(m_b/m_t)^2 + 1] = -c_{W^+} = -0.39$ (assuming the reconstruction of the W^+ boson direction of flight). That is, for an ensemble of 100 % polarized top quarks, the probability for the ℓ^+ being emitted in the direction of the t spin is maximal, while it is zero for the emission opposite to the t spin. The circumstance that the charged lepton has a larger t spin-analyzing power than its mother, the W boson, seems curious at first sight. But this is due to the fact that the ℓ^+ distribution is generated by the amplitudes with intermediate $W^+(\lambda_W = 0)$ and $W^+(\lambda_W = -1)$ bosons which interfere, and this leads to constructive and completely destructive interference in the direction parallel and opposite to the t-spin, respectively. This information about the t spin contained in the interference terms is missing in the distributions (3.11) for $f = W^+$ and $f = b$.

To order α_s the CKM allowed final states are (i) $\ell\nu_\ell + b$ jet and $\ell\nu_\ell + b$ jet + gluon jet in semileptonic decays and (ii) a b jet plus two or three non-b jets in nonleptonic decays. The spin-analyzing power of a final state particle/jet f decreases slightly due to gluon radiation.

The correlation coefficients c_f were computed to order α_s for the semi- and nonleptonic channels in [44] and in [45], respectively, and are collected, together with the lowest-order values in table 3. For the nonleptonic channels, $j_<$ and $j_>$ denote the least energetic and most energetic non-b jet, respectively, defined by the Durham clustering algorithm. As the identification of the flavours of the quark jets from CKM allowed W decay is not

Table 3: Spin-analyzing power c_f to lowest order and to $O(\alpha_s)$ for semileptonic [44] and nonleptonic [45] top quark decays for $m_t = 171$ GeV.

	ℓ^+	$\bar{d}$	u	b	$j_<$	**T**	$j_>$
LO:	1	1	-0.32	-0.39	0.51	-0.32	0.2
NLO:	0.999	0.97	-0.31	-0.37	0.47	-0.31	

possible – or inefficient in the case of the $c\bar{s}$ final state –, table 3 shows that, in the case of nonleptonic decays, the least energetic non-b jet is the most efficient top-spin analyzer. Again, this is a consequence of $V-A$ and angular momentum conservation. The vector **T** denotes the oriented thrust axis for nonleptonic final states, defined by the requirement $\mathbf{T}\cdot\mathbf{p}_b > 0$. The coefficients $c_f \neq c_\ell$ in table 3 depend slightly on the value of m_t.
The analogous angular distributions for the decays of antitop quarks, $\bar{t} \to \bar{f} + \cdots$, are

$$\frac{1}{\Gamma_{\bar{f}}}\frac{\mathrm{d}\Gamma_{\bar{f}}}{\mathrm{d}\cos\theta_{\bar{f}}} = \frac{1}{2}(1 + p\, c_{\bar{f}} \cos\theta_{\bar{f}}), \quad c_{\bar{f}} = -c_f\,. \tag{3.12}$$

The last relation is valid if *CP* invariance holds. Violation of this relation requires that the respective decay amplitude has a *CP*-violating absorptive part [49]. Within the SM such an effect is negligibly small.
If the $t \to b$ transition, i.e., the decays $t \to b f_1 f_2$ are affected by new interactions, the values of the c_f given in table 3 will change in general – see sections 3.2.1 and 3.2.2.
SM predictions including QCD corrections for lepton-energy and energy-angular distributions in (polarized) semileptonic top-quark decay are also available [37, 44, 46]. The shapes of the ℓ and ν_ℓ energy distributions are good probes of the chirality of the current which induces the $t \to b$ transition. For a small $V+A$ admixture to this current these distributions were determined in [47, 48].

3.2. Top-quark decays in SM extensions

In the SM all decay modes other than $t \to Wb$ are rare, as their branching ratios are $O(10^{-3})$ or less. Nevertheless, exotic decay modes with branching ratios of the order of a few percent are still possible. Several examples will be reviewed below. If new particles/interactions affect top quarks, they may not lead to new decay modes, but they should, in any case, have an effect on the tbW vertex. LHC experiments should be able to determine this vertex quite precisely, as will be discussed now.

3.2.1. Anomalous couplings in the tbW vertex:

A model-independent analysis of the structure of the tbW vertex can be made as follows. The amplitude $\mathcal{M}_{tbW}$ of the decay $t(p) \to b(k) W^+(q)$, where all particles are on-

shell (p, k and $q = p - k$ denote four-momenta) has the general form-factor decomposition [49, 50]

$$\mathcal{M}_{tbW} = -\frac{g_W}{\sqrt{2}}\varepsilon^{*\mu}\overline{u_b}\left[(V_{tb}^* + f_L)\gamma_\mu P_L + f_R\gamma_\mu P_R + \mathrm{i}\sigma_{\mu\nu}q^\nu(\frac{g_L}{m_W}P_L + \frac{g_R}{m_W}P_R)\right]u_t\,. \quad (3.13)$$

Here $P_{L,R} = (1 \mp \gamma_5)/2$ and the two chirality conserving and flipping form factors[9] $f_{L,R}$ and $g_{L,R}$, respectively, are dimensionless (complex) functions of the squared W boson four-momentum q^2. The parameterization in (3.13) is chosen such that non-zero values of $f_{L,R}$ and $g_{L,R}$ signify deviations from the structure of the tree-level Born vertex. An equivalent description of the $t \to bW$ vertex is obtained using an effective Lagrangian approach [51]. In this context, the above form factors evaluated at $q^2 = m_W^2$ correspond to anomalous couplings.

In SM extensions corresponding to renormalizable theories, $f_{L,R} \neq 0$ can appear at tree-level while $g_{L,R} \neq 0$ must be loop-induced. The form factors are gauge-invariant, but in general not infrared-finite. They should be used to parameterize only possible new "infrared safe" short-distance contributions to the tbW vertex, caused for instance by the exchange of new heavy virtual particles. A search for anomalous couplings in $t \to bf\bar{f}'$ decay-data should proceed as follows. One computes decay distributions within the SM including radiative corrections, and adds the contributions linear in the anomalous form factors $f_{L,R}$ and $g_{L,R}$ which are generated by the interference of (3.13) with the SM Born amplitude. This assumes that these anomalous effects are small, which can be checked a posteriori.

For a small $V + A$ admixture to the SM current, energy and higher-dimensional distributions were computed in this fashion in [47, 48]. In this case neutrino energy-angular distributions turn out to be most sensitive to $f_R \neq 0$. It is important to take the QCD corrections into account in (future) data analyses, as gluon radiation can mimic a small $V + A$ admixture.

There are tight indirect constraints on some of the anomalous couplings from the measured branching ratio $B(\bar{B} \to X_s\gamma)$, in particular on f_R and g_L, as the contributions of these couplings to B are enhanced by a factor m_t/m_b [52, 53]. A recent analysis [54] arrives at the bounds given in table 4. (For earlier work, see [55, 56].) These bounds were obtained by allowing only one coupling to be non-zero at a time.

One should keep in mind that these bounds are not rock-solid as the effects of different couplings might cancel among each other or might be off-set by other new physics contributions.

The possible size of these anomalous couplings was investigated in several SM extensions. While in the minimal supersymmetric extension of the SM the radiative corrections to the lowest order $V - A$ tbW vertex due to supersymmetric particle exchanges are only at the level of 1% or smaller [57, 58], effects can be somewhat larger in some alternative models of electroweak symmetry breaking [59].

[9] If the W bosons are off-shell, two additional form factors appear in the matrix element. However, they do not contribute in the limit of vanishing masses of the fermions into which the W boson decays.

Table 4: Current 95 % C.L. upper and lower bounds on anomalous couplings in the tbW vertex from $B(\bar{B} \to X_s\gamma)$ [54]. The couplings are assumed to be real.

	f_L	f_R	g_L	g_R
upper bound	0.03	0.0025	0.0004	0.57
lower bound	-0.13	-0.0007	-0.0015	-0.15

The level of precision with which the helicity fractions are presently known from Tevatron experiments (see table 2) do not imply constraints on the anomalous couplings which can compete with those given in table 4. However, future high statistics data on top quark decays at the LHC can provide information on the couplings f_R, g_L, and g_R at the level of a few percent – i.e., there is the prospect of directly determining these couplings with good precision. Simulation studies for the LHC analyzed $t\bar{t}$ production and decay into lepton plus jets channels [22, 43] and also dileptonic channels [22]. Basic observables for determining the anomalous couplings are the W-boson helicity fractions (whose estimated measurement uncertainties are given in table 2) and the forward-backward asymmetries (3.10), which were used in [43]. These observables are not sensitive to the absolute strength of the tbW vertex and to f_L. Both studies assume real form factors. The parametric dependence of the observables on the anomalous couplings yields estimates for the expected confidence intervals. Assuming that only one non-standard coupling is nonzero at a time, [43] concludes that f_R, g_L, or g_R should be either detected or excluded at the 2 s.d. level (statistics plus systematics) if their values lie outside the following intervals:

$$f_R\,(2\sigma):\ [-0.055, 0.13]\,, \quad g_L\,(2\sigma):\ [-0.058, 0.026]\,, \quad g_R\,(2\sigma):\ [-0.026, 0.031]\,. \tag{3.14}$$

The analysis of [22] arrived, as far as g_R is concerned, at a sensitivity level of the same order. Thus the sensitivity to g_R expected at the LHC is an order of magnitude better than the current indirect bound given in table 4.

Single top-quark production and decay at the LHC will also provide a sensitive probe of these anomalous couplings [60, 61]. If the single-top-production cross sections for the t-channel and s-channel processes (see section 5) will be measured at the LHC with reasonable precision, then this additional information will allow to determine/constrain also f_L and the absolute strength of the tbW vertex [62].

In general the form factors $f_{L,R}$ and $g_{L,R}$ can be complex, which need not necessarily be due to CP violation. Because the form factors are in the timelike region, $q^2 > 0$, they can have absorptive parts. CP invariance implies, apart from the requirement of a real CKM matrix, that the following relations hold between the form factors $f_{L,R}, g_{L,R}$ and the corresponding form factors $f'_{L,R}, g'_{L,R}$ in the $\bar{t} \to \bar{b}W^-$ decay amplitude [49]:

$$f_i = f'_i, \quad g_i = g'_i, \tag{3.15}$$

where $i = L, R$. Thus, absorptive parts due to *CP*-invariant interactions satisfy (3.15) while dispersive (and absorptive) parts generated by *CP*-violating interactions violate these relations. The T-odd triple correlation $O = \mathbf{S}_t \cdot (\hat{\mathbf{p}}_{\ell^+} \times \hat{\mathbf{p}}_b)$ in polarized semileptonic t decay, where $\mathbf{S}_t$ denotes the top spin, is sensitive to *CP* violation and *CP*-invariant absorptive parts in the tbW vertex. Measuring O and the the corresponding correlation $\bar{O}$ in t and $\bar{t}$ decay and taking the difference would be a clean *CP*-symmetry test in top decay. One finds that $\langle O \rangle - \langle \bar{O} \rangle \propto \mathrm{Im}(g_R - g'_R)$ [49, 63]. Other *CP* asymmetries in top-quark decay were discussed in [50].
A general analysis of the semi- and nonleptonic (anti)top-quark decays via W exchange was made in terms of helicity parameters in [64–66].
While the b-jet, ℓ, $\nu_e ll$ energy distributions and the b-jet and $\nu_e ll$ angular distributions from top-quark decay can be used to probe anomalous couplings (3.13) in the tbW vertex, the angular distribution (3.11) of the charged lepton is insensitive to small anomalous couplings $f_{L,R}$, $g_{L,R}$ [67,68]. This holds for the secondary lepton distribution $\sigma^{-1} \mathrm{d}\sigma / \mathrm{d}\cos\theta_\ell \mathrm{d}\phi_e ll$ irrespective of the top-quark production process [69].

3.2.2. Decays to charged Higgs bosons:

Many SM extensions which involve a larger Higgs sector predict the existence of charged Higgs bosons $H^\pm$, apart from the existence of more than one neutral Higgs state. One of the simplest extensions of the SM results from the addition of a second Higgs doublet field. This leads to three physical neutral (h, H, A) and a pair of charged $(H^\pm)$ spin-zero bosons. The non-supersymmetric two-Higgs doublet models (2HDM) are conventionally classified into three types: In the type I model only one of the two Higgs doublet fields Φ_1, Φ_2 is coupled to the quarks and leptons at tree level, while in the type II 2HDM the Higgs doublets Φ_1 and Φ_2 couple only to right-handed down-type fermions (d_{iR}, ℓ_{iR}) and up-type fermions (u_{iR}, ν_{iR}), respectively. Type III 2HDM allow for tree-level couplings to both up-type and down-type fermions for each of the Higgs doublets [70]. In type III models the exchange of neutral Higgs bosons can mediate transitions between quarks (and leptons) of the same charge at tree level. Such couplings are strongly constrained for transitions between b, s, d quarks (and between charged leptons) [19] – contrary to transitions $t \to c$. This will be discussed in section 3.2.4.
In the phenomenology of 2HDM extensions of the SM discussed here, two new parameters enter, which are taken to be the mass m_{H^+} of the charged Higgs boson and $\tan\beta = v_2/v_1$, where v_1, v_2 is the vacuum expectation value of Φ_1 and Φ_2, respectively.
In 2HDM the mass of $H^\pm$ is strongly constrained by the data on the radiative decays $\bar{B}^0 \to X_s \gamma$ from the B meson factories. The measured inclusive branching ratio agrees very well with the SM prediction, leaving only a small margin for possible new physics contributions. For the 2HDM type-II models this implies the lower bound $m_{H^\pm} > 350$ GeV [71]. Thus, within these models, a charged Higgs boson can affect top quark decays only by mediating, in addition to W boson exchange, three-body decays like $t \to bc\bar{s}$, $b\tau^+\nu_\tau$. However, because of the strong lower bound on m_{H^+} the possible changes of the respective branching ratios are very small compared to the values (3.6) predicted by the SM.

A model-independent lower bound, $m_{H^\pm} > 79.3$ GeV at 95% C.L., was obtained at the LEP2 collider [19] from the non-observation of $e^+e^- \to H^+H^-$.
The minimal supersymmetric extension of the SM (MSSM) includes a two-Higgs doublet sector of type II. Within the MSSM the constraint from $B(b \to s\gamma)$ on the mass of $H^\pm$ does not apply, as the one-loop contributions from H^- exchange to the $b \to s\gamma$ amplitude can be compensated to a large extent by the contributions from the exchange of supersymmetric particles (in particular of charginos and top squarks). Thus, within the MSSM, $m_{H^+} < m_t$ and the decay of a top quark into a b quark and an on-shell H^+ is still possible. To Born approximation the decay rate is (putting $m_b = 0$ in the phase space function, but not in the coupling to H^+):

$$\Gamma^B(t \to bH^+) = \frac{G_F}{8\pi\sqrt{2}} m_t^3 |V_{tb}|^2 \left(1 - \frac{m_{H^+}^2}{m_t^2}\right)^2 \left(\frac{m_b^2}{m_t^2}\tan^2\beta + \cot^2\beta\right). \tag{3.16}$$

The $O(\alpha_s)$ QCD corrections to (3.16) are also known [72, 73] and are such that the ratio of the rates for $t \to bH^+$ and $t \to bW^+$ remains almost unaffected by these corrections. Comparing (3.16) with (3.4) one sees that the decay rate for $t \to bH^+$ becomes comparable in size to $t \to bW^+$ for small and large values of $\tan\beta$ if m_{H^+} is not too close to the phase space limit. For fixed m_{H^+} the rate (3.16) is smallest at $\tan\beta = \sqrt{m_t/m_b} \sim 6$. For instance, putting $m_{H^+} = 140$ GeV, we have $B(t \to bH^+) \simeq 0.01$ and $\simeq 0.1$ for $\tan\beta = 6$ and 30, respectively. The quantum corrections to (3.16) within the MSSM are also known [74]. The corrections depend strongly on the parameters of the model; they can be large, especially for $\tan\beta \gg 1$ [75]. Values of $\tan\beta \lesssim 1-3$ are not tolerable within the MSSM, because this would push the mass of the lightest neutral Higgs boson of this model below its present experimental lower bound [19]. Moreover, values of $\tan\beta \gtrsim O(m_t/m_b) \sim 50$ are both theoretically and experimentally disfavored.
The main two-body decays of a charged Higgs boson with mass $79\,\text{GeV} < m_{H^+} < m_t$ are $H^\pm \to \tau\nu_\tau$, cs, cb. The tree-level partial widths are given by

$$\Gamma^B(H^+ \to f_u \bar{f}_d) = N_c \frac{G_F}{4\pi\sqrt{2}} m_{H^+} |V_{f_u f_d}|^2 \left(m_{f_d}^2 \tan^2\beta + m_{f_u}^2 \cot^2\beta\right). \tag{3.17}$$

Here $f_u\bar{f}_d = c\bar{s}, c\bar{b}, \nu_\tau\tau^+$, $N_c = 3\,(1)$ for quarks (leptons), and the CKM matrix elements involved are $|V_{cs}| \simeq 0.96$ and $|V_{cb}| \simeq 4 \times 10^{-2}$. In (3.17) the fermion masses were again neglected in the phase space function, but not in the couplings to H^+. Thus for $\tan\beta > 1$, $H^\pm \to \tau\nu_\tau$ is the dominant channel; we have $B(H^+ \to \tau^+\nu_\tau)/B(H^+ \to c\bar{s}) > 10$ for $\tan\beta > 2$, and $B(H^+ \to c\bar{b})/B(H^+ \to c\bar{s}) > 1$ for $\tan\beta \gtrsim 2.6$. For $m_{H^+} > 130$ GeV the decay $H^+ \to W^+ b\bar{b}$ (via a virtual t quark) becomes also relevant. Therefore, one expects the appearance of the decay modes

$$t \to bH^+ \to b\tau\nu_\tau,\ bc\bar{s},\ cb\bar{b},\ W^+ b\bar{b}, \tag{3.18}$$

with branching ratios being considerably larger than the respective SM predictions.
The existence of a charged Higgs boson would not significantly change the total $t\bar{t}$ or single-top cross sections at the Tevatron and LHC. Instead one searches for the appearance

of any of the signatures from $t \to H^{\pm} b$ decay just mentioned – i.e., for violations of the (CKM modified) universality of the charged weak current interactions which is reflected in the SM predictions for the branching ratios into the different dilepton, single-lepton, and all-jets final states from $t\bar{t}$ decay. At the LHC such investigations should also be possible for single top production and decay.

Searches by the D0 and CDF experiments [76–78] for $t \to H^{+} b$ in $t\bar{t}$ events at the Tevatron were negative so far. Resulting exclusion limits on the mass of $H^{\pm}$ and its couplings to fermions are model-dependent. Analyses are mostly done within the framework of the MSSM, assuming the appearance of the above-mentioned final states from top decay. Exclusion limits in the $\tan\beta$, m_{H^+} plane ($m_{H^+} < m_t$) are given in [77]. Assuming that $H^{\pm}$ decays exclusively to $\tau\nu_\tau$ then $B(t \to H^{+} b) < 0.4$ at 95% C.L. [77].

The discovery potential of the LHC for this top-quark decay mode has been investigated in simulation studies both by the ATLAS and CMS collaborations, considering $t\bar{t} \to H^{\pm} W^{\mp} b\bar{b}$ events with decays $W \to \ell\nu_\ell$ ($\ell = e, \mu$), $H^{\pm} \to \tau\nu_\tau$ [23], and also $H^{\pm} \to cs$ [79]. These studies indicate that almost all of the region in the $\tan\beta$, m_{H^+} plane ($m_{H^+} < m_t$) not yet excluded so far can be covered by the LHC.

For the decay of polarized top quarks $t \to H^{+} b$ the angular distribution $\Gamma_H^{-1} \mathrm{d}\Gamma_H / \mathrm{d}\cos\theta_H$ is of the form (3.11), where θ_H is the angle between the top-spin vector and the H^+ direction of flight in the t rest frame. For m_{H^+} not too close to m_t, the correlation coefficient c_{H^+} is given in type II 2HDM to good approximation by

$$c_{H^+} = \frac{1 - (m_b/m_t)^2 \tan^4\beta}{1 + (m_b/m_t)^2 \tan^4\beta} \,. \tag{3.19}$$

The $\mathrm{O}(\alpha_s)$ corrections to (3.19) are also known [80]. For the corresponding b-jet angular distribution we have $c_b = -c_{H^+}$. The observation of this decay mode and the measurement of these distributions would allow the determination of the parameter $\tan\beta$.

3.2.3. Decays into supersymmetric particles:

In the MSSM the lightest neutralino ($\tilde{\chi}_1^0$) is likely to be the lightest supersymmetric particle, which is stable and is a candidate for the non-baryonic dark matter of the universe. The reason for the lightest supersymmetric particle being stable in the MSSM is R-parity conservation. The model is constructed such that a discrete symmetry, R parity, is conserved in any reaction. Each particle is assigned the quantum number $R \equiv (-1)^{3B+L+2S}$, where B, L, S denotes baryon number, lepton number, and spin, respectively – i.e., $R = 1$ for the known particles and the Higgs bosons, and $R = -1$ for their superpartners.

Moreover, one of the two spin-zero superpartners $\tilde{t}_{1,2}$ of the top quark – $\tilde{t}_1$ by convention – may also be relatively light. This is because quantum corrections involving the large top mass lead to a large splitting of the masses of $\tilde{t}_1$ and $\tilde{t}_2$ [81]. The non-observation of top-squark pair production at the LEP2 collider yields the (almost model-independent) lower bound of about 90 GeV on the masses of these squarks [19].

If $m_t > m_{\tilde{\chi}_1^0} + m_{\tilde{t}_1}$ then the top quark can have the new decay mode

$$t \to \tilde{t}_1 \tilde{\chi}_1^0 \,. \tag{3.20}$$

A priori, this tree-level process can have a rather large branching ratio. The subsequent decay channels of $\tilde{t}_1$ depend on the masses and couplings of the supersymmetric particles. 1a) If the lightest chargino $\tilde{\chi}_1^+$ is the second lightest supersymmetric particle and its mass satisfies $m_{\tilde{\chi}_1^+} < m_{\tilde{t}_1} - m_b$ then the tree-level decay $\tilde{t}_1 \to b\tilde{\chi}_1^+$ dominates, and $\tilde{\chi}_1^+$ decays via $\tilde{\chi}_1^+ \to \tilde{\chi}_1^0 \ell^+ \nu_\ell$ and $\tilde{\chi}_1^+ \to \tilde{\chi}_1^0 q\bar{q}'$. Thus we have a new set of final states in top-quark decay, $t \to b f \bar{f}' \tilde{\chi}_1^0 \tilde{\chi}_1^0$. In this case hadronic $t\bar{t}$ production, with one top quark decaying into Wb, leads to the new final states

$$t\bar{t} \to W^+ b \bar{b} q \bar{q}' \tilde{\chi}_1^0 \tilde{\chi}_1^0, \quad W^+ b \bar{b} \ell^- \bar{\nu}_\ell \tilde{\chi}_1^0 \tilde{\chi}_1^0 \tag{3.21}$$

plus the charge-conjugated channels, with the two neutralinos escaping undetected.
1b) If $m_{\tilde{\chi}_1^+} > m_{\tilde{t}_1} - m_b$, the chargino is virtual and $\tilde{t}_1$ will decay primarily via the three-body decays $\tilde{t}_1 \to W^+ b \tilde{\chi}_1^0$, $H^+ b \tilde{\chi}_1^0$, and $\tilde{t}_1 \to b\ell^+ \tilde{\nu}_\ell$, $b\tilde{\ell}^+ \nu_\ell$ [82–84], provided the sleptons $\tilde{\nu}_\ell$, $\tilde{\ell}$ and the charged Higgs boson H^+ are light enough. In this case we have, for instance,

$$t\bar{t} \to W^+ b W^- \bar{b} \tilde{\chi}_1^0 \tilde{\chi}_1^0, \quad W^+ b \bar{b} \ell^- \tilde{\nu}_\ell \tilde{\chi}_1^0 . \tag{3.22}$$

2) If the both the lightest chargino $\tilde{\chi}_1^\pm$ and the scalar leptons are heavier than $\tilde{t}_1$, the following situations can arise, depending on the parameters of the model. a) The dominant decay of $\tilde{t}_1$ is $\tilde{t}_1 \to c\tilde{\chi}_1^0$, a process induced at one-loop [82]. In this case, hadronic $t\bar{t}$ production yields the final state

$$t\bar{t} \to W^+ b \bar{c} \tilde{\chi}_1^0 \tilde{\chi}_1^0 \tag{3.23}$$

plus the charge-conjugated channel. The signature of the decay $t \to c\tilde{\chi}_1^0 \tilde{\chi}_1^0$ is similar to the flavour-changing neutral current decay mode $t \to cZ \to c\nu\bar{\nu}$ which will be discussed in section 3.2.4. b) Actually in this kinematic situation, the four-body decay modes $\tilde{t}_1 \to b\tilde{\chi}_1^0 f \bar{f}'$ can have larger rates than $\tilde{t}_1 \to c\tilde{\chi}_1^0$ in a wide range of the MSSM parameter space [85]. In this case the final states from top-decay are identical to those in 1a) and to a subset of 1b), and the final states from $t\bar{t}$ decay are identical to those in (3.21) and to the first set in (3.22).
The signals associated with the final states (3.21) and (3.22) – charged leptons (if $W \to \ell\nu_\ell$), two or four jets including two b jets, and substantial missing transverse energy/momentum – are identical to those from SM $t\bar{t}$ dilepton and single lepton decays (see section 4). However, the transverse momentum and angular distributions differ. The CDF experiment has searched for events of this type at the Tevatron, with no evidence found [86].
The signal (3.23) in the alternative scenario for $\tilde{t}_1$ decay consists of an isolated high-p_T lepton (if $W \to \ell\nu_\ell$), a b and c jet, and substantial missing transverse energy/momentum. Background is mainly due to the production of W plus jet events. The conclusion of [87] is that experiments at the Tevatron should eventually either discover the decay $t \to \tilde{t}_1 \tilde{\chi}_1^0$ in the channel (3.23) or place an upper bound of about 1% on its branching ratio. Analyses should account for the possibility that hadronic production of supersymmetric particles can increase the number of top and stop events. For instance, a gluino $\tilde{g}$ being lighter than the non-top squarks would decay into $\tilde{g} \to t\tilde{t}_1^*, \bar{t}\tilde{t}_1$ if $m_{\tilde{g}} > m_t + m_{\tilde{t}_1}$ [83].

In addition, experiments at the Tevatron have explored the possibility of top-squark pair production in $q\bar{q}$ annihilation and gluon fusion, $q\bar{q}, gg \to \tilde{t}_1\tilde{t}_1^*$. The search in [88, 89] was conducted under the assumption that both $\tilde{t}_1$ decay to $\tilde{t}_1 \to b\ell^+\tilde{\nu}_\ell$. Searches for signatures of three- and four-body decays of top squarks and of both top squarks decaying to $c\tilde{\chi}_1^0$ were made in [90] and [91–93], respectively. All these searches were negative and have excluded substantial parts of the kinematically accessible regions in the $m_{\tilde{t}_1}, m_{\tilde{\nu}}$ and $m_{\tilde{t}_1}, m_{\tilde{\chi}_1^0}$ planes.

Experiments at the Tevatron should be able to answer whether or not i) a top squark lighter than the top quark exists and ii) the decay (3.20) exists with a branching fraction $\gtrsim 1\%$. In any case, these questions will eventually be clarified at the LHC.

The answer to question i) is of great interest to cosmology. Among the scenarios that try to explain the observed matter-antimatter asymmetry of the universe, there is an attractive (viz. testable) class that relates the generation of this asymmetry to the electroweak phase transition in the early universe (which happens at a temperature $T \sim 100$ GeV). These electroweak baryogenesis scenarios require this phase transition to cause a thermal non-equilibrium situation, i.e., to be of first order. This is excluded within the SM, but is possible for instance within the MSSM if $m_{\tilde{t}_1} < m_t$ (see, e.g., [94]).

3.2.4. Flavour-changing neutral current (FCNC) decays:

In the SM FCNC decays are induced by quantum corrections (at the one-loop level) and are governed by the Glashow-Iliopoulos-Maiani (GIM) mechanism [95]. The transitions $t \to c$ and $t \to u$ are severely suppressed, because the rates are determined, apart from the CKM matrix elements, by the differences of the squared masses of the b, s, d quarks which are very small compared to m_t^2. This leads to tiny branching ratios [96–98] that are many orders of magnitude below the detection limits of the LHC [23, 99].

In a number of SM extensions the branching ratios of these decays can be be significantly enhanced. Supersymmetric extensions contain new flavour-violating interactions involving supersymmetric particles. As a consequence, GIM suppression of the $t \to c, u$ transitions may be overcome to a large extent in these models. Type-III 2-Higgs doublet extensions of the SM (see section 3.2.2) allow for tree-level FCNC couplings of neutral Higgs bosons to quarks which are, as far as $t \to c$ transitions are concerned, not yet severely constrained. Tree-level FCNC quark couplings of the Z boson are present in models with exotic quarks, for instance extra heavy quarks being $SU(2)_L$ singlets. Sizeable $t \to c$ transitions naturally appear in models of dynamical electroweak symmetry breaking, where the top quark plays a special role [100, 101].

For the decay modes $t \to cX^0$ ($X^0 = \gamma, Z, g, h$) the order of magnitude of the maximally possible values of the branching ratios B are collected in table 5, where h denotes either the SM Higgs boson or a light Higgs boson in one of the above-mentioned SM extensions (assuming $m_h \sim 120$ GeV). Constraints from low-energy data were taken into account. The SM values are from [102], for predictions in type-III 2HDM, in the MSSM and in R-parity violating ($\not{R}$) SUSY models see [103, 104], [105–109], and [110, 111], respectively. Topcolour-assisted technicolour models allow for $B(t \to cZ) \sim 10^{-5}$ [112]. In models

with exotic quarks, for instance extra heavy quarks of charge $Q = 2/3$ being $SU(2)_L$ singlets, $B(t \to qZ)$ may be as large as 10^{-4} [113]. As to the expectations for the transitions $t \to u$: in the SM they are even smaller than $t \to c$, as they are CKM-suppressed with respect to this mode. This is not the case in the MSSM and in $\not{R}$ SUSY: in these models $B(t \to cX^0) \simeq B(t \to cX^0)$. If kinematically possible, the decay mode $t \to c$ + sneutrino can have a branching $B \sim 10^{-5}$ in $\not{R}$ SUSY models [114].

Table 5: Branching ratios B of some FCNC top quark decay modes, $t \to cX^0$, in the SM and several of its extensions. Expected sensitivities at the LHC are for a signal at the 5σ level and 100fb^{-1} integrated luminosity.

Decay mode	SM	type-III 2HDM	MSSM	$\not{R}$ SUSY	LHC sensitivity
$t \to c\,\gamma$	$\sim 5 \times 10^{-14}$	$\sim 10^{-6}$	$\sim 5 \times 10^{-7}$	$\sim 10^{-6}$	2×10^{-4}
$t \to c\,Z$	$\sim 10^{-14}$	$\sim 10^{-7}$	$\sim 10^{-6}$	$\sim 3 \times 10^{-5}$	3×10^{-4}
$t \to c\,g$	$\sim 5 \times 10^{-12}$	$\sim 10^{-4}$	$\sim 3 \times 10^{-5}$	$\sim 10^{-4}$	2×10^{-3}
$t \to c\,h$	$\sim 3 \times 10^{-15}$	$\sim 10^{-3}$	$\sim 6 \times 10^{-5}$	$\sim 10^{-5}$	

So far, the experimental limits on the strength of possible FCNC transitions of the top quark are not extremely tight [19, 115–118]. The presently most precise experimental upper bound on FCNC top decays to a Z boson was recently obtained by the CDF experiment, $B(t \to Zq) < 3.7\%$ [119]. At the LHC FCNC transitions can be searched for in (single) top production, which is sensitive to anomalous gqt couplings (see section 5.4), and in top-decays, e.g., in $t\bar{t}$ events where one top quark decays via the Wb decay mode and the other one into cX^0 or uX^0. The best identification will be reached for $t \to q\gamma$ and $t \to qZ \to q\ell^+\ell^-$. Simulation studies were made by the D0 and the ATLAS collaboration [23, 99]. Resulting estimates are given in table 5 for the minimum size of the respective branching ratio allowing a discovery at the LHC with $100\,\text{fb}^{-1}$ integrated luminosity.

4. Top-quark pair production

The main physics goal associated with $t\bar{t}$ events at the Tevatron, and even more so at the LHC, is the detailed investigation of the top-quark pair production and top-quark decay dynamics. Besides the determination of the top-mass, key measurements at the LHC will include the total cross section and differential distributions. Specifically, top-spin effects, which offer additional means to explore the interactions of these quarks, will also be measurable. The LHC provides also the opportunity to dramatically extend the search for heavy resonances (which may or may not be associated with electroweak symmetry breaking) that strongly couple to $t\bar{t}$ pairs.

At the Tevatron, and according to the SM also at the LHC, $t\bar{t}$ pairs are produced by the strong interactions. The main partonic subprocesses are quark-antiquark annihilation, $q\bar{q} \to t\bar{t}$, which dominates at the Tevatron, and gluon-gluon fusion, $gg \to t\bar{t}$, which makes up most of the $t\bar{t}$ cross section at the LHC. As discussed in section 3 the t and $\bar{t}$ quarks decay almost exclusively into a W boson and a b-jet. The $t\bar{t}$ signals are then classified according to the decays of the W^+W^- bosons from $t\bar{t} \to bW^+\bar{b}W^-$ as dilepton, lepton + jets, and fully hadronic decay channels.

$$p\bar{p}, pp \to t\bar{t}X \to \begin{cases} \ell^+ + \ell'^- + j_b + j_{\bar{b}} + p_T^{miss} + n \geq 0 \text{ jets}, \\ \ell^\pm + j_b + j_{\bar{b}} + p_T^{miss} + n \geq 2 \text{ jets}, \\ j_b + j_{\bar{b}} + n \geq 4 \text{ jets}. \end{cases} \tag{4.1}$$

From (3.6) we obtain a branching fraction of 10.5%, 43.5%, and 45.5% for the dilepton, lepton + jets, and all jets modes, respectively. Many top-physics analyses (will) use dilepton and lepton + jets final states with $\ell = e, \mu$ only. In this case the respective branching ratios are 4.7%, 29%, and 45.5%.

All the channels (4.1) were observed and analyzed at the Tevatron (see [6–8] for reviews). Detailed simulation studies were made for the LHC by the ATLAS [79, 120] and, more recently, by the CMS collaboration [23].

The cleanest signals for $t\bar{t}$ production are provided by the dilepton and the lepton + jets channels. The signature for the $\ell\ell$ channel consists of two high p_T, isolated, and oppositely charged leptons, large missing transverse energy/momentum, and at least two jets which originate from b quarks. The main background reactions with final states that can mimic the signal are the production of Z + jets, VV + jets ($V = W, Z$), $\ell + 4j$, and fully hadronic $t\bar{t}$ channels. After setting appropriate selection criteria including the requirement of b-tagging, a signal-to-background ratio $S/B = 12$ and a selection efficiency $\varepsilon \simeq 5\%$ was estimated [23] for the $\ell\ell$ channel at the LHC.

The signature for the ℓ + jets channel consists of an isolated, high p_T charged lepton, large missing transverse energy/momentum, and at least four jets, two of which originate from b quarks. The main backgrounds come from the production of $Wb\bar{b}$ + 2 jets, W + 4 jets, and from the other $t\bar{t}$ channels. For the ℓ + jets channel very pure samples should be obtained at the LHC ($S/B \simeq 27$ and $\varepsilon \simeq 6.3\%$ [23]). In this channel the complete final state can be reconstructed (up to a two-fold ambiguity which results from the solution of a quadratic equation) by solving kinematic equations, assuming that $E_T^{\text{miss}} = E_T^{\nu}$.

The fully hadronic channel has at least 6 jets in the final state. It has the largest branching ratio of the three modes (4.1), and the event kinematics can be fully reconstructed. However, this channel is polluted by a large QCD multijet background. Requiring b-tagging and requiring the signal events to contain rather high p_T, the simulation study [120] obtained a ratio $S/B = 1/9$ and a selection efficiency $\varepsilon \simeq 2.7\%$ for the low-luminosity phase of the LHC. A similar result was reached in [23].

In view of the rather large $t\bar{t}$ cross section and the distinct signatures of the dilepton and lepton + jets channels, these modes are perfect physics events to analyze during the first data taking phase of the LHC detectors (with a few hundred pb^{-1} of integrated luminosity). In this phase the focus will be on detector issues such as measuring the factors that

determine the calibration of the jet-energy scale, and measuring the b-tagging efficiency. As far as top quark physics is concerned, first measurements will include the $t\bar{t}$ cross section in the various channels and the determination of the top mass [121].
In the "discovery phase" of the LHC millions of $t\bar{t}$ pairs will be produced already with $10\,\mathrm{fb}^{-1}$ of integrated luminosity (c.f. table 1). For most top-quark observables, statistical uncertainties will then be below the percent level; i.e., the measurements will eventually be systematics dominated.
In the following subsections we shall discuss $t\bar{t}$ production mostly from the perspective of considering the top quark to be a signal. Production of $t\bar{t}$ pairs is, on the other hand, also an important background to the search for new particles, including the searches for the SM and/or non-standard Higgs bosons and for signals of supersymmetry. Obviously, both roles the top quark plays at the Tevatron and at the LHC require accurate predictions of $t\bar{t}$ production and decay.

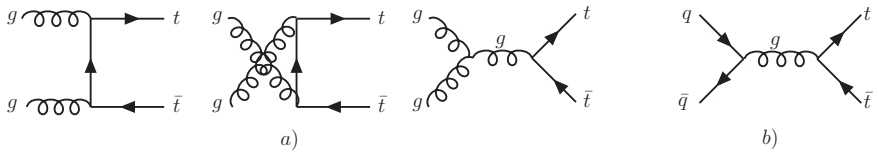

Figure 2: Lowest order Feynman diagrams for $t\bar{t}$ production by the strong interactions: $gg \to t\bar{t}$ (a) and $q\bar{q} \to t\bar{t}$ (b).

4.1. Status of theory

Because $m_t \gg \Lambda_{QCD}$, top-quark production and decay processes are hard scattering reactions which can be computed in (QCD) perturbation theory. The $t\bar{t}$ production processes are depicted to lowest-order QCD in figure 2. At next-to-leading order (NLO) in the QCD coupling α_s, also qg and $\bar{q}g$ scatterings produce $t\bar{t}$ pairs. To arbitrary order in QCD perturbation theory, the total $t\bar{t}$ cross section for

$$p\bar{p}, pp \to t\bar{t} + X \tag{4.2}$$

is given as a convolution of the cross sections for the partonic subprocesses and the parton distribution functions (PDF) – up to terms which are suppressed with some power of the hadronic center-of-mass energy $\sqrt{s}$ (so-called higher twist terms):

$$\sigma^{t\bar{t}}_{h_1 h_2}(s, m_t) = \sum_{i,j} \int_0^1 \mathrm{d}x_1 \mathrm{d}x_2 \, f_i^{h_1}(x_1, \mu_F) \, f_j^{h_2}(x_2, \mu_F) \, \hat{\sigma}_{ij}(\hat{s}, m_t, \alpha_s(\mu_R), \mu_R, \mu_F) \,. \tag{4.3}$$

Here $i, j = g, q, \bar{q}$, and $h_1, h_2 = p, \bar{p}$. The PDF $f_i^h(x, \mu_F)$ is the probability density of finding parton i with longitudinal momentum fraction x in hadron h at the factorization scale μ_F. This scale, which is arbitrary in principle, is usually set equal to a typical scale of the problem, e.g. m_t, in order to avoid large logarithms in perturbation theory. The

cross section of a partonic subprocess is denoted by $\hat{\sigma}_{ij}$, $\hat{s} = x_1 x_2 s$ is the square of the partonic center-of-mass energy, and μ_R denotes the renormalization scale. This scale is also arbitrary and need not be the same as μ_F; but again one should take it to be of the order of a typical energy scale of the partonic processes in order not to generate large logarithms. The hadronic cross section must not – as an observable – depend on the choice of μ_R and μ_F – but computed in fixed-order perturbation theory, it does. The dependence of a hadronic observable O_H on μ_R and μ_F decreases with increasing order of the perturbation series. Often one varies μ_R and μ_F in some range and takes the resulting spread in the value of O_H – for no deeper reason – as an estimate of the theoretical error, i.e., of the size of the uncalculated higher-order perturbative contributions. In higher-order QCD the total cross section should be calculated in terms of a short-distance mass parameter, e.g. the $\overline{\rm MS}$ mass $\overline{m}_t$ rather than the pole mass m_t. (Recall that in lowest-order perturbation theory the mass parameter is not yet specified.)
Formula 4.3 applies also when electroweak (and non-SM) interactions are taken into account. Analogous formulae hold for differential distributions, like the p_T distributions of the t and $\bar{t}$ quarks or the $t\bar{t}$ invariant-mass distribution. Unlike the total cross section, differential distributions often involve more than one typical scale. For instance, if $p_T, M_{t\bar{t}} \gg m_t$, the choice of μ_R and μ_F requires more scrutiny. Moreover, for adequate predictions, top-quark decay must also be taken into account in the computation of $\mathrm{d}\hat{\sigma}_{ij}$.

4.1.1. SM results:

Quite a number of theoretical investigations have been made on hadronic $t\bar{t}$ production. The results which were obtained to higher orders in the SM couplings may be classified as follows.
1) Predictions for on-shell $t\bar{t}$ states, summed over their spins:

- NLO QCD corrections ($\mathrm{O}(\alpha_s^3)$) for the total cross section [122,123], p_T and rapidity distributions [124, 125], and double-differential spectra including the $t\bar{t}$ invariant-mass distribution and azimuthal correlations [126, 127]. The cross section and single particle distributions such as p_T and rapidity distributions are insensitive to the t and $\bar{t}$ spin degrees of freedom, and it is acceptable to calculate these quantities for on-shell stable top quarks.

- Threshold resummations: The NLO QCD differential cross sections $\mathrm{d}\hat{\sigma}_{ij}$ of the hard scattering subprocesses contain logarithms that become large near threshold. Here 'threshold' refers not only to the $t\bar{t}$ production threshold, but more generally to the boundary of phase space where $M_{t\bar{t}}/\hat{s}$ becomes equal to 1. These threshold logarithms can be summed [128, 129]. This has been done, in various approaches, for the total cross section [130–133] and for the p_T distributions [133, 134].

- Mixed electroweak-QCD corrections ($\mathrm{O}(\alpha_s^2\alpha)$): The weak corrections (W, Z, and Higgs boson exchange) were first computed in [135], and later in a more complete fashion for $q\bar{q} \to t\bar{t}$ [136, 137, 139], $gg \to t\bar{t}$ [138, 140, 141], and $gq(\bar{q}) \to t\bar{t}q(\bar{q})$ [138, 139]. The photonic corrections were determined by [142]. Here partonic

$t\bar{t}$ production processes involving an initial-state photon appear, the most important one being $\gamma g \to t\bar{t}$. The $O(\alpha_s^2\alpha)$ contributions to the $t\bar{t}$ cross section are smaller than the present QCD uncertainties, but these corrections are relevant for distributions, especially in the high-energy regime (see section 4.4).

- $t\bar{t}$ + jet production: The NLO QCD corrections ($O(\alpha_s^4)$) to the cross section of this process were computed in [143]. It is important to know these corrections, as $t\bar{t}$ plus one hard jet constitutes a significant fraction of the inclusive $t\bar{t}$ sample. Moreover, this process is an important background for Higgs boson searches at the LHC.

2) For on-shell $t\bar{t}$ states, with t and $\bar{t}$ spin degrees of freedom fully taken into account, the differential cross sections for $t\bar{t}$ production by $gg, q\bar{q}, gq\,(\bar{q})$ initial states were determined to NLO QCD [144, 145]. The mixed weak-QCD corrections were also computed [136, 138]. These results allow for predictions of distributions induced by top-spin effects (see section 4.5).
3) For off-shell t and $\bar{t}$ intermediate states, the non-factorizable QCD corrections of $O(\alpha_s^3)$ are known [146, 147] – see below.
The physics effects of these corrections will be discussed in the following subsections. In addition to the above list, results were published [148, 149] for the two-loop virtual QCD corrections for $q\bar{q}, gg \to t\bar{t}$: these corrections were determined by [148, 149] in the kinematic limit where all Mandelstam invariants are much larger than m_t^2. Recently, the two-loop QCD corrections to $q\bar{q} \to t\bar{t}$ were computed in the whole kinematic regime [150]. These are ingredients required for a computation of the inclusive $t\bar{t}$ cross section to $O(\alpha_s^4)$ (c.f. also [151]). Such a computation requires, in addition, an efficient method to handle the soft and collinear singularities to NNLO QCD associated with real radiation.
In the remainder of this subsection we have a closer look at $t\bar{t}$ production and decay at NLO QCD. This involves the following $2 \to 6$ and $2 \to 7$ parton reactions:

$$q\bar{q} \xrightarrow{t\bar{t}} b + \bar{b} + 4\ f\ (+g), \tag{4.4}$$

$$gg \xrightarrow{t\bar{t}} b + \bar{b} + 4\ f\ (+g), \tag{4.5}$$

$$g\,q \xrightarrow{t\bar{t}} b + \bar{b} + 4\ f\ + q, \tag{4.6}$$

$$g\,\bar{q} \xrightarrow{t\bar{t}} b + \bar{b} + 4\ f\ + \bar{q}, \tag{4.7}$$

where $f = q, \ell, \nu_\ell$. Because $\Gamma_t \ll m_t$, the $t, \bar{t}$ quarks are narrow resonances. Thus the double pole approximation is appropriate (we consider here top as signal, not as background); i.e., the S matrix elements of the reactions (4.4) - (4.7) (which can proceed through many intermediate states other than $t\bar{t}$) are expanded around their poles in the complex $t, \bar{t}$ energy planes, and only the term $\propto (D_t D_{\bar{t}})^{-1}$ of each matrix element is kept. ($D_t = p_t^2 - m_t^2 + \mathrm{i} m_t \Gamma_t$.)
In the double pole approximation the radiative corrections – both the real and virtual ones – can be classified into factorizable and nonfactorizable corrections. In figure 3 this classification is illustrated for virtual corrections. While in figure 3 (left) the radiative corrections are confined to the $t\bar{t}$ production and/or the t and/or $\bar{t}$ decay parts of the amplitude, the gluon exchange depicted in figure 3 (right) connects the production and decay

parts. This classification applies also to the squared matrix elements $|\mathcal{M}|^2$ of real gluon radiation.

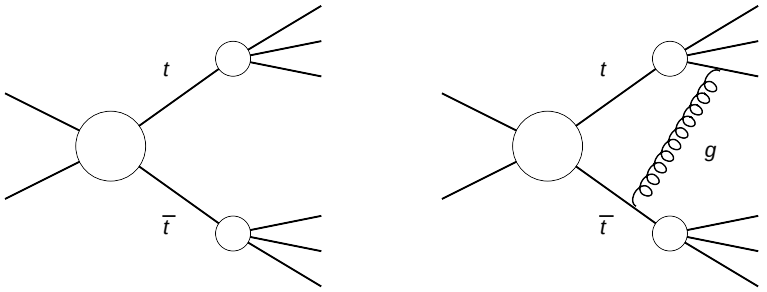

Figure 3: Illustration of factorizable (left) and nonfactorizable (right) virtual QCD corrections.

The differential cross sections for the above parton reactions (4.4) - (4.7) are to $O(\alpha_s^3)$:

$$d\hat{\sigma}_{ij} = d\hat{\sigma}_{ij,B} + d\hat{\sigma}_{ij,fact} + d\hat{\sigma}_{ij,nf}\,, \tag{4.8}$$

where $i,j = q,\bar{q},g$ and $d\hat{\sigma}_{ij,B}$ is the lowest order differential cross section. For $ij = gq, g\bar{q}$ there is only $d\hat{\sigma}_{ij,B}$ to this order in α_s. In computing $d\hat{\sigma}_{ij,fact}$ we may apply the narrow width approximation, $\Gamma_t/m_t \to 0$, for t and $\bar{t}$. This means one neglects terms of order $\alpha_s\Gamma_t/m_t$ with respect to the Born term, which are parametrically smaller than the uncalculated NNLO QCD corrections. Then

$$d\hat{\sigma}_{ij,fact} \propto \mathrm{Tr}\left(R^{(ij)}\rho_{f_1}\bar{\rho}_{\bar{f}_2}\right). \tag{4.9}$$

Here $(R^{(ij)})_{\alpha\alpha',\beta\beta'}$ are the $t\bar{t}$ production density matrices, where $\alpha\alpha'$ and $\beta\beta'$ are the spin labels of the t and $\bar{t}$ quarks, respectively. The density matrices that describe the decays $t \to f_1$ and $\bar{t} \to \bar{f}_2$ are denoted by ρ_{f_1} and $\bar{\rho}_{\bar{f}_2}$, respectively. The trace in (4.9) refers to the t and $\bar{t}$ spin labels. The $R^{(ij)}$ are known to $O(\alpha_s^3)$ and $O(\alpha_s^2\alpha)$ for the initial states $ij = q\bar{q}, gg, gq, g\bar{q}$ and intermediate states $t\bar{t}$ and $t\bar{t}g$ [136, 138, 145]. The NLO decay density matrices can be extracted from the results of [44, 45]; for details, see [145]. The $R^{(ij)}$, ρ_{f_1}, and $\bar{\rho}_{\bar{f}_2}$ serve also as building blocks in the computation of $d\hat{\sigma}_{ij,fact}$ when the intermediate $t,\bar{t}$ quarks are taken to be off-shell (in the double pole approximation).
To order α_s^3, nonfactorizable QCD corrections contribute to the differential cross sections of the reactions (4.4) and (4.5). Figure 3 (right) shows an example of a virtual nonfactorizable correction. The real corrections can be grouped into diagrams where a gluon is radiated from an initial, intermediate, or final state, and the nonfactorizable real corrections arise from the interference of these different classes. The nonfactorizable QCD corrections are dominated by gluon exchange/radiation with energy $E_g \lesssim O(\Gamma_t)$ [146]. (Gluons with energies $E_g \gg \Gamma_t$ drive the intermediate t and/or $\bar{t}$ quark far off-shell, and these contributions to $d\hat{\sigma}_{ij}$ can be neglected.) They contribute, e.g., to $t,\bar{t}$ momentum distributions, and the $t,\bar{t}$, and $t\bar{t}$ invariant mass distributions. However, when computing

observables which are inclusive in both the t and $\bar{t}$ invariant masses, the nonfactorizable QCD corrections of order α_s^3 cancel [146, 152, 153].
Studies where the intermediate t and $\bar{t}$ quarks are non-resonant were made at leading-order by [154, 155]. This is relevant for $t\bar{t}$ as background to new physics searches.

4.1.2. Simulation tools:

A crucial ingredient in analyzing and interpreting experimental data on top-quark production and decay is the accurate modeling of the signal and background events. It must provide a description of events for colour-singlet hadrons, while the perturbative results listed in section 4.1.1 make only predictions at the level of coloured final-state partons. This modeling is done – on the theoretical side – with computer simulation programs, so-called Monte Carlo (MC) generators. These are very complex and sophisticated tools, which we can mention here only in passing. (For an introductory review, see [156].) General purpose programs like PYTHIA [157, 158] or HERWIG [159, 160] not only contain (lowest order) hard scattering parton matrix elements, but simulate also the emission of additional partons from the initial and final-state partons in the hard process (parton showering), and model the formation of hadrons from partons. A number of programs exist that simulate hard hadronic collisions a the level of partonic final states; for a detailed list, see [161]. Tools that include $t\bar{t}$ and single-top production and decay and background processes at tree-level are the program packages TopRex [162], ALPGEN [163], MadGraph/MadEvent [164], and GR@PPA [165]. MC codes which incorporate $t\bar{t}$ and single-top production at NLO QCD are MC@NLO [166], MCFM [167, 168], and POWHEG [169, 170]. For the simulation of single top events at NLO QCD, see also [171]. An important aspect of these codes is the use of a consistent method of interfacing the hard scattering part with a parton shower algorithm in order to avoid double counting. This problem arises when both the hard-scattering and the shower algorithm generate the same final state.
A further important issue in interpreting top-physics data, which is least understood in terms of ab initio calculations, is how the fragments of the (anti)proton that do not take part in the hard scattering process evolve and affect the final states from single top or $t\bar{t}$ decay. Some (long range) interaction between this so-called underlying event and the partons involved in the hard scattering must occur in order to maintain the over-all colour neutrality and the conservation of baryon number. Empirical models are tuned with data on multiple interactions in hadronic collisions [156].

4.2. The total cross section

The basic observable for the reactions (4.2) is the inclusive $t\bar{t}$ cross section. Predictions involve the cross sections $\hat{\sigma}_{ij}$ for the parton processes $ij \to t\bar{t}X$ and the parton luminosities $L_{ij}^{h_1h_2}$. Formula (4.3) can be cast into the form [175]:

$$\sigma_{h_1h_2}^{t\bar{t}}(s, m_t) = \sum_{i,j} \int_{4m_t^2}^{s} \mathrm{d}\hat{s} L_{ij}^{h_1h_2}(s, \hat{s}, \mu_F)\, \hat{\sigma}_{ij}(\hat{s}, m_t, \mu_R, \mu_F)\,, \tag{4.10}$$

where

$$L_{ij}^{h_1 h_2}(s,\hat{s},\mu_F) = \frac{1}{s}\int_{\hat{s}}^{s} \frac{\mathrm{d}s'}{s'} f_i^{h_1}\left(\frac{s'}{s},\mu_F\right) f_j^{h_2}\left(\frac{\hat{s}}{s'},\mu_F\right), \tag{4.11}$$

and $\hat{s} = x_1 x_2 s$.

At the Tevatron the largest parton flux is $L_{q\bar{q}}$, followed by $L_{qg} = L_{g\bar{q}}$, while L_{gg} is the smallest one. On the other hand, $\hat{\sigma}_{qg}$ is much smaller than $\hat{\sigma}_{q\bar{q}}$ and $\hat{\sigma}_{gg}$, as the former is a NLO correction of order α_s^3. Using the PDF sets from the CTEQ [172] or MRST [173,174] collaborations one arrives, to NLO QCD, at the following relative contributions to the $t\bar{t}$ cross section: $\sim 85\%$ $(q\bar{q})$ and $\sim 15\%$ (gg), while the contribution from qg and $g\bar{q}$ initial states is only at the percent level.

At the LHC the qg scattering occurs with the highest parton luminosity, but the overall contribution to the hadronic cross section is again small because of the small partonic cross section compared with $\hat{\sigma}_{gg}$ and $\hat{\sigma}_{q\bar{q}}$. The $\bar{q}g$ contribution, which involves a smaller parton flux than qg scattering, is even further suppressed. At the LHC the most important contribution to σ_{pp}^{tt} comes from gluon-gluon fusion, where a large partonic cross section combines with the second-largest flux, followed by the one from $q\bar{q}$ annihilation. At NLO QCD, the gg and $q\bar{q}$ processes contribute about 90% and 10% to $\sigma_{pp}^{t\bar{t}}$, respectively, while that of the qg channel is at the percent level. One should note that the $t\bar{t}$ cross section calculated to leading-order QCD has large uncertainties and is significantly smaller than σ_{NLO}: the ratio $\sigma_{\mathrm{NLO}}/\sigma_{\mathrm{LO}}$ (computed with NLO and LO PDF sets, respectively) is ~ 1.25 for the Tevatron and ~ 1.5 for the LHC.

Detailed updates of the $t\bar{t}$ cross section at the Tevatron and the LHC at NLO QCD – with threshold resummations included – have recently been made by [175] and by [176]. Uncertainties were taken into account which arise from the choice of μ_R, μ_F and from uncertainties in the PDF sets (which are due to the uncertainties of the experimental data used in the PDF fits). Previous predictions include [131–133, 177].

In [175] also an approximate next-to-next-to-leading order (NNLO) result for the $t\bar{t}$ cross section was derived. The argumentation of [175] yields all powers in $\ln\beta_t$ at two loops (where β_t is the top-quark velocity), the exact NNLO scale dependence, and also the two-loop Coulomb corrections at the $t\bar{t}$ threshold – up to some constants. They can be obtained only by an explicit NNLO computation of the $q\bar{q}$ and gg initiated $t\bar{t}$ cross sections.

Replacing the upper endpoint s in the integral (4.10) by $\hat{s}_{max}$, it is interesting to determine the value of $\hat{s}_{max}$ of the squared parton center-of-mass energy for which the resulting σ saturates the total $t\bar{t}$ cross section to a large fraction, say 80% (95%). At the Tevatron this happens at $\sqrt{\hat{s}} \lesssim 470$ (600) GeV. At the LHC the available phase space is significantly larger and a 80% (95%) saturation occurs at $\sqrt{\hat{s}_{max}} \simeq 600$ (1000) GeV [175].

This means that at the Tevatron most of the $t\bar{t}$ production occurs near threshold. Putting the momentum fractions of the initial-state partons $x_i \simeq x_j = x_{thr}$, one gets $x_{thr} \simeq 2m_t/\sqrt{s} \simeq 0.17$ for the Tevatron. At these values the valence quark PDFs are considerably larger than the gluon density. The latter is rather poorly known in this regime. The near-threshold domination of the cross section at the Tevatron had motivated the application of the threshold resummation methods (see section 4.1.1). The computations of the cross section to fixed order ($\mathrm{O}(\alpha_s^3)$) and with threshold resummation included (properly incorporated in

order to avoid double counting) differ only $\sim 5\%$; but the inclusion of threshold resummation reduces the dependence of the prediction on variations of μ_F and μ_R, which is reassuring. Several approximation schemes have been employed in the evaluation of $\sigma^{t\bar{t}}_{p\bar{p}}(\sqrt{s} = 1.96\,\text{TeV})$. In [175, 176] analyses were made based on the NLO cross section including the resummed leading and next-to-leading threshold logarithms (NLO+NLL approximation). Spreads of $\sigma^{t\bar{t}}_{p\bar{p}}$ are computed which arise from scale variations in the range $m_t/2 \leq \mu_F, \mu_R \leq 2m_t$, and from the use of two recent PDF sets, CTEQ6.5 [179] and MRST-2006 [180], including their uncertainties. The resulting values of the cross section, obtained as a function of m_t, have an uncertainty of about $\pm 12\%$. For instance, for $m_t = 171$ GeV, [176] obtains $\sigma^{t\bar{t}}_{p\bar{p}} = 7.35^{+0.30}_{-0.53}\,(scales)\,^{+0.53}_{-0.36}\,(PDF)$ pb using the CTEQ6.5 set. This is in accord with [175]. Employing the MRST-2006 set results in smaller PDF uncertainties. The use of the approximate NNLO cross section of [175] drastically reduces the uncertainty due to scale variations, and results in an estimated total uncertainty for $\sigma^{t\bar{t}}_{p\bar{p}}$ of $\pm 8\%$ (CTEQ6.5) and $\pm 6\%$ (MRST-2006) [175].

The cross section decreases with increasing m_t; the change is approximately given by $\Delta\sigma/\sigma \approx -5\Delta m_t/m_t$ [178].

At the Tevatron the CDF and D0 collaborations have measured the $t\bar{t}$ cross section in the channels (4.1) with several methods (see [29, 181, 182] and references therein, and [28] for a recent overview). The combination of the CDF results as of summer 2007 yields $\sigma^{t\bar{t}}_{p\bar{p}} = 7.3 \pm 0.5(stat.) \pm 0.6(syst.) \pm 0.4(lumi.)$ pb [28]. From a recent combined measurement of the cross section and the ratio R defined in (3.2), D0 obtained $\sigma^{t\bar{t}}_{p\bar{p}} = 8.18^{+0.90}_{-0.84}(stat. + syst.) \pm 0.50(lumi.)$ pb [29]. The SM predictions cited above are in agreement with these values.

As discussed above, most of the $t\bar{t}$ cross section at the LHC comes from gg fusion, and a simple kinematic consideration as done above shows that $\sigma^{t\bar{t}}_{\text{LHC}}$ probes the gluon density in a regime where it is quite well known ($x \sim x_{thr} \sim 0.025$). The cross section shown in figure 4 exhibits the computation of [175] based on the NLO+NLL approximation. The range of $\sigma^{t\bar{t}}_{\text{LHC}}$ is plotted as a function of m_t, where scale and PDF uncertainties are added linearly. For a given m_t the uncertainty of $\sigma^{t\bar{t}}_{\text{LHC}}$ with respect to its central value is about $\pm 15\%$ and is dominated by the scale uncertainty. The figure shows that $\Delta\sigma/\sigma \approx -5\Delta m_t/m_t$ holds also at the LHC. The results obtained in [176] have slightly smaller errors. Again, the approximate NNLO calculation of $\sigma^{t\bar{t}}_{\text{LHC}}$ by [175] drastically reduces the scale uncertainites, and results in an estimated total uncertainty for $\sigma^{t\bar{t}}_{LHC}$ of $\pm 6\%$ (CTEQ6.5) and $\pm 4\%$ (MRST-2006). While it is gratifying that this calculation is in accord with the NLO+NLL approximation of figure 4, it is – needless to say – no substitute[10] for an complete NNLO computation of $\sigma^{t\bar{t}}$.

The weak [138, 140] and electromagnetic [142] corrections of $O(\alpha_s^2\alpha)$ are, as far as the total cross section is concerned, smaller than the uncertainties of the present QCD predictions. With respect to the NLO QCD cross section, the weak and photonic contributions amount to a correction of about 0.5% and -1.4% for the Tevatron and about -1% and 0.5% for the LHC, respectively.

[10] The recent suggestion [183] to use top-quark pair production at the LHC as an additional calibration process for the parton luminosities requires a rather precise prediction of $\sigma^{t\bar{t}}$.

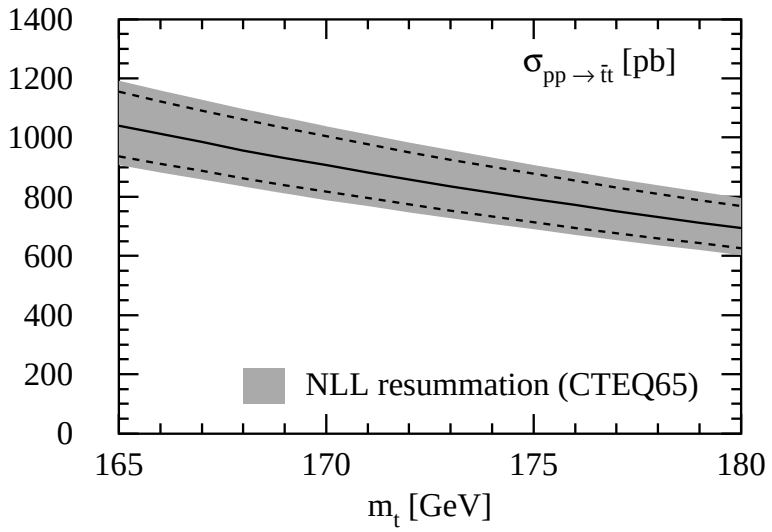

Figure 4: The total $t\bar{t}$ cross section at the LHC ($\sqrt{s} = 14$ TeV) resummed to NLL accuracy in QCD as a function of m_t [175]. The solid line is the central value for $\mu = m_t$, the dashed lower and upper lines correspond to $\mu = 2m_t$ and $\mu = m_t/2$, respectively. The shaded band denotes the range with the PDF uncertainty of the CTEQ6.5 set [179] included.

With which precision will the $t\bar{t}$ cross section be measurable at the LHC? Simulation studies were made by the ATLAS [79] and the CMS collaboration [23]. The lepton + jets and the dilepton channels (4.1) offer measurements with the smallest systematic uncertainties. The analysis [23] concludes that $\Delta\sigma/\sigma = 10.5\%\,(syst.) \pm 0.6\%\,(stat.) \pm 3\%\,(lumi.)$ and $\Delta\sigma/\sigma = 11\%\,(syst.) \pm 0.9\%\,(stat.) \pm 3\%\,(lumi.)$ are possible for the lepton + jets (with 5 fb^{-1} of integrated luminosity) and dilepton channels (with 10 fb^{-1}), respectively ($\ell = e, \mu$). The cross section measurement in the fully hadronic channel has an estimated systematic uncertainty of 20%.
One may optimistically expect that a measurement of $\sigma^{t\bar{t}}_{\rm LHC}$ will eventually be achievable with a total relative error between 5% and 10%. This goal necessitates and motivates improvements in the theory of the inclusive hadronic $t\bar{t}$ cross section.

4.3. Determination of the top-quark mass

As discussed in section 2.1 the top-quark mass is a key parameter of the SM, but also of many of its extensions, and should therefore be determined as precisely as possible. It is, like any other quark mass, a convention-dependent quantity. Distinguishing between differently defined top-mass parameters requires the computation of observables (which depend on this parameter) beyond the tree-level in a specific renormalization scheme. The $t\bar{t}$ cross section discussed above is such an observable. As we have seen, its sensitivity to the top-quark mass is rather good; we have $\Delta\sigma/\sigma \simeq -5\Delta m_t/m_t$ both for the the Tevatron and the LHC. One may eventually compute the hadronic $t\bar{t}$ cross section to higher-order QCD in terms of a well-defined short-distance mass, for instance the running

$\overline{\rm MS}$ mass $\overline{m}_t(\mu_R)$, rather than in terms of the (ambiguous) pole mass m_t. Comparison of the measured cross section with $\sigma^{t\bar{t}}_{h_1h_2}(s,\alpha_s,\overline{m}_t)$ for a specified value of μ_R, the running mass $\overline{m}_t(\mu_R)$. The present and expected experimental uncertainties at the Tevatron and the LHC, respectively, and the ones on the theory side preclude for the time being a precise determination of $\overline{m}_t(\mu_R)$ in this way. In any case, it allows, at some level of precision, to cross-check mass determinations that use other techniques (see below). In fact, in a recent determination of m_t in the dilepton channel by the CDF collaboration at the Tevatron, the dependence of $\sigma^{t\bar{t}}$ on m_t was combined with the top mass determination from event kinematics [184].

As an aside we recall the well-known result, based on many studies [185], that the top-quark mass could be determined with unprecedented precision by a counting experiment at a future linear e^+e^- collider. A scan of the cross section through the $t\bar{t}$ production threshold and a fit of the resulting line-shape to the theoretical predictions for $\sigma_{e^+e^-\to t\bar{t}}(s)$, which can be made in terms of well-defined short-distance masses[11] (c.f., e.g., [186]), would yield the $\overline{\rm MS}$ mass with an overall error of $\delta\overline{m}_t \simeq 150$ MeV.

Determination of the top mass at hadron colliders use the kinematic reconstruction of the events. A measure of the top mass is the invariant mass $M_t = [(\sum_i p_i)^2]^{1/2}$ of the top-quark decay products. However, the peak M_t^* of the invariant mass distribution cannot be equal to m_t, as this parameter is associated with a coloured object, while the measured M_t distribution involves leptons and hadrons which are colour singlets. In the "partonic phase" of the $t\bar{t}$ event, many additional partons are present and at least one antiquark $\bar{q}$ must combine with the partons from top-decay to form colour-singlet states. Colour exchange occurs between the various stages of the hard scattering event and between the final-state partons from this event and the underlying event (see sections 4.1.1 and 4.1.2). When computing $\mathrm{d}\sigma/\mathrm{d}M_t$ in perturbation theory one gets the following: As long as one considers only factorizable corrections, figure 3 (left), the peak value M_t^* of this distribution is equal to m_t, to any order in the perturbation expansion. Nonfactorizable (semisoft) gluon exchange, figure 3 (right), shifts the peak of $\mathrm{d}\sigma/\mathrm{d}M_t$ away from m_t, but the effect, computed to $\mathrm{O}(\alpha_s^3)$, is very small. Near the production threshold, $\hat{s} \gtrsim 4m_t^2$, a shift ΔM_t of ~ -15 MeV and $\sim +10$ MeV occurs for gg and $q\bar{q}$ initial states, respectively, [146] and the sizes of the shifts, which are of opposite sign for the two $t\bar{t}$ production channels, decrease with increasing parton center-of-mass energy $\sqrt{\hat{s}}$. When folded with the PDF the overall effect on $\mathrm{d}\sigma/\mathrm{d}M_t$ is negligibly small.

However, no conclusion can be drawn from this on the non-perturbative aspects of colour reconnection, which includes the effect of long-wavelength colour fields from the underlying event on the formation of hadrons in top decay. A study based on a heuristic model of non-perturbative colour reconnection concludes that in top-mass determinations an uncertainty $\delta m_t \sim \pm 0.5$ GeV is associated with this phenomenon [190].

The experiments at the Tevatron use complex modeling techniques in order to extract a value of the top-quark mass from the raw data. The modeling of the events involves simulations that use lowest-order parton matrix elements for $t\bar{t}$ production and decay, various

[11] For $e^+e^- \to t\bar{t}$ far above threshold, an interesting theoretical analysis of a top-mass determination from the invariant mass distribution was made in [187].

parton showering algorithms, and modeling of the hadronization and of the underlying event. The methods are reviewed in [7, 8]. Recent results on the top-mass from the fully hadronic, dileptonic, and lepton + jets channels were obtained in [182,184,188,189]. The average of all measurements was recently determined to be $m_t^{exp} = 172.6 \pm 0.8\,(stat.) \pm 1.1\,(syst.)$ GeV [16]. Adding the uncertainties in quadrature yields a total uncertainty of 1.4 GeV. As the top-mass determinations at the Tevatron are based on kinematic reconstructions it seems natural to identify this value with the pole mass m_t. One should, however, be careful with this interpretation. For instance, the value of the upper bound on the SM Higgs boson mass, derived by assuming that m_t is known with this precision, may perhaps be premature.

For the LHC, simulation studies have been made by the ATLAS and the CMS collaborations in order to estimate the precision with which the top mass can be determined in the three channels (4.1). Based on kinematic reconstructions and modeling similar to that used by the Tevatron experiments, the CMS study [23] concludes that the top mass can be determined with an uncertainty of $\Delta m_t^{exp} \simeq 1.2\,(1.9)$ GeV in the dilepton (lepton + jets) channel with $10\,\mathrm{fb}^{-1}$ of integrated luminosity, if the goal of a precise determination of the b-jet energy scale can be achieved. The ATLAS study [120] arrived at a total error of 2 GeV for the same integrated luminosity.

In the high luminosity phase of the LHC the top mass can also be determined precisely from $t\bar{t}$ events with a J/ψ from exclusive b decay in the final state [191]. Consider $t\bar{t} \to (b \to J/\psi)\ell\nu_\ell\, bqq'$ with $J/\psi \to \ell^+\ell^-$. The top quark mass is correlated with the invariant mass $M_{J/\psi\ell}$ of the J/ψ and the lepton from the W decay which comes from the same top quark as the b that decays into J/ψ. This correlation allows a determination of the top mass, and this method considerably reduces the uncertainty related to the knowledge of the jet energies. There are, however, other uncertainties, in particular theoretical ones associated with colour reconnection and quark fragmentation. When combining the top-mass measurement with the direct measurement methods mentioned in the previous paragraph, an uncertainty on m_t^{exp} of 1 GeV is feasible [23, 120].

The mean distance that b hadrons from $t\bar{t}$ events travel before they decay is also correlated with the top-quark mass, and this correlation provides another method for determining m_t^{exp} [192]. Here, systematic uncertainties are associated with Monte Carlo modeling, b fragmentation, and the average b hadron lifetime.

Another observable that may be useful for determining the top-quark mass at the LHC is the $t\bar{t}$ invariant mass distribution. The average $\langle M_{t\bar{t}} \rangle$ and higher moments have some sensitivity to m_t [193]. This distribution is also affected by colour reconnection.

Thus, in view of the goal of determining at the LHC a well-defined top-quark mass with an overall uncertainty of ~ 1 GeV, there is still some effort required, especially on the theoretical side. This includes the investigation of the theoretical uncertainties of observables sensitive to the top-mass.

4.4. Distributions

Besides $\sigma^{t\bar{t}}$, kinematic distributions are also important probes of the dynamics of $t\bar{t}$ production. Investigations including higher-order SM corrections were listed in section 4.1.1, and most of the higher-order QCD results were incorporated in the NLO Monte Carlo codes mentioned in section 4.1.2. Predictions for the p_T or (pseudo)rapidity distribution of the t or $\bar{t}$ quark can be made to good approximation for on-shell, stable top quarks averaged over their spins. In general (multi-particle) distributions should be computed at the level of the t and $\bar{t}$ decay products, and a number of distributions depend also on the spin configuration of the intermediate $t\bar{t}$ state. Some of them will be discussed in the next subsection. Some variables, for instance $p_T^{t\bar{t}} = |\mathbf{p}_T^t + \mathbf{p}_T^{\bar{t}}|$ or the difference $\Delta\phi$ of azimuthal angles of the t and $\bar{t}$ quark, have a non-trivial distribution only beyond the leading-order, due to real radiation. This makes them sensitive to multiple gluon emission.

The precise measurement of the $M_{t\bar{t}}$ distribution at the $t\bar{t}$ production threshold would allow for interesting studies of $J = 0$ colour singlet $t\bar{t}$ resonance effects [194]. On the other side of the energy spectrum, the measurement of the p_T and $t\bar{t}$ invariant mass distributions up to the highest possible values is crucial in the search for new (TeV-scale) physics, such as heavy s-channel resonances (c.f. section 4.7.2). Therefore they should be known as precisely as possible within the SM. The electroweak corrections, computed to $O(\alpha_s^2\alpha)$, contribute to these distributions. The weak corrections grow in "exclusive" $t\bar{t}$ production (i.e., no real radiation of W and Z bosons) due to the appearance of weak-interaction Sudakov logarithms. The electroweak corrections are negative, both for the Tevatron and the LHC, above some minimum p_T or $M_{t\bar{t}}$ and increase in magnitude relative to the LO QCD corrections. At the LHC, for example, the weak corrections to the LO p_T and $M_{t\bar{t}}$ distribution at $p_T = 1$ TeV and $M_{t\bar{t}} = 2$ TeV are -11% and -6% (for a Higgs boson mass $m_H = 120$ GeV), respectively, [138, 140], while the purely photonic corrections at these values of p_T and $M_{t\bar{t}}$ are -2% and $+0.5\%$ [142]. A complete assessment of the significance of these corrections requires inclusion of the NLO QCD corrections and a discussion of the uncertainties resulting from PDF errors and scale variations. On the experimental side, a measurement of these distributions in the TeV range requires special $t\bar{t}$ identification criteria [195]. In this energy region the t and $\bar{t}$ quarks are highly Lorentz-boosted, which leads to overlapping and merged jets in the case of hadronic top decays.

For $p\bar{p} \to t\bar{t} + X$ kinematic distributions in QCD need not be symmetric with respect to the interchange of the t- and $\bar{t}$-quark charges. This is because the initial state, $|p(\mathbf{q})\bar{p}(-\mathbf{q})\rangle$, is not an eigenstate of charge conjugation. A charge asymmetry is generated at NLO QCD by the interference of C-even and -odd terms of the amplitudes for $q\bar{q}$ annihilation and, likewise, for gq and $g\bar{q}$ fusion [124, 125, 196–198]. (The contribution of the latter two processes to the asymmetry is small.) One may define a differential and a total charge asymmetry

$$A(y) = \frac{N_t(y_t) - N_{\bar{t}}(y_{\bar{t}})}{N_t(y_t) + N_{\bar{t}}(y_{\bar{t}})}, \quad A = \frac{N_t(y_t \geq 0) - N_{\bar{t}}(y_{\bar{t}} \geq 0)}{N_t(y_t \geq 0) + N_{\bar{t}}(y_{\bar{t}} \geq 0)}, \tag{4.12}$$

where y_t and $y_{\bar{t}}$ are the rapidities of the t and $\bar{t}$ quark, and $N(y) = \mathrm{d}\sigma/\mathrm{d}y$. Notice that $A(y)$ and A are of order α_s. A recent LO analysis [199] obtained $A = 0.051 \pm 0.006$ for the

integrated asymmetry, where the given uncertainty is due to scale variations and variations of m_t within the error given in (2.2). The electroweak QCD interferences, which increase the LO QCD result by a factor 1.09, are included. If one takes only the strong interactions into account, then one can invoke C invariance which implies $N_{\bar{t}}(y_{\bar{t}}) = N_t(-y_t)$. With this proviso, A is equal to the forward-backward asymmetry $A_{FB}^t = [N(y_t > 0) - N(y_t < 0)]/[N(y_t > 0) + N(y_t < 0)]$ of the t quark. As the initial $p\bar{p}$ state is a CP eigenstate in the laboratory frame, CP invariance implies $A_{FB}^{\bar{t}} = -A_{FB}^t$. Non-standard CP-violating interactions, if existent, can lead to small deviations from this relation [200].

For the production of $t\bar{t}$ pairs in association with a hard jet, the integrated charge asymmetry was calculated to NLO QCD by [143]. Here $A = A_{FB}^t$, which to leading-order is -7%, is drastically reduced at NLO to $-1.5 \pm 1.5\%$. From this result, no conclusion can however be drawn concerning the size of the unknown NLO QCD corrections to the inclusive $t\bar{t}$ asymmetry discussed in the previous paragraph.

Recent measurements at the Tevatron by the CDF and D0 collaborations use an asymmetry different from (4.12). Defining the difference $\Delta y = y_t - y_{\bar{t}}$ of the rapidities of the t and $\bar{t}$ quark, these experiments use $A' = (N_> - N_<)/(N_> + N_<)$, where $N_>$ ($N_<$) is the number of events with positive (negative) Δy. The leading-order SM prediction is $A' = 0.078 \pm 0.009$ [199]. The lepton + jets final states of the $t\bar{t}$ pair is well suited for this measurement, as the charge of the lepton tags the charge of the top quark. The size of this asymmetry (and of (4.12)) is strongly dependent on acceptance cuts, as shown by a calculation of A' [201] with the MC@NLO event generator. The D0 collaboration measured $A'_{D0} = 0.12 \pm 0.08\,(\text{stat.}) \pm 0.01\,(\text{syst.})$ [201]. This result must be unfolded for detector efficiencies and migration effects [201] before it can be compared with predictions. The CDF experiment also measured this asymmetry and obtained, after performing the unfoldings just mentioned: $A' = 0.24 \pm 0.13\,(stat.) \pm 0.04\,(syst.)$ [202]. The central value of this result is higher than the SM expectation, but the result is still consistent with the SM Monte Carlo prediction.

The asymmetries A, A', and A_{FB}^t are useful tools in the search for new physics effects that involve axial vector couplings to quarks. This has been demonstrated for some hypothetical heavy s-channel resonances, namely "leptophobic" Z' vector bosons (with vector- and axial-vector couplings to quarks) [201] and axigluons (with axial vector couplings to quarks) [199, 203].

At the LHC, the initial state $|p(\mathbf{q})p(-\mathbf{q})\rangle$ is an eigenstate of parity. Thus, $A_{FB}^t = A_{FB}^{\bar{t}} = 0$ in the laboratory frame, as long as only parity-invariant interactions – more general, only parity-even terms in the scattering operator – are taken into account. The charge asymmetries A, A' induced by the SM interactions are very small. They result from $t\bar{t}$ production by $q\bar{q}$ annihilation and gq and $g\bar{q}$ fusion, which are subdominant processes at the LHC. The size of the effect was investigated in [197, 199], within the SM and for an axigluon with a mass in the TeV range, in appropriately chosen kinematic regions.

4.5. Top quark polarization and spin correlations

As emphasized in section 2.2, the top quark is unique among quarks in that polarization and spin correlation phenomena provide important tools in exploring the dynamics of these quarks. The SM predicts only a small polarization of the t- and $\bar{t}$-quark ensembles when pair-produced in hadronic collisions. Strong interactions lead to a polarization of t and $\bar{t}$ quarks orthogonal to the scattering plane, due to absorptive parts of the scattering amplitudes of $q\bar{q} \to t\bar{t}$ and $gg \to t\bar{t}$, which are of $O(\alpha_s^3)$. This polarization of $O(\alpha_s)$, the size of which is dependent on the parton center-of-mass energy and on the scattering angle, does not exceed $\sim 2\%$ in magnitude [204,205]. Parity-violating weak interactions, which affect both $q\bar{q} \to t\bar{t}$ and $gg \to t\bar{t}$, induce a top quark polarization in the scattering plane (more general, along some polar vector), which is, however, also small – see below.

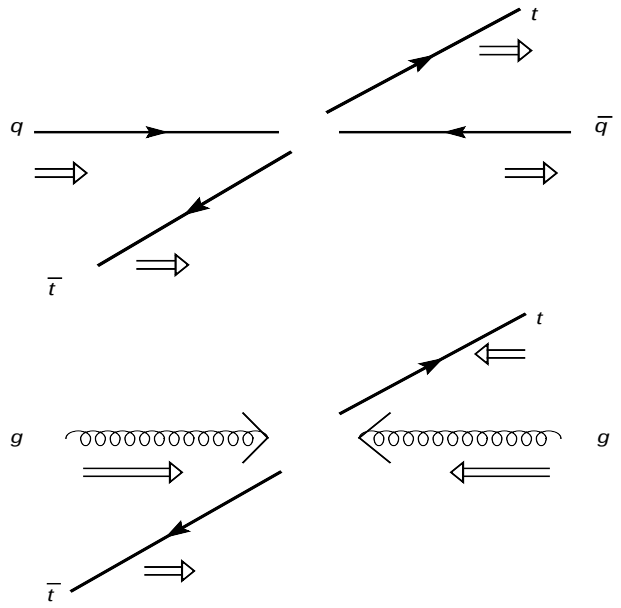

Figure 5: Illustration of the correlation of the t and $\bar{t}$ spins in the $q\bar{q}$ and gg production channels near threshold.

On the other hand the correlation of the t and $\bar{t}$ spins in the QCD-induced production reactions is known to be sizeable [206–211]. In fact, the strength of this correlation depends, like the t and $\bar{t}$ polarization, on the choice of suitable reference axes, which can be interpreted as t and $\bar{t}$ spin quantization axes (i.e. as t and $\bar{t}$ spin bases) in the approximation of on-shell $t\bar{t}$ production and decay. The correlation of the t and $\bar{t}$ spins with respect to arbitrary reference axes $\hat{\mathbf{a}}$, $\hat{\mathbf{b}}$ is given by the expectation value $\mathcal{A} = \langle 4(\hat{\mathbf{a}} \cdot \mathbf{S}_t)(\hat{\mathbf{b}} \cdot \mathbf{S}_{\bar{t}}) \rangle$. This correlation is equal to the $t\bar{t}$ double spin asymmetry

$$\mathcal{A} = \frac{N(\uparrow\uparrow) + N(\downarrow\downarrow) - N(\uparrow\downarrow) - N(\downarrow\uparrow)}{N(\uparrow\uparrow) + N(\downarrow\downarrow) + N(\uparrow\downarrow) + N(\downarrow\uparrow)}, \tag{4.13}$$

where the first (second) arrow refers to the t ($\bar{t}$) spin projection onto $\hat{\mathbf{a}}$ ($\hat{\mathbf{b}}$). Useful choices

are the helicity basis, $\hat{\mathbf{a}} = \hat{\mathbf{k}}_{\mathbf{t}}$, $\hat{\mathbf{b}} = \hat{\mathbf{k}}_{\bar{\mathbf{t}}}$, the so-called beam basis $\hat{\mathbf{a}} = \hat{\mathbf{b}} = \hat{\mathbf{p}}$, and off-diagonal basis $\hat{\mathbf{a}} = \hat{\mathbf{b}} = \hat{\mathbf{d}}$. Here $\hat{\mathbf{p}}$ denotes the direction of one of the hadron beams (i.e., the z axis in the laboratory frame), and $\hat{\mathbf{d}}$ is given by

$$\hat{\mathbf{d}} = \frac{-\hat{\mathbf{p}} + (1-\gamma)(\hat{\mathbf{p}} \cdot \hat{\mathbf{k}}_{\mathbf{t}})\hat{\mathbf{k}}_{\mathbf{t}}}{\sqrt{1-(\hat{\mathbf{p}} \cdot \hat{\mathbf{k}}_{\mathbf{t}})^2(1-\gamma^2)}}, \quad \gamma = E_t/m_t\,. \tag{4.14}$$

Let us briefly discuss the significance of these reference axes. At the Tevatron most of the $t\bar{t}$ pairs are produced by $q\bar{q}$ annihilation not too far away from threshold. At threshold the $t\bar{t}$ pair, being produced in an s wave, is in a $^3S_1$ state – c.f. the illustration in figure 5. Thus, when the top-quark velocity $\beta_t \to 0$, angular momentum conservation implies that the t and $\bar{t}$ spins are 100% correlated with respect to the beam axis, while this correlation is smaller for any other axis. On the other hand, in the ultra-relativistic regime, $\beta_t \to 1$, there is 100% correlation of the t and $\bar{t}$ spins with respect to the t and $\bar{t}$ helicity axes. This follows from the helicity conservation of quark-gluon interaction. The vector (4.14) defines the so-called off-diagonal basis [212] with respect to which the t and $\bar{t}$ spins are 100% correlated for any β_t. This holds for $q\bar{q} \to t\bar{t}$ to Born approximation.

For $gg \to t\bar{t}$ no spin basis with this property exists. This may be seen as follows. For $\beta_t = 0$ the $t\bar{t}$ is in a $^1S_0$ state (recall the Landau-Yang theorem for ortho/para-positronium decay). Thus close to threshold mostly $t\bar{t}$ pairs with like helicities are produced in gg fusion, while the opposite is the case for $\beta_t \to 1$.

These considerations imply that for the Tevatron the off-diagonal basis [212] and the beam basis [144, 145] yield the strongest correlations, while for the LHC, where the top quarks have on average larger velocities, the helicity basis is a good choice. A prescription was given by [213] to obtain at the LHC a correlation which is somewhat stronger than in the helicity basis.

Notice that the number of $t\bar{t}$ events with like and unlike spin projections in (4.13) is determined by the diagonal terms $(R^{(ij)})_{\alpha\alpha,\beta\beta}$ of the production density matrices (c.f. section 4.1.1).

At Born level the vectors involved in these three bases may be defined in the center-of-mass frame of the colliding partons. However, this frame is of no use, once QCD corrections are taken into account [145]. The reconstruction of this frame requires the measurement of the four-momenta of all final state particles/jets; but for real gluon radiation being collinear to one of the initial partons this is not possible. Thus in this frame the correlation (4.13) is not collinear-safe when using the helicity and the off-diagonal basis. A suitable frame is the zero-momentum frame of the $t\bar{t}$ pair. In the following the three bases above are defined with respect to that frame.

The correlations of the t and $\bar{t}$ spins manifest themselves in decay angular correlations which are to be measured with respect to the chosen reference axes. If the t ($\bar{t}$) decays semileptonically then, as discussed in section 3.1.3, the charged lepton is the best spin analyzer, while for non-leptonic t ($\bar{t}$) decays the least-energetic non-b jet will be the best choice, at least from a theoretical point of view. This choice will be made in the following.

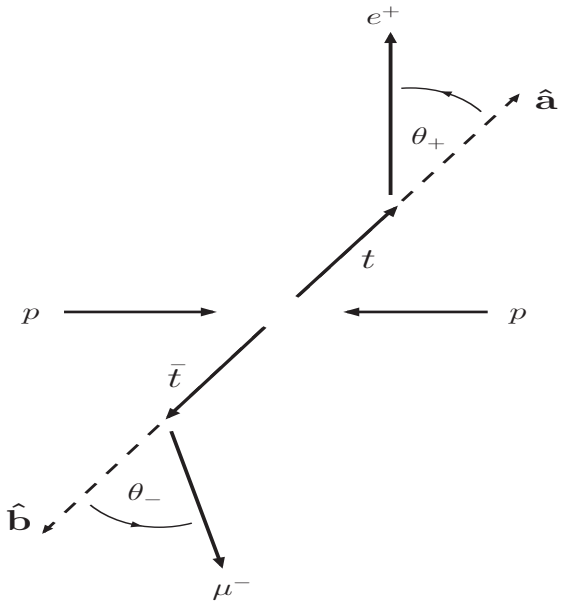

Figure 6: Illustration of the helicity axes in $t\bar{t} \to \ell^+\ell'^- X$.

The dilepton and the lepton + jets channels

$$pp,\ p\bar{p} \longrightarrow t\bar{t}\,X \to a\,b\,X\,, \tag{4.15}$$

where $a\,b = \ell^+\,\ell'^-$, $\ell\,j_<$, and $j_<\,\ell$ ($\ell = e,\mu$), are best suited for measurements of top-spin effects. A useful observable is the following double distribution

$$\frac{1}{\sigma}\frac{\mathrm{d}^2\sigma}{\mathrm{d}\cos\theta_a \mathrm{d}\cos\theta_b} \;=\; \frac{1}{4}\left[1 + B_1\cos\theta_a + B_2\cos\theta_b - C\cos\theta_a\cos\theta_b\right], \tag{4.16}$$

where θ_a (θ_b) is the angle defined between the direction of flight of the particle/jet $a\,(b)$ in the t ($\bar{t}$) rest frame and the reference axis $\hat{\mathbf{a}}$ ($\hat{\mathbf{b}}$). For the helicity axes these angles are illustrated in figure 6. The coefficients $B_{1,2}$ reflect the polarization of t and $\bar{t}$ with respect to the axes $\hat{\mathbf{a}}$ and $\hat{\mathbf{b}}$, respectively. When choosing the beam, off-diagonal, or helicity basis, then QCD absorptive parts cannot generate a t and $\bar{t}$ polarization along these axes. Within the SM only weak interaction corrections lead to non-zero coefficients B_i, which are however small: $|B_1|, |B_2| < 1\%$ (see below). The coefficient C reflects the correlation of the t and $\bar{t}$ spins. Because (4.16) is inclusive in the t and $\bar{t}$ invariant masses, the $\mathrm{O}(\alpha_s^3)$ nonfactorizable QCD corrections, discussed in section 4.1.1, do not contribute. For factorizable corrections, the following formula holds to all orders in α_s [144]:

$$C \;=\; -c_a c_b\,\mathcal{A}\,, \tag{4.17}$$

where $\mathcal{A}$ is the double spin asymmetry (4.13) and c_a, c_b are the t, $\bar{t}$ spin-analyzing powers of a, b given in table 3. This formula tells us that the double distribution (4.16) picks

Table 6: Coefficient C of the angular distribution (4.16) that reflects $t\bar{t}$ spin correlations, at LO and NLO in α_s, for the dilepton and lepton + jets channels [145]. For the LHC C_{beam} and C_{off} are not given, as they are very small.

	Tevatron, $\sqrt{s} = 1.96$ TeV		LHC, $\sqrt{s} = 14$ TeV	
$\ell\ell$	LO	NLO	LO	NLO
$C_{\rm hel}$	-0.471	-0.352	0.319	0.326
$C_{\rm beam}$	0.928	0.777	-0.005	-0.072
$C_{\rm off}$	0.937	0.782	-0.027	-0.089
D	0.297	0.213	-0.217	-0.237
$\ell + j$				
$C_{\rm hel}$	-0.240	-0.168	0.163	0.158
$C_{\rm beam}$	0.474	0.370		
$C_{\rm off}$	0.478	0.372		
D	0.151	0.101	-0.111	-0.115

out the diagonal terms $(R^{(ij)})_{\alpha\alpha,\beta\beta}$ in the production density matrices. (In the helicity basis $\alpha,\beta = R,L$, where $R(L)$ refers to positive (negative) helicity of the t or $\bar{t}$ quark.) Off-diagonal terms can be probed with higher-dimensional distributions [64, 214, 215].
Another useful observable for investigating $t\bar{t}$ spin correlations is the opening angle distribution [145, 266]:

$$\frac{1}{\sigma}\frac{d\sigma}{d\cos\varphi} = \frac{1}{2}(1 - D\cos\varphi)\,, \tag{4.18}$$

where $\varphi = \angle(\mathbf{p_a}, \mathbf{p_b})$, with the directions of flight of a, b being defined in the respective t, $\bar{t}$ rest frames. This distribution reflects the correlation of t and $\bar{t}$ spins when projected onto each other, $\langle \mathbf{S}_t \cdot \mathbf{S}_{\bar{t}} \rangle$.
The structures displayed on the right hand sides of (4.16) and (4.18) apply if no phase space cuts are made. For estimators of C and D in the presence of cuts, see [145].
The measurement of (4.16) and (4.18) requires the reconstruction of the t and $\bar{t}$ rest frames. For the ℓ + j channel this can be done, as was discussed in section 4. Here, m_t should be considered to be known. In the case of $t\bar{t}$ dilepton events, the equations which result from the kinematics for the unknown ν and $\bar{\nu}$ momenta can be solved up to a four-fold ambiguity, if besides the W mass also the value of the top-quark mass is put in. A weight can be assigned to the different solutions by Monte Carlo simulation. The fully hadronic channels can be completely reconstructed, but the spin-correlation effects in the pertinent distributions are small. Moreover, the signal-to-background ratio is unfavourable for these events (c.f. section 4).
Table 6 contains the predictions at LO and NLO in the QCD coupling for the distributions (4.16) and (4.18) for the dilepton and lepton + jets channels. Predictions for the fully hadronic channel can be found in [145]. For the results of table 6, the LO and NLO PDFs of [172] were used, and $\mu_F = \mu_R = m_t = 175$ GeV.

We add the following remarks: (i) The NLO predictions given in table 6 remain basically unchanged when using the PDF set [174]. (ii) Table 6 shows that for the Tevatron the beam basis is practically as good as the off-diagonal basis for detecting the $t\bar{t}$ spin correlations. From the experimental point of view the beam basis is perhaps the best choice. (iii) For the LHC good choices are the double distribution (4.16) in the helicity basis and the opening angle distribution (4.18). The correlation coefficients C_{hel} and D can be enhanced by cutting away events with large $t\bar{t}$ invariant mass. (iv) Based on a Monte Carlo analysis of dilepton and lepton + jets events, the ATLAS study [22] concludes that these correlations can be measured at the LHC with a relative error of $\delta D/D \simeq 4\%$ and $\delta C_{hel}/C_{hel} \simeq 6\%$, including systematics and detector effects. The CMS study of the distribution (4.16) in the $\ell + j$ channel draws a more pessimistic conclusion: they estimate the relative measurement uncertainty of C_{hel} to be 17%. (v) $q\bar{q}$ annihilation and gg fusion contribute with opposite sign to the above distributions. This makes them quite sensitive to the quark and gluon content of the (anti)proton. (vi) The spin correlations are sensitive to new interactions in $t\bar{t}$ production, especially when their chiral structure differs from the dominant QCD vector coupling (see section 4.7).

For a complete discussion of SM top-spin effects (electro)weak corrections must also be taken into account. The mixed weak QCD corrections of $O(\alpha_s^2\alpha)$ to (4.16) and (4.18) are also known [136, 138]. They contribute to the coefficients C_{hel} and D only at the percent level. For large $t\bar{t}$ invariant masses, $M_{t\bar{t}} \gtrsim 1$ TeV, where the event numbers become small, these corrections amount to about -10% of the LO QCD values.

In addition, the weak interaction corrections generate P-violating spin effects, in particular a polarization $\langle \mathbf{S}_t \cdot \hat{\mathbf{a}} \rangle$, $\langle \mathbf{S}_{\bar{t}} \cdot \hat{\mathbf{b}} \rangle$ of the t and $\bar{t}$ quarks along a polar vector, e.g., along the beam direction or along the t and $\bar{t}$ directions of flight. P-violating (single) spin effects are again best analyzed in the $\ell\ell$ and $\ell + j$ channels. If one considers $pp, p\bar{p} \to t\bar{t}X \to \ell^+ + X$, information on the t polarization may be obtained from the angular distribution

$$\frac{1}{\sigma}\frac{d\sigma}{d\cos\theta_+} = \frac{1}{2}(1 + B\cos\theta_+) , \tag{4.19}$$

where $\theta_+ = \angle(\ell^+, \hat{\mathbf{a}})$, and $\hat{\mathbf{a}}$ may be chosen to be the beam axis (Tevatron) or the helicity axis (LHC). (Of course, (4.19) follows from (4.16).) The distribution leads to the P-violating spin asymmetry $A_{PV} = (N_> - N_<)/(N_> + N_<) = B/2$, where $N_>$ ($N_<$) is the number of events with $\cos\theta_+$ larger (smaller) than zero. The spin asymmetry, considered as a function of $M_{t\bar{t}}$, increases with increasing $M_{t\bar{t}}$. Eventually one should measure this asymmetry bin-wise at the LHC, especially at large $M_{t\bar{t}}$, provided that sufficiently large data samples have been collected. In the helicity basis it becomes larger than 1% at the LHC only for $M_{t\bar{t}} \gtrsim 2$ TeV. However, the integrated asymmetry A_{PV} stays well below 1% [138, 139]. Such a small asymmetry will hardly be measurable – yet this makes (4.19) a sensitive tool in the search for non-standard P-violating interactions of top quarks.

4.6. Associated production of $t\bar{t}X^0$, $X^0 = \gamma, Z, H$

The couplings of the top quark to a photon and a Z boson have not yet been directly measured[12]. At hadron colliders this can be done in the associated production of a $t\bar{t}$ pair with a hard photon or a Z boson. In the high luminosity phase of the LHC the $t\bar{t}\gamma$ and $t\bar{t}Z$ event rates are large enough to allow for rather sensitive tests of the top-quark couplings to the neutral gauge bosons. Model-independent phenomenological analyses may be done using a general form-factor decomposition of the ttV vertices ($V = \gamma, Z$) or equivalently, an effective, gauge-invariant Lagrangian which describes possible ttV interactions in terms of anomalous couplings. In the approximation where apart from the V boson both top quarks in the ttV vertex are put on-shell, this vertex can be parameterized, for each boson, in terms of four anomalous couplings: a vector, an axial vector, a magnetic dipole moment and an electric dipole moment coupling (for a parameterization see, for instance, [216]).
In the SM at tree level, the photonic vector coupling is equal to the top-quark charge $Q_t e$, while the axial vector coupling is zero, and the ttZ vector and axial vector couplings are given by the well-known neutral current couplings $v_t^Z e$ and $a_t^Z e$. The magnetic and weak magnetic dipole moments are induced by quantum fluctuations: to $\mathrm{O}(\alpha_s^2)$ the anomalous (weak) magnetic moment of the top quark is $0.02\ (0.007)$ [217]. The SM radiative corrections to the vector and axial vector couplings involving the Z boson are of $\mathrm{O}(10^{-2})$ [217, 218]. One should note that the correct description of the $t\bar{t}V$ events involves the S matrix element of the respective process and not, in general, these anomalous couplings or form factors. (See e.g. [217] for a discussion.) The primary use of anomalous couplings is to parameterize new physics effects, in the same fashion as described in section 3.2.1.
Some of these effective couplings may be modified significantly by new interactions. For instance in several models of non-standard electroweak symmetry breaking, such as technicolour [100] or Little Higgs models [219], deviations may reach the level of 10%. If the top quark were a composite object, one might expect an anomalously large $t\bar{t}\gamma$ event rate, due to de-excitation of higher-energetic top states. The electric dipole moment and weak electric dipole moment of the top quark in the $tt\gamma$ and ttZ vertex, respectively, which are generated by CP-violating interactions, are tiny within the SM. If non-standard CP violation, in particular Higgs sector CP violation exists, a sizeable top-quark (weak) electric dipole moment can be induced [220].
How precisely can these couplings be measured in $t\bar{t}\gamma$ and $t\bar{t}Z$ events at the LHC? Rather detailed studies have been made in [216, 221, 222]. As to $t\bar{t}\gamma$ events, one is interested in photon emission from top quarks. Cuts have been identified which suppress the contributions of photon radiation from the other particles involved in $t\bar{t}$ production and decay [216]. Assuming $300\,\mathrm{fb}^{-1}$ of integrated luminosity at the LHC, [216] concludes that the $t\bar{t}\gamma$ vector and axial vector couplings could be measured with a 1 s.d. error of $\sim \pm 0.07$, while the magnetic and electric moments may be determined with an accuracy of aobut ± 0.20. The event rate for $t\bar{t}Z$ with subsequent leptonic Z boson decay is considerably smaller than the $t\bar{t}\gamma$ rate. Therefore, one expects that the $t\bar{t}Z$ couplings cannot be deter-

[12] The ttZ couplings are, however, constrained by data from LEP, especially by $Z \to b\bar{b}$.

mined as precisely as the $t\bar{t}\gamma$ couplings. Yet, for the axial vector coupling an accuracy of $\sim \pm 0.10$ could be reached [222]. As far as the axial vector couplings are concerned this sensitivity is competitive with the measurement expectations in $e^+e^- \to t\bar{t}$ at a future linear collider [185].

An important objective at the LHC is the search for the associated production of a $t\bar{t}$ pair with a Higgs boson, $pp \to t\bar{t}H$. For a SM Higgs boson H, this channel may be observable if H is light, $m_H \lesssim 150$ GeV. In view of its cross section being significantly smaller than those of other H production reactions, this is very probably not the channel where H will be discovered (if it exists). Yet, once a Higgs boson is found, it will be important to measure its couplings to other particles in order to check whether these couplings are really those of a standard-model Higgs boson. The $t\bar{t}H$ channel provides a direct way to explore the top Yukawa coupling λ_t, which the SM predicts to be $\lambda_t^{SM} = m_t/v = m_t/(246\text{GeV})$. The cross section and distributions for this process are known to NLO QCD [223–226]. The QCD corrections increase the total $t\bar{t}H$ cross section at the LHC by about 20%.

A measurement of the absolute value of the top Yukawa coupling by counting the events $t\bar{t}H, H \to f$ is not possible without further input. The determination requires, apart from a precise prediction of the production cross section $\sigma(t\bar{t}H) \propto |\lambda_t|^2$, the knowledge of the branching ratio $B(H \to f)$. One can, however, measure ratios of couplings in a model-independent way. For instance, a measurement of the ratio between the rate of ttH production and that of WH production, where in both cases H decays to the same final state, would yield the ratio of the Higgs couplings to the top quark and to the W boson. These coupling ratios would also allow to discriminate between SM and non-SM Higgs bosons.

A light Higgs boson decays dominantly into $b\bar{b}$ pairs. Observation of the signal $t\bar{t}H$ followed by $H \to b\bar{b}$ is difficult in view of the large background [23, 79]. The decay channel $H \to W^+W^-$ (where one or both W bosons are virtual in the case of a light Higgs boson) is also an option, because $B(H \to W^+W^-) \sim 10\%$. The reaction $t\bar{t}H, H \to \gamma\gamma$ has a rather clean signature and allows to reconstruct the Higgs mass peak, but has a much smaller rate than the $b\bar{b}$ and W^+W^- channels. For the $\gamma\gamma$ decay mode, a signal in excess of 3 s.d. should be observable in the high luminosity phase of the LHC [23].

In SM extensions with more than one Higgs (doublet) field, the couplings of the Higgs bosons to the other particles depend on additional parameters which are unknown. In two-Higgs doublet extensions like the MSSM, a key parameter is $\tan\beta$, introduced in section 3.2.2. For the MSSM to be phenomenologically viable, $\tan\beta$ is required to be larger than one. This implies, for a large parameter range, that the Yukawa coupling of the lightest MSSM Higgs boson h to top quarks is smaller than the corresponding SM coupling, while its coupling to b quarks is enhanced. In the MSSM one expects that Higgs-boson radiation off b quarks, $b\bar{b}h$, dominates over $t\bar{t}h$.

4.7. BSM effects in $t\bar{t}$ production

The existence of physics beyond the standard model (BSM) could affect $t\bar{t}$ production in several ways. New particles which strongly couple to top quarks could show up as resonance bumps in the $t\bar{t}$ invariant-mass spectrum, or may be produced in association

with $t\bar{t}$ pairs. Virtual new particle exchanges may significantly modify the total cross section and/or kinematic distributions. Some effects of this type were already discussed in section 4.6. Of particular interest in the search for BSM effects in (future) high-statistics data is the measurement of distributions/observables that signify P or CP violation in $t\bar{t}$ production, because such effects are small to tiny according to the SM.

4.7.1. Effects of virtual particle exchanges:

The effects of virtual new particle exchanges on the $t\bar{t}$ cross section and distributions has been extensively studied in the literature for a number of SM extensions. If resonance effects are absent, one expects significant deviations from SM predictions only if the new particles X that couple to top quarks are not too heavy, $m_X \sim$ a few hundred GeV, assuming that the associated couplings are not much stronger than g_{QCD}.

Popular new physics models with such particles include non-supersymmetric two-Higgs doublet extensions and the MSSM. For a 2HDM of type II the one-loop corrections to hadronic $t\bar{t}$ production were computed in [227–230]. Within the MSSM the full supersymmetric QCD (SQCD) corrections (squark and gluino exchanges) were determined by [231], both for the cross section and for a number of distributions. (In this paper earlier discrepancies in the literature [232, 233] were resolved.) The corrections due to the exchange of colour-singlet supersymmetric particles were calculated by [229,230,234,235], and more recently by [236] which incorporated also the SQCD corrections.

As to the size of these corrections: in a 2HDM they arise from the exchange of one charged and three neutral Higgs bosons. In a large region of the parameter space of the model, the corrections to the cross section are negative and amount to not more than a few percent of the Born cross section, even if one or several of the Higgs bosons are relatively light ($m_{Higgs} = \mathrm{O}(100\,\mathrm{GeV})$) [229]. However, if one of the neutral Higgs bosons is heavier than $2m_t$ it can be resonantly produced in the gluon fusion subprocess, $gg \to t\bar{t}$, and produce a peak in the $M_{t\bar{t}}$ spectrum. This scenario is relevant for the LHC – see section 4.7.2. Of special interest are P-violating asymmetries, for instance the spin asymmetry A_{PV} defined below (4.19), to which charged Higgs boson exchanges can contribute, assuming that the neutral Higgs states have a definite CP parity. The resulting effect was found to be small: even for a rather light charged Higgs boson, $|A_{PV}| \lesssim 1\%$ [230]. In general, the Higgs self-interactions, i.e., the (effective) Higgs potential of a 2HDM – but also of the MSSM [237] – may break CP invariance. As a consequence, the pseudoscalar state, A, having CP parity -1, mixes with the two scalar, $CP = +1$ states h and H. The resulting mass eigenstates $\phi_i\,(i = 1,2,3)$ no longer have a definite CP parity – they couple to both scalar and pseudoscalar lepton and quark currents. As the Yukawa couplings of the ϕ_i are proportional to the mass of the respective fermion, the top-quark scalar and pseudoscalar Yukawa couplings can be of order one. Resulting P- and CP-violating effects in top-quark reactions may reach observable levels. CP-violating phenomena were investigated for non-resonant [238] and resonant ϕ_i exchanges [239, 240] in hadronic $t\bar{t}$ production; c.f. also [241,242]. For non-resonant ϕ_i exchanges the CP-violating effects in $t\bar{t}$ production at the LHC are small, they are below the percent level [238–240]. We shall

discuss appropriate observables in somewhat more detail in section 4.7.2 for the case of resonant Higgs production and decay into $t\bar{t}$ pairs where the effects become larger.
The one-loop MSSM corrections to hadronic $t\bar{t}$ production comprise, apart from the exchange of the Higgs bosons h, H, A, and $H^{\pm}$, the contributions of the non-coloured and coloured SUSY particles. In general the SQCD corrections are the dominant ones. The largest corrections occur if the mass of the gluino is close to its present experimental lower bound, $m_{\tilde{g}} \gtrsim 230$ GeV, and the splitting between the masses of the two top squarks $\tilde{t}_1$, $\tilde{t}_2$ is large. In this case the contribution to the $t\bar{t}$ cross section at the Tevatron and at the LHC can reach $\pm 5\%$ of the Born cross section, where the sign of the correction depends on the stop mixing angle [231]. In a large portion of the parameter space of the model the SQCD corrections to the $M_{t\bar{t}}$ and p_T distributions are of moderate size, of the order of a few percent, both for the Tevatron and the LHC. However, the gluino pair which appears in the intermediate state can become resonant, $q\bar{q}, gg \to \tilde{g}\tilde{g} \to t\bar{t}$. For rather light gluinos, $m_{\tilde{g}} \gtrsim 230$ GeV, this would show up as a bump in the $M_{t\bar{t}}$ spectrum and would cause also a significant distortion of the p_T distribution [231]. As the gluino-quark-squark interactions violate parity, the SQCD corrections contribute also to parity-odd asymmetries such as A_{PV}. For the LHC, effects can reach 2% at the differential level, i.e. in some $M_{t\bar{t}}$ bins, but the corrections to the integrated asymmetry are below 1% [231].
The gluino-quark-squark interactions not only violate parity, but can also break *CP*. This effect can be parameterized by a phase in the interaction Lagrangian. While for light quarks this possibility is strongly constrained by the experimental upper bound on the electric dipole moment of the neutron, no such strong constraint exists for a possible *CP* phase in the $\tilde{g}t\tilde{t}_{1,2}$ interaction. The observables with which this interaction was investigated in [241, 243] yield, however, effects below the percent level.
BSM effects in $t\bar{t}$ production may be parameterized in a (rather) model-independent way by effective quark-gluon interactions (induced by heavy particle exchanges), the strength of which is described anomalous couplings. There is a vast literature on this topic, which we cannot cover in detail here (see, for instance, [5]). Hadronic $t\bar{t}$ production is obviously the right place to search for anomalous $tt\bar{g}$ interactions, in particular for chromomagnetic and chromoelectric top-quark couplings, which are described by the effective Lagrangian

$$\mathcal{L}_{eff} = -\frac{\mu_t^c}{2}\bar{t}\sigma_{\mu\nu}G^{\mu\nu}t - i\frac{d_t^c}{2}\bar{t}\sigma_{\mu\nu}\gamma_5 G^{\mu\nu}t\,, \tag{4.20}$$

where $G^{\mu\nu} = G^{a\mu\nu}T^a$ is the gluon field strength tensor, $\mu_t^c = \hat{\mu}_t^c/m_t$ and $d_t^c = \hat{d}_t^c/m_t$ denote the dimensionful chromomagnetic and -electric dipole moments of the top quark, and $\hat{\mu}_t^c$ and $\hat{d}_t^c$ their dimensionless analogues. In renormalizable theories they are induced at the loop level; $d_t^c \neq 0$ requires *CP*-violating interactions. The chromoelectric moment generated by the CKM phase is tiny. Therefore, any observable effect would signify a new *CP*-violating interaction.
The contribution of the dimension-five interactions to the partonic differential cross sections $q\bar{q}, gg \to t\bar{t}$ grows with $\hat{s}$ relative to the Born terms. If the dipole moments are nearly constant or vary only weakly with $\hat{s}$, then the anomalous contributions (4.20) would considerably distort the high-end tail of the p_T and $M_{t\bar{t}}$ spectra. A number of other top-quark

distributions would also be affected by (4.20), in particular the $t\bar{t}$ spin correlations discussed in section 4.5. Effects of an anomalous chromomagnetic moment were investigated in [5, 244–246]. A non-zero chromoelectric top-quark dipole moment would leave its mark in suitably constructed *CP*-odd and/or *T*-odd triple correlations or energy asymmetries[13]. These observables are best measured in the dilepton and lepton + jets channels. Such effects were studied in [245, 247–250]. Assuming these form factors to be real, one finds that anomalous couplings as small as $|\hat{\mu}_t^c|, |\hat{d}_t^c| \sim 0.04$ can be detected at the LHC. As these form factors are probed in the time-like region, they can have real and imaginary parts, which can be measured separately with appropriate correlations.
Decay angular correlations can also be used to search for new physics effects in top quark decay. The exclusion limits on the mass and couplings of a charged Higgs boson implied by the negative searches of the D0 and CDF experiments [76–78] do not yet preclude the existence of the decay mode $t \to bH^+$. If it exists one would expect a preference of $t \to b\tau^+\nu_\tau$ over the other semileptonic decay modes (c.f. section 3.2.2). For the $t\bar{t} \to \tau + 2j_b + 2j + E_T^{miss}$ channels one can construct appropriate azimuthal angle correlations that are sensitive to the Lorentz structure of a charged Higgs-boson coupling [251].

4.7.2. Heavy resonances:

Many BSM physics scenarios predict heavy, electrically neutral bosons X^0, with masses m_{X^0} up to a few TeV, that (strongly) couple to $t\bar{t}$ pairs. Thus these resonances would show up as bumps in the $M_{t\bar{t}}$ invariant mass distribution. 2HDM or supersymmetric extensions predict a spectrum of neutral Higgs bosons, some of which can be heavy enough to decay into $t\bar{t}$. Models that aim to explain the mechanism of electroweak gauge symmetry breaking "dynamically" by a new strong force, like technicolour models and their descendants [100], contain new spin-zero and spin-one states. In top-colour [252, 253] and Little Higgs models [254] (c.f. [255] for a review) the top quark plays a special role. New vector resonances appear in these models with reasonably strong couplings to top quarks. Models with extra dimensions [256–258] have massive spin-one and spin-two Kaluza-Klein (KK) excitations. In some of these models the couplings of the new states to light quarks and gluons is suppressed [259–263], and their decay into $t\bar{t}$ is expected to be their main discovery channel.
The prime observable in the search for such objects is of course the $M_{t\bar{t}}$ spectrum, but also the p_T distribution and distributions due to top-quark polarization and spin correlation effects are useful tools. Phenomenological studies on resonance production in the $t\bar{t}$ channel were made for Higgs bosons (more general, spin-zero resonances) [264–266], for spin-one bosons from technicolour [267], topcolour [253], and Little Higgs models [255], axigluons [268], for KK excitations of the graviton [260, 269, 270], and KK excitations of the weak [271, 272] and strong [259, 260, 262, 263, 273, 274] gauge bosons. Recent

[13] A general kinematic analysis of observables in hadronic $t\bar{t}$ production obtained the result [240] that interactions which violate both *P* and *CP* induce a *CP*-odd transverse spin-spin correlation and/or a *CP*-odd longitudinal polarization asymmetry (see section 4.7.2).

model-independent resonance studies include [193, 275]. The expected discovery reach in the $t\bar{t}$ channel at the LHC for such states is typically $m_{X^0} \sim$ a few TeV, depending on the couplings and widths of these particles.

These new states may also be produced in association with a top-quark pair, $t\bar{t}X^0$. If X^0 couples predominantly to quarks of the third generation, one expects an enhanced $t\bar{t}t\bar{t}$ production cross section [276, 277]. An enhanced production rate of this four top state could also be a sign of a top-quark substructure [278].

The experiments at the Tevatron have searched for (colour) neutral, narrow spin-one resonances, Z', that decay into $t\bar{t}$, with no evidence found for such objects so far. Exclusion limits depends on the mass and couplings of Z'. Assuming that such a particle has the same couplings as the Z boson, masses $m_{Z'} \lesssim 700$ GeV can be excluded [279, 280]. However, some new resonances with lower masses may be produced dominantly in gluon fusion (see the next paragraph), so a precise measurement of the $M_{t\bar{t}}$ spectrum over the whole accessible energy range is indispensable at the LHC.

For brevity we discuss here only one scenario which is of interest for the LHC, namely heavy non-standard Higgs bosons which strongly couple to top quarks, as predicted by many SM extensions. Consider, for instance, a 2HDM or the MSSM where the spectrum of physical Higgs particles contains three neutral states: two scalars h, H with $J^{PC} = 0^{++}$ and a pseudoscalar A with $J^{PC} = 0^{-+}$. Depending on the parameters of the respective model some of these states may be heavy, e.g., H and A, with masses of the order of 300 GeV or larger. Of particular interest here is the case of a pseudoscalar, as $A \not\to W^+W^-, ZZ$ in lowest order. If the ratio of the vacuum expectation values of the two Higgs doublet fields, $\tan\beta$, is of order 1, these states will strongly couple to top quarks. Consider the production of a heavy Higgs boson ϕ via gluon fusion at the LHC. If $\phi = A$ this boson will dominantly decay into $t\bar{t}$ pairs, $gg \to \phi \to t\bar{t}$, but also for $\phi = H$ this channel will be significant. The amplitude of this reaction interferes with the amplitude of the QCD-induced non-resonant $t\bar{t}$ background, $gg \to t\bar{t}$, and this interference is not negligible, even in the vicinity of the resonance, $\sqrt{\hat{s}} \sim m_\phi$, because the width Γ_ϕ of the Higgs particle is not necessarily very small compared to m_ϕ; i.e., the resonance need not be narrow. In the case of a non-narrow resonance the interference generates a peak-dip structure in the $t\bar{t}$ invariant mass distribution $M_{t\bar{t}}$. For a scalar Higgs boson his was investigated first in [264], and for scalar and pseudoscalar states in [265, 266]. The "golden" channel to search for resonances in $t\bar{t}$ production is the ℓ + jets final state. An example of the signature of a pseudoscalar Higgs boson with parameters $m_A = 400$ GeV, $\Gamma_A = 10$ GeV, and $\tan\beta = 1$ is shown in figure 7. In the MSSM one expects $\tan\beta > 1$. In this case the $At\bar{t}$ coupling and therefore also the width Γ_A will be smaller. This results in a narrower and higher peak in the $M_{t\bar{t}}$ spectrum. Analogous studies were made for a scalar resonance [193, 266]. A scalar Higgs boson H with mass $m_H \gtrsim 350$ GeV and SM couplings to the other particles would, however, to be too broad to be visible in the $M_{t\bar{t}}$ distribution. Statistically significant signals for scalar and pseudoscalar resonances are possible in the mass range 350 GeV $\lesssim m_\phi \lesssim$ 500 GeV, depending on the strength of the Yukawa couplings and on the width of ϕ [79, 266]. Needless to say, this is a difficult channel which requires a very good resolution of the $M_{t\bar{t}}$ distribution and a precise knowledge of the SM background

contribution.

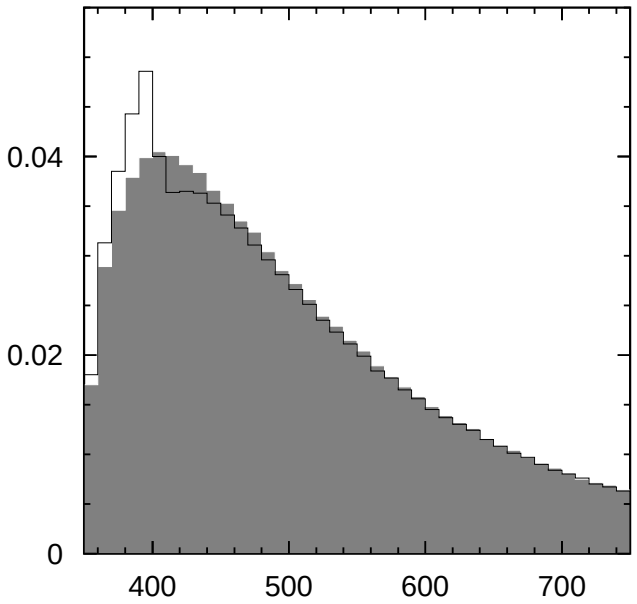

Figure 7: Signal of a heavy pseudoscalar Higgs boson resonance A in the $M_{t\bar{t}}$ spectrum of the $t\bar{t}$ lepton + jets channel [266]. ($m_A = 400$ GeV, $\Gamma_A = 10GeV$, $\tan\beta = 1$.) The solid line represents signal plus background, and the shaded area is the non-resonant $t\bar{t}$ background only.

Suppose experiments will be lucky and discover a heavy boson in $t\bar{t}$ production. The spin of this resonance may be inferred from the polar angle distribution of the top quarks. Another observable which is sensitive to the spin of such an intermediate state is the Collins-Soper angle [193, 281]. Let's assume the outcome of such an analysis is that the resonance has spin zero. How to find out whether it is a scalar or a pseudoscalar? In [266] it was proposed to use spin correlations for answering this question, and it was found that $\langle \mathbf{S}_t \cdot \mathbf{S}_{\bar{t}} \rangle$ is the best choice, which is easy to understand in simple quantum mechanical terms. Consider $gg \to \phi \to t\bar{t}$. If ϕ is a scalar ($J^{PC} = 0^{++}$) then $t\bar{t}$ is in a ${}^3P_0$ state, and a straightforward calculation yields $\langle \mathbf{S}_t \cdot \mathbf{S}_{\bar{t}} \rangle = 1/4$. If ϕ is a pseudoscalar ($J^{PC} = 0^{-+}$) then $t\bar{t}$ is in a ${}^1S_0$ state and $\langle \mathbf{S}_t \cdot \mathbf{S}_{\bar{t}} \rangle = -3/4$. The non-resonant $t\bar{t}$ background dilutes this striking difference in the values of this correlation. As discussed in section 4.5 the correlation $\langle \mathbf{S}_t \cdot \mathbf{S}_{\bar{t}} \rangle$ induces the opening angle distribution (4.18) which is best studied in the dilepton channel. Depending on the couplings and on the width of ϕ a statistically significant effect may be found with this distribution. In order to preserve the discriminating power of the underlying spin correlation, this distribution should be measured only for $t\bar{t}$ events that lie in a suitably chosen $M_{t\bar{t}}$ bin below m_ϕ [266].

However, things could be more complex. If the (effective) Higgs potential does not conserve *CP*, the scalars h, H and the pseudoscalar A will mix, and the Higgs states ϕ_i of definite mass will no longer have a definite *CP* quantum number (as already mentioned in section 4.7.1). While in a non-supersymmetric 2HDM this can occur at tree level it is a loop-induced effect in the MSSM, but it can nevertheless be sizeable [237]. If this is the case, the states ϕ_i will have both scalar and pseudoscalar couplings to fermions; i.e., the $t\bar{t}\phi_i$ interactions violate both *P* and *CP*. Then the spin correlation $\langle \mathbf{S}_t \cdot \mathbf{S}_{\bar{t}} \rangle$ and the resulting coefficient D in (4.18) will lie between the pure scalar and pseudoscalar cases discussed above. Their values depend on the ratio of the scalar and pseudoscalar $t\bar{t}\phi_i$ couplings. Yet (non-resonant and resonant) ϕ_i exchange induces in addition the *CP*-odd and *T*-odd transverse spin-spin correlation $\langle O_1 \rangle = \langle \hat{\mathbf{k}}_t \cdot (\mathbf{S}_t \times \mathbf{S}_{\bar{t}}) \rangle$ and the *CP*-odd and *T*-even longitudinal polarization asymmetry $\langle O_2 \rangle = \langle \hat{\mathbf{k}}_t \cdot (\mathbf{S}_t - \mathbf{S}_{\bar{t}}) \rangle$ [239, 240]. The latter asymmetry corresponds to a difference in the produced numbers of $t\bar{t}$ pairs with negative and positive helicities, $N(t_L\bar{t}_L) - N(t_R\bar{t}_R) \neq 0$. If one or several of the ϕ_i have masses near or above the $t\bar{t}$ threshold, *s*-channel ϕ_i exchanges become resonant, and the induced *CP*-odd correlations can become quite sizeable. They, in turn, generate corresponding angular correlations and asymmetries in the various $t\bar{t}$ decay channels [240, 282]. Again, the dilepton and lepton + jets channels are most suited for such investigations. For instance, once sufficiently large $t\bar{t}$ data sets have been collected, one may consider the samples $t\bar{t} \to \ell^+ X$ and $t\bar{t} \to \ell^- X$. For each sample one can measure the $\cos\theta_+$ ($\cos\theta_-$) distribution, which was defined in (4.19), where θ_+ (θ_-) in the angle between the ℓ^+ (ℓ^-) and the t ($\bar{t}$) direction of flight. The ℓ^+ (ℓ^-) direction is taken to be in the t ($\bar{t}$) rest frame, while the t ($\bar{t}$) direction of flight is to be determined in the $t\bar{t}$ ZMF of the respective sample. A signal of *CP* violation would be a difference in the two distributions; that is, a difference in the expectation values, $\Delta_{CP} = \langle \cos\theta_+ \rangle - \langle \cos\theta_- \rangle \neq 0$. This difference results from $\langle O_2 \rangle \neq 0$. For resonant ϕ exchange, $\Delta_{CP} \sim 5\%$ is possible if these expectation values are evaluated in suitably chosen $M_{t\bar{t}}$ bins in the vicinity of a resonance [282]. The spin correlation $\langle O_1 \rangle$ leads to triple correlations among the momenta of the final state particles/jets. For instance, for the dilepton channel $t\bar{t} \to \ell^+\ell'^- X$ one may measure $\hat{\mathbf{k}}_t \cdot (\hat{\mathbf{p}}_\ell \times \hat{\mathbf{p}}_{\ell'})$. Its expectation value, evaluated in a $M_{t\bar{t}}$ bin near the resonance, can reach a value of several percent [282].

The search for non-standard *CP* violation, in particular Higgs sector *CP* violation, at the LHC is of great interest, not only to particle physics but also to cosmology. Viable scenarios that try to explain the matter-antimatter asymmetry as a dynamical effect require non-standard *CP* violation. The discovery of Higgs bosons with *CP*-violating couplings would support the hypothesis that this asymmetry was generated at the electroweak phase transition [283]. There are several reactions where one can search for Higgs sector *CP* violation (c.f. [284] for a review), and $t\bar{t}$ production is among the more promising ones. One should note that the *CP*-odd observables referred to above probe non-standard *CP* violation, irrespective of whether or not such effects are induced by Higgs bosons.

5. Single-top-quark production

In the hadronic production of single (anti)top quarks the weak interactions are involved in an essential way. Therefore, these reactions provide, besides top-quark decay, another important opportunity to study the charged weak current interactions of this quark. In the SM there are three main hadronic production modes, namely top-quark production via the exchange of a virtual W boson in the t-channel and in the s-channel, and the associated production of a t quark and real W boson:

$$q(\bar{q})\,b \to q'(\bar{q}')\,t\,, \quad q\bar{q}' \to \bar{b}t\,, \quad bg \to W^- t\,. \tag{5.1}$$

These reactions are depicted to lowest order in the gauge couplings in figure 8. The cross sections of these processes are proportional to $|V_{tb}|^2$. Thus, single-top-quark production provides a means of directly measuring the strength of the Wtb vertex. Moreover, the reactions (5.1) are a source of highly polarized top quarks, which allow for dedicated investigations of the structure of the charged weak current interactions of this quark. Exotic t and $\bar{t}$ production processes involving new particles/interactions are also conceivable; for instance, the associated production of a top quark and charged Higgs boson, or enhanced production of single top quarks by sizeable flavour-changing neutral currents.

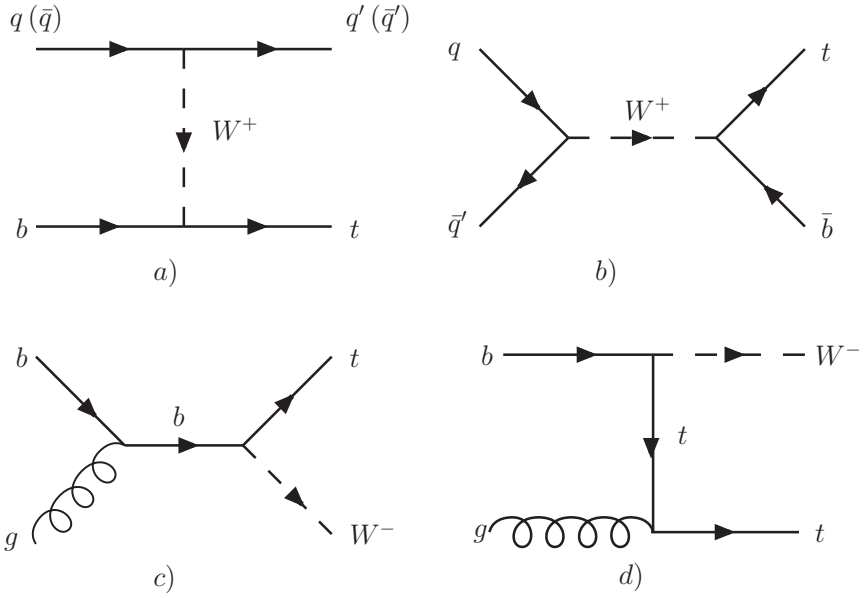

Figure 8: Lowest order Feynman diagrams for single-top-quark production processes: t channel (a), s channel (b), and associated tW production (c,d).

Thus, there are interesting physics issues associated with the hadronic production of single top quarks. However, their observation is much more challenging than detecting $t\bar{t}$ pairs. This is partly due to smaller cross sections, but mainly due to the fact that the final-state signatures suffer from larger backgrounds (see below). Although a few thousand single t

and $\bar{t}$ have been produced at the Tevatron (with 1 fb^{-1} of integrated luminosity), is was only in 2006 that the D0 collaboration [3] – and recently also CDF [4] – reported evidence for the detection of these processes. At the LHC prospects are brighter, as this collider will not only be a factory for the production of $t\bar{t}$ pairs, but also for single top quarks.
Single-top-quark production constitutes also an important background to a number of possible new physics processes. Prominent examples include the associated production of a neutral (SM) Higgs boson and a W boson, $p\bar{p}, pp \to W^+HX$, $H \to b\bar{b}$, for which $p\bar{p}, pp \to tbX \to W^+bbX$ is a significant background. The tW mode is an important background to Higgs production and decay into W bosons, $gg \to H \to W^+W^-$. Needless to say that also this aspect requires the theoretical description of single-top processes to be as precisely and detailed as possible.

5.1. The production cross sections: status of theory

The three modes (5.1) probe the charged-current interactions of the top quark in different kinematical regions. Moreover, these reactions are sensitive to different types of new particles/interactions. Each mode has a relatively distinct event kinematics. Therefore they may eventually be observable separately. In the following subsections, we review the theoretical results for the three modes within the SM. The reactions (5.1) are hard scattering processes. Thus, formulae analogous to (4.3) apply for predictions of the cross sections and distributions.

5.1.1. t-channel production:

This production process is the most important one for the Tevatron and for the LHC, as it has the largest cross section of the three channels (5.1) for both colliders.
At the LHC the dominant t-channel parton processes are $ub \to dt$ (which makes up about 74% of the cross section), $d\bar{b} \to \bar{u}t$ ($\sim 12\%$), $\bar{s}b \to \bar{c}t$ ($\sim 8\%$), and $cb \to st$ ($\sim 6\%$). In addition there are a number of CKM-suppressed reactions. At the Tevatron the same reactions take place, but with with different percentage contributions to the cross section, the most important ones being $ub \to dt$ ($\sim 70\%$) and $d\bar{b} \to \bar{u}t$ ($\sim 21\%$).
The production of a $\bar{t}$ quark requires initial-state $\bar{u}$, d, s, $\bar{c}$ quarks. The relative contributions of the CKM-allowed subprocesses to the t-channel cross section at the LHC are $d\bar{b} \to u\bar{t}$ ($\sim 56\%$), $s\bar{b} \to c\bar{t}$ ($\sim 13\%$), $\bar{u}\bar{b} \to \bar{d}\bar{t}$ ($\sim 20\%$), and $\bar{c}\bar{b} \to \bar{s}\bar{t}$ ($\sim 11\%$). As the proton contains more valence u quarks than d quarks, the t-quark production cross section at the LHC, which is a pp collider, is larger than the $\bar{t}$-quark cross section. The SM predicts these cross sections to be equal at the Tevatron.
Figure 8a shows the Feynman diagrams for the t-channel processes to leading-order QCD in the so-called 5-flavour scheme, where the (anti)proton is considered to contain also b and $\bar{b}$ quarks in its partonic sea, with a b-quark PDF which is obtained from QCD evolution of the gluon and light-quark PDFs. The b and $\bar{b}$ quarks in the (anti)proton sea arise from the splitting of virtual gluons into nearly collinear $b\bar{b}$ pairs, $g \to b\bar{b}$. Thus, if one considers the (anti)proton to be composed only of the four lightest quarks and

gluons, one would take into account the reactions $qg \to q't\bar{b}$ instead of $qb \to q't$. (That is why the t-channel reactions are often called "W-gluon fusion processes" in the literature.) However, the cross section for the W-gluon fusion process contains terms proportional to $\alpha_s \ln(m_t/m_b)^2$ from the region where the outgoing $\bar{b}$ is parallel to the gluon in the initial state. These logarithmically enhanced terms, which make perturbation theory in α_s unreliable, can be summed up by introducing a b-quark PDF [285]. In this approach, the process $qg \to q't\bar{b}$ (with the contribution from the collinear region subtracted) is one of the next-to-leading order QCD contributions to the LO cross section.

To NLO QCD the t-channel cross section was calculated in [286–288]. The corrections are relatively modest, they increase the LO t-quark cross section at the LHC (Tevatron) by about about 5% (9%). NLO QCD results for the fully differential cross section were presented in [289–291]. NLO QCD analyses including the semileptonic top decays were made in [292] and in [293, 294], where also top-spin effects were taken into account. Matching of the next-to-leading order QCD results with parton shower Monte Carlo simulations, according to the prescription used in the Monte Carlo program MC@NLO, was made in [295]. The electroweak corrections were computed in [296, 297] within the SM and the MSSM. The corrections turn out to be small in both models, at the percent level and below.

Table 7: Predictions for single top-quark production cross sections at the Tevatron and the LHC according to the recent update [298, 299]. The given errors include scale uncertainties, PDF uncertainties, and uncertainties in m_t. The value $m_t = 171.4 \pm 2.1$ GeV was used. At the Tevatron the SM prediction for $\bar{t}$ production is equal to σ^t.

cross section	t channel	s channel	tW mode
$\sigma^t_{\text{Tevatron}}$	1.15 ± 0.07 pb	0.54 ± 0.04 pb	0.14 ± 0.03 pb
σ^t_{LHC}	150 ± 6 pb	7.8 ± 0.7 pb	44 ± 5 pb
$\sigma^{\bar{t}}_{\text{LHC}}$	92 ± 4 pb	4.3 ± 0.3 pb	44 ± 5 pb

Table 7 contains predictions for the t-channel cross sections which were updated in [298, 299]. The value given for the Tevatron was obtained taking higher-order soft gluon corrections into account. For the LHC the incorporation of these threshold corrections is not meaningful in the case of the t-channel processes. Therefore the values for σ^t_{LHC} and $\sigma^{\bar{t}}_{\text{LHC}}$ given in table 7 are based on the fixed-order NLO QCD results. The predictions were made with the parton distribution functions MRST2004 [173, 174] and with $m_t = 171.4 \pm 2.1$ GeV. The given errors include the uncertainties in the PDF, in m_t, and those due to variation of the factorization and renormalization scales, μ_F and μ_R, between $m_t/2$ and $2m_t$. For fixed-order NLO predictions, see [289, 290].

5.1.2. *s*-channel production:

At the Tevatron the *s*-channel processes $q\bar{q}' \to \bar{b}t$ have the second largest cross section of the three single-top-production modes (5.1), while at the LHC this channel is very small compared to the other ones. The dominant process is $u\bar{d} \to \bar{b}t$. Additional $q\bar{q}'$ annihilation channels are $\bar{s}c \to \bar{b}t$ and CKM-suppressed reactions.
The leading-order processes are depicted in figure 8b. To NLO QCD the cross section was calculated in [300], and in fully differential form in [289]. The corrections are rather large; they increase the LO *t*-quark cross section at the LHC (Tevatron) by about 44% (47%). NLO QCD results including the semileptonic top decays were presented in [292, 301].
Effects on the cross section due to resummation of higher-order soft gluon radiation are quite sizable for this channel, both for the Tevatron and the LHC [298, 299, 302], so one may take them into account. The values given in table 7 from [298, 299] are based on incorporating such corrections. The errors arise from the uncertainties mentioned at the end of section 5.1.1.
The hadronic *s*-channel cross section has a rather small PDF uncertainty, because it arises mostly from light quarks in the initial state. The largest part of the errors given in table 7 is due to $\Delta m_t = \pm 2.1$ GeV. If the uncertainty on m_t will be significantly reduced (and the precise meaning of the measured value m_t^{exp} will be clarified), the predictions for the *s*-channel cross section will become quite precise. Thus from a theoretical point of view, the *s*-channel mode is well suited to determine the strength of the tbW vertex, i.e., to directly measure $|V_{tb}|$. This is of relevance for the Tevatron, where this mode makes up about 30% of the single *t* cross section.

5.1.3. Associated tW production:

Associated tW production proceeds via $gb \to tW^-$. The CKM-suppressed contributions from gs and gd initial states are negligibly small. This mode plays no role at the Tevatron, but is of interest for the LHC.
The leading-order Feynman diagrams are shown in figure 8c, d. A key issue for this mode is the separation of final states arising from tW and $t\bar{t}$ intermediate states. This problem shows up when one considers real radiation corrections to NLO QCD. The process $gg \to tW^-\bar{b}$, where one gluon splits into a virtual b and a real $\bar{b}$, is among the QCD corrections to $gb \to tW^-$ (c.f. the analogous discussion in section 5.1.1). However, $gg \to tW^-\bar{b}$ can proceed also via a intermediate $t\bar{t}$ state, where not only the t, but also the $\bar{t}$ is on-shell (resonant) and decays into $W^-\bar{b}$. When integrated over the total available phase space the contribution from the $t\bar{t}$ amplitude to the cross section is, at the LHC, about one order of magnitude larger than the lowest order tW cross section. Thus, if one wants to investigate the "genuine" tW mode, the $t\bar{t}$ terms must be suppressed by appropriate cuts.
Several methods were proposed and studied in the literature. One approach is to make a cut on the invariant mass of the $W^-\bar{b}$ system to prevent the $\bar{t}$ propagator from becoming resonant [303, 304]. Another method [305, 306] is to use a veto on the additional $\bar{b}$ jet, namely to accept only $\bar{b}$ with a transverse momentum below some value, typically $p_T^b <$ 50 GeV at the LHC. This suppresses contributions from $t\bar{t}$ intermediate states, too. In

order to obtain the "genuine" tW cross section to NLO QCD one should subtract from $\sigma(gg \to tW^-\bar{b})$ the leading-order $t\bar{t}$ contribution, i.e., $\sigma_{LO}(gg \to t\bar{t})B(\bar{t} \to W^-\bar{b})$ [305].
The NLO QCD corrections to the tW cross section were investigated in [307, 308]. NLO QCD predictions taking into account the semileptonic top decays and the leptonic W decays are also available [306]. Applying a b-jet veto, the NLO QCD corrections are moderate: $\sigma_{NLO}(p_T^{\bar{b}} < 50\text{GeV})/\sigma_{LO} \simeq 1.1$. Table 7 contains the results of [298, 299] for the hadronic tW cross sections at the Tevatron and LHC, where higher-order soft gluon corrections were taken into account, but no cut on $p_T^{\bar{b}}$ was applied. Input and error estimates are as mentioned at the end of section 5.1.1.

5.2. Signals and backgrounds; prospects for the LHC

Table 7 and the results given in section 4 imply that the total production rate for single t- and $\bar{t}$-quarks at the Tevatron and LHC is about 48% and 38% of the $t\bar{t}$ production rate, respectively. Thus, as already stated, the LHC will be also a single-top factory, with $\sim 3 \times 10^6$ t- and $\bar{t}$-quarks being produced already with $10\,\text{fb}^{-1}$ of integrated luminosity. However, observing singly produced top quarks is much more difficult than observing $t\bar{t}$ pairs, because the final states from single-top events are clouded by large backgrounds. Let us briefly discuss this, first for the t-channel production mode. In order to suppress the QCD background one is forced to search for semileptonic top-decays and to rely on b tagging. Thus one searches for the final states $tq \to Wbq \to \ell\nu_\ell bq$. A fair fraction of the signal events contain also an additional $\bar{b}$ jet, which has, however, most of the time a transverse momentum too low to be observable. A characteristic signature is provided by the light-quark jet. The t-channel W boson by which tq is produced deflects the initial-state light quark only a bit. At the Tevatron, the outgoing light-quark jet is therefore emitted most of time at large rapidity, i.e., very forward in the detector. At the pp collider LHC the light jets are emitted preferentially both into the forward and backward direction. Thus the signal consists of an isolated, high p_T charged lepton, large missing transverse energy/momentum, and two jets – one of which is a b jet and the other, light-quark jet has large pseudorapidity η ($|\eta|$) at the Tevatron (LHC).
For the s-channel production mode the signal is $t\bar{b} \to \ell\nu_\ell b\bar{b}$, i.e., an isolated, high p_T charged lepton, large missing transverse energy/momentum, and two b-jets.
The background to these modes is huge and consists of a number of processes. Irreducible background arises from gauge boson plus heavy-quark production: Wdb, $Wb\bar{b}$, WZ, with $W \to \ell\nu_\ell$ and $Z \to b\bar{b}$. Considerable background arises also from Wc and $Wc\bar{c}$ production. Moreover, a significant background is due to the production of W + two light jets, where one of the jets fakes a b quark. Severe background is due to $t\bar{t}$ production with subsequent decay into dileptonic and lepton + jets channels, when only one of the leptons (in the $\ell\ell$ channels), respectively only 2 jets (in the $\ell + j$ channels) are observed. QCD multijet events have a huge cross section, but such background can be reduced substantially by considering only the above-mentioned signals.
The D0 and CDF collaborations reported evidence for single-top production at the Tevatron [3, 4]. The analyses used a number of discriminating variables and sophisticated

statistical methods. Using $0.9\,\mathrm{fb}^{-1}$ of data, D0 obtained for the sum of the t- and $\bar{t}$-quark production cross sections $\sigma^t + \sigma^{\bar{t}} = 4.7 \pm 1.3$ pb [3]. Assuming SM physics – i.e. putting the anomalous couplings in the tWb vetex to zero – this cross-section measurement implies the bound $0.68 < |V_{tb}| \leq 1$ (95% C.L.) on the CKM matrix element V_{tb}. The CDF experiment reports the result $\sigma^t + \sigma^{\bar{t}} = 2.2 \pm 0.7$ pb [4], based on $2.2\,\mathrm{fb}^{-1}$ of data. From this measurement the value $|V_{tb}| = 0.88 \pm 0.14\,(exp.) \pm 0.07\,(th.)$ was extracted. While the central value of the D0 and CDF cross-section result is a bit on the high and low side, respectively, compared with the t- plus s-channel predictions collected in table 7, the measurements are nevertheless in agreement with the SM.

For the LHC prospects are brighter to actually disentangle the different single-top production modes and to use them for a detailed exploration of the physics involved. Simulation studies were performed by the ATLAS [79] and the CMS collaboration [23]. For the t-channel mode a signal-to-background ratio $N_S/N_B = 1.34$ and a significance $S_{\mathrm{stat}} = N_S/\sqrt{N_S + N_B} = 37$ can be reached [23]. The t-channel cross section is expected to be measurable with a total error of 10%. This implies, assuming SM physics, that the CKM matrix element V_{tb} can be determined with 5% accuracy.

The tW mode, which has the second-highest yield at the LHC, has two W bosons and a b quark in the final state. In the simulation [23] only leptonic W decays were considered. Then the signals for this mode are $\ell^+\ell'^- b E_T^{\mathrm{miss}}$ and $\ell^\pm b\,j\,j\,E_T^{\mathrm{miss}}$ if the top quark decays semi- and non-leptonically, respectively. The dominant background arises from $t\bar{t}$ events. Other background comes from $Wb\bar{b}$, W + jets, WW + jets, from QCD multijets, and from t-channel single-top production. The study concludes that a statistical significance of 6.4 can be reached by combining the two channels. The estimated uncertainties for the cross section measurements in the dilepton and single lepton channels is 26% and 23%, respectively.

For the cross section of the s-channel top production mode at the LHC a measurement uncertainty of 36% was estimated [23].

5.3. Top-quark polarization

Because the weak interactions are involved in single-top production, the produced sample of t and $\bar{t}$ quarks is highly polarized, and the decay products are correlated with the top spin – c.f. the decay-angular distributions (3.11), (3.12). These distributions depend not only on the structure of the top-decay vertex, but also on the polarization degree p_t ($p_{\bar{t}}$) of the (anti)top quark. The polarization degree characterizes the production dynamics of the top quark. Sizeable contributions from the exchange of new particles, for instance, heavy $W'^\pm$ bosons having also right-handed couplings, or charged Higgs bosons $H^\pm$ would leave their mark in this observable. Thus, these decay angular distributions contain important information about top quark production and decay. (See, however, the remark at the end of section 3.2.1.)

For a specific production dynamics the top polarization degree depends on the choice of the reference axis, i.e., on which "top-spin quantization axis" is chosen. Within the SM this issue was investigated exhaustively for the s- and t-channel modes at the Tevatron

[309] and for the t-channel mode at the LHC [310]. Here we review only the case of the t-channel mode at the LHC in some detail, for which the experimental investigation of top-spin effects may be feasible with reasonable precision. First we recall that about 80% of the processes for t-quark production, $ub \to dt$ and $cb \to st$, have a d-type quark in the final state. Crossing symmetry relates the lowest-order amplitude for these processes, figure 8a, to the amplitude for nonleptonic top-decay, $t \to bu\bar{d}$. From the discussion in section 3.1.3 we know that the spin of the t quark is maximally correlated with the direction of the d-type quark. For the case at hand this implies that the sample of t quarks produced by these processes is 100% polarized in the direction of the d-type jet – the spectator jet – with the jet direction determined in the top-quark rest frame. This direction is called the spectator basis. Higher-order QCD corrections (gluon radiation) will dilute this maximal correlation somewhat. Considering the subsequent semileptonic decay of the t quark, i.e., $pp \to dt \to d\ell^+\nu_\ell b$, we have the decay-angular distribution

$$\frac{1}{\sigma^t}\frac{\mathrm{d}\sigma^t}{\mathrm{d}\cos\theta_+} = \frac{1}{2}\,(1 + p_t\, c_+ \cos\theta_+)\,, \quad p_t = \frac{N_\uparrow - N_\downarrow}{N_\uparrow + N_\downarrow}\,, \tag{5.2}$$

where θ_+ is the angle between the direction of charged lepton ℓ^+ and the chosen spin axis, in the t rest frame. The coefficient c_+ is the spin-analyzing power of ℓ^+ which is $+1$ in the SM (see table 3). This distribution implies a lepton asymmetry with respect to the chosen axis, $A^t_{\uparrow\downarrow} = p_t c_+$. From the above discussion – and the remark in brackets in the middle of the next paragraph – we expect $A^t_{\uparrow\downarrow} \sim 100\%$ for the spectator basis.

In the case of $\bar{t}$ production, the probability for the spectator jet being a d-type jet is only about 31%, while in about 69% the d-type quarks are in the initial state, being supplied by one of the proton beams (c.f. section 5.1.1). At first sight it seems that using the spectator direction as spin basis for the $\bar{t}$ quark is not a good choice. However, as was discussed in section 5.2, the direction of the spectator jet nearly coincides with the direction of the incoming light quark. Thus, even when the d-type quark is in the initial state, the polarization degree $p_{\bar{t}}$ will not be degraded very much when choosing the spectator direction as spin basis. (This applies also to the case of t-quark production discussed above, where about 20% of the events arise from d-type quarks in the initial state.) Considering again the crossed process, $\bar{t} \to \bar{b}d\bar{u}$, we know from section 3.1.3 that the spin of the $\bar{t}$ quark is maximally anti-correlated with the direction of the d-type quark. Thus the produced sample of $\bar{t}$ quarks will have a large negative polarization $p_{\bar{t}}$, close to -100%, with respect to the direction of the spectator jet. For the subsequent semileptonic decay of the $\bar{t}$ quark, $pp \to j\bar{t} \to j\ell^-\bar{\nu}_\ell\bar{b}$, we have, in analogy to (5.2), the decay-angular distribution

$$\frac{1}{\sigma^{\bar{t}}}\frac{\mathrm{d}\sigma^{\bar{t}}}{\mathrm{d}\cos\theta_-} = \frac{1}{2}\,(1 + p_{\bar{t}}\, c_- \cos\theta_-)\,, \tag{5.3}$$

where $c_- = -1$ is the spin-analyzing power of ℓ^-. Thus the spin-asymmetries $A^t_{\uparrow\downarrow}$ and $A^{\bar{t}}_{\uparrow\downarrow}$ which appear in the distributions (5.2) and (5.3) are both positive. This implies that in experimental analyses the t- and $\bar{t}$-quark samples may be combined without diluting the resulting decay-angular distribution. This would be necessary if the sign of the charged lepton cannot be determined.

This discussion suggests that another good choice for the top-spin axis should be the direction of one of the proton beams, as seen in the $\bar{t}$ (respectively t) quark rest frame. As the two beams are not back-to-back in this frame, one should choose the direction of that beam which is most closely aligned with the spectator jet on an event-by-event basis [309, 310]. This reference axis is called the beamline basis.

As the top quarks produced in the t-channel process at the LHC have relatively large velocities, one might envisage also the traditional helicity basis. In fact, inspection of the spin configurations allowed by the $V-A$ law and angular momentum conservation in the $2 \to 2$ processes figure 8a yields that the t and $\bar{t}$ quarks have negative and positive helicities, respectively, in the center-of-mass frame of the initial partons. However, this frame is not collinear-safe, as discussed in section 4.5. One may determine the t- and $\bar{t}$-quark directions of flight in the laboratory frame (lab. helicity basis), which is unambiguous theoretically. With respect to this frame a sizable fraction of t ($\bar{t}$) quarks has however also positive (negative) helicities. Thus the polarization degrees p_t and $p_{\bar{t}}$ with respect to the laboratory helicity basis of the t and $\bar{t}$ quarks are expected to be smaller than in the above spin bases.

Table 8 contains the results of a leading-order computation [310] of the spin fractions and polarization degrees p_t and $p_{\bar{t}}$, for the case of the LHC and the three spin bases discussed above. The $2 \to 3$ processes $qg \to q' t \bar{b}$ (see section 5.1.1) were also taken into account. The applied selection cuts for p_T^{ℓ}, $p_T^{\rm miss}$, p_T^b, and the p_T and pseudorapidity range of the spectator jet increase the spin fractions. The results corrobate the qualitative discussion above: the spectator and the beamline bases yield the highest polarization degrees in the SM. Nevertheless, the t- and $\bar{t}$-quark polarizations should be measured for all spin bases in order to explore the production dynamics in detail. If single-top production is influenced by new interactions with a chiral structure different from $V-A$ then this can affect the polarization degree for each spin basis in a different way.

An experimental issue is the precision with which the top-quark rest frame can be reconstructed. The unobserved momentum of the neutrino from semileptonic top decay leads to a two-fold ambiguity in the kinematic reconstruction (c.f. section 4.5). More detailed studies must take into account also the effect of background contributions to and the effects of energy smearing on the distributions (5.2) and (5.3). Studies made so far include [5, 79].

As to the polarization of top quarks produced by the tW mode, which has the second-largest cross section at the LHC, the situation is more complicated. Consider the lowest-order amplitude, given by the sum of the diagrams figure 8c and 8d. While in the contribution figure 8c the top-quark state has left-handed chirality at the production vertex (btW vertex), left- and right-handed chiralities appear with equal strength in the diagram figure 8c ($gt\bar{t}$ vertex), which will dilute the top-quark polarization degree. The issue was analyzed in [311]. For the final states $tW^- \to b\ell^+\nu_\ell \ell'^- \bar{\nu}_{\ell'}$ it was found that one can select a sample of top quarks with polarization vector preferentially close to the direction of of the charged lepton ℓ'^- from W^- decay by applying appropriate cuts which reduce top-quark contributions with opposite polarization. It remains to be demonstrated whether polarization measurements with reasonable precision are feasible for the tW mode at the

Table 8: SM predictions for the dominant spin fraction and polarization degree of t and $\bar{t}$ quarks for several t and $\bar{t}$ spin bases in the t-channel mode at the LHC [310], with selection cuts as specified in this reference. The acronym bml denotes the beamline basis; L, R denote negative and positive helicity, respectively.

	basis	fraction	polarization p
t:	lab. helicity	74% $\downarrow$ (L)	-0.48
	spectator	99% $\uparrow$	0.99
	bml	98% $\uparrow$	0.96
$\bar{t}$:	lab. helicity	70% $\uparrow$ (R)	0.41
	spectator	98% $\downarrow$	-0.96
	bml	99% $\uparrow$	-0.97

LHC.

5.4. New physics effects

New physics effects in single-top production could manifest themselves by modifications of the strength and structure of the SM tWb vertex or, more generally, by the effects of virtual new particle exchanges. New particles might also appear as resonances in s-channel single-top production or in association with a top quark. New mechanisms like FCNC interactions could lead to enhanced production rates or exotic final states, e.g., "like-sign" tt or $\overline{tt}$ events.

First of all, single-top production probes the strength of the charged weak interactions of the top quark. The expected measurement uncertainty of the t-channel cross section at the LHC (see section 5.2) implies that this strength may be determined eventually with an accuracy of about 5%. If one assumes that the main effect of new physics is the modification of the SM tWb vertex, one may use the general parameterization (3.13) and compute the effects of the anomalous couplings on the single-top production cross sections. (More generally, one may take additional couplings into account [312], which appear when the t and b quarks involved are off-shell.) In combination with the helicity fractions $F_{0,\pm}$ discussed in sections 3.1.2 and 3.2.1 one can uniquely determine the four anomalous couplings by fits to (future) data [62]. For analyses taking into account also effective $qq'tb$ production vertices, see for instance [313, 314].

A number of investigations were made in specific extensions of the SM to determine the effects on the production rates of virtual new particle exchanges, in particular in the MSSM, the presently most popular paradigm for new physics. The supersymmetric QCD corrections to the three single-top production modes were calculated in [315], and the electroweak MSSM corrections to the t-channel and tW modes were computed in [296, 316]. The effects on the cross sections and on distributions are modest to small, of the

order of a few percent at most. This complies with the smallness of the supersymmetric quantum corrections in top decays $t \to b f f'$ – c.f. section 3.2.

New heavy charged boson resonances may exist that (strongly) couple to top quarks. Heavy vector bosons $W'^{\pm}$ are predicted by several SM extensions, such as left-right-symmetric models [317–319], or technicolour models and their descendants [100, 320]. Heavy charged Higgs bosons $H^{\pm}$ appear in many SM extensions, for instance in the MSSM. Topcolour models predict top-pions $\pi_t^{\pm}$ [100] whose masses might be as low as several hundred GeV. If such resonances exist they can contribute significantly to the s-channel rate, $q\bar{q}' \to W'^{+}, W^{+} \to t\bar{b}$ (with interference effects which might be significant, depending on the mass and width of W') and $c\bar{b} \to \phi^{+} \to t\bar{b}$ ($\phi^{+} = H^{+}, \pi_t^{+}$) [320–323]. The LHC should eventually be sensitive to resonances which preferentially couple to heavy quarks, with masses up to a few TeV. The t-channel exchange of heavy charged bosons $X^{\pm}$ is marginal to negligible, as their contribution to the cross section is suppressed by $1/m_X^2$. Heavy W' bosons with SM couplings and masses below 1 TeV have been excluded by the D0 collaboration at the Tevatron from the search for their leptonic decays $W' \to \ell\nu_\ell$ [324]. The CDF experiment has searched for $W' \to tb$ and excludes a W' with a mass below 790 GeV having this decay mode [93]. Lower bounds on the masses and couplings of such resonances can also be derived from the measurement of the sum of the s- and t-channel single top-production cross section at the Tevatron [23] which is in agreement, within errors, with the SM prediction.

Charged bosons could also be produced in association with top quarks. For charged Higgs bosons $H^{\pm}$ this was investigated for the LHC in [325], with the conclusion that some perspectives for a discovery exist if the $H^{\pm}$ are rather light.

Single-top production is also a good place to search for FCNC interactions involving the top quark. If sizeable $t \leftrightarrow c, u$ transitions exist, they would lead not only to new top-decay modes (as discussed in section 3.2.4), but also to new production processes, e.g., $cg \to t$, $gg \to t\bar{c}$, $cg \to tX^0$ ($X^0 = g, Z, \gamma, h$). Many theoretical investigations have been made on this subject. A rather general approach is to use effective Lagrangians, i.e., to classify the relevance of possible FCNC interactions of the top quark in terms of inverse powers of some large scale $\Lambda \sim 1$ TeV, and to parameterize them by dimensionless anomalous couplings [5, 326–329]. Other studies have investigated the above FCNC production processes within specific SM extensions, in particular in the MSSM [109, 330, 331] and in topcolour-type models [332]. In the MSSM the supersymmetry-breaking terms provide a new source of flavour violation, which leads to FCNC processes at one-loop order. A systematic investigation of various FCNC single-top production and decay processes in the MSSM was made in [109]. Taking into account phenomenological constraints, this study and [331] conclude that the cross section for $gg \to t\bar{c}$ is at most 0.7 to 1 pb. However, this mode has a huge irreducible SM background: the $t\bar{c}$ production rate in the SM is more than 12 times larger. Moreover, it is unlikely that this final state can be separated from the much more frequent $t\bar{q}$ events (see section 5.1.1). A cleaner signature arises from the FCNC process $cg \to t$, whose cross section in the MSSM is, however, also not larger than about 1 pb [109]. Topcolour-type models predict somewhat larger FCNC effects [332].

An interesting signature caused by FCNC gqt couplings is the production of like-sign

top pairs, $qq \to tt$, $\overline{qq} \to \overline{tt}$ $(q = u, c)$ [328, 333] whose signature is two like-sign high p_T leptons plus two hard b-jets. The ATLAS collaboration has investigated the potential reach of the LHC to this mode in terms of sensitivity limits to anomalous gtc and gtu couplings [79].

While the best place to search for FCNC transitions $t \leftrightarrow c, u$ involving the photon and Z boson are top decays, hadronic single-top production is mostly sensitive to FCNC couplings involving the gluon. The D0 collaboration at the Tevatron searched for the production of single top quarks by FCNC gtc and gtu couplings and set upper limits on respective anomalous coupling parameters, as no significant deviation from the SM prediction was observed [118]. At the LHC the sensitivity to FCNC gluon top-quark couplings should increase by one to two orders of magnitude [5].

In summary, from the measurements of the cross sections of the three production modes (5.1) and the t- and $\bar{t}$-quark polarizations, and from the search for exotic final states, a detailed exploration of the weak interactions – or, more general, flavour-changing interactions – of the top quark should be possible at the LHC.

6. Summary and outlook

An impressive amount of insight has been gained to date into the properties and interactions of the top quark. Yet it seems fair to say that the physics of this quark remains to be fully explored in the years to come, both in $t\bar{t}$ and single top-quark production and decay. This particle provides the unique opportunity to explore the physics of a bare quark at distances below the attometer scale. LHC experiments will probe, in the $t\bar{t}$ channel, the existence of heavy resonances with masses up to several TeV. These searches will, in particular, help to clarify the mechanism of electroweak gauge symmetry breaking. The search for non-standard Higgs bosons and/or non-standard CP violation will provide important laboratory tests of electroweak baryogenesis scenarios. A precise measurement of the $M_{t\bar{t}}$ and p_T distributions, especially of their high-energy tails, and of correlations and asymmetries will be an important issue in the high-luminosity phase of the LHC. Angular distributions and correlations due to top-spin effects should become, at the LHC, important tools in the investigations of the dynamics of top quarks. At the LHC the sensitivity to FCNC interactions involving the top quark should reach a level $\sim 10^{-4}$.

The standard model predictions for top quarks as a signal at the LHC are, by and large, in reasonably good shape. Yet there are still a number of challenges which include the following issues: As reviewed above, the top mass has been determined already with a relative uncertainty of 0.8%, and this error on m_t^{exp} will be further reduced in future measurements. An interpretation of m_t^{exp} in terms of a Lagrangian mass parameter is, however, presently not possible at this level of precision. Observables should be identified, which can be both computed and measured with reasonable precision, that allow the determination of a well-defined top mass parameter with an uncertainty of about 2 GeV or better. Furthermore, the $t\bar{t}$ cross section at the LHC may eventually be measurable with an uncertainty of about 5%. This requires the SM prediction for $\sigma_{LHC}^{t\bar{t}}$ to reach

the same level of precision, which necessitates the complete computation of the NNLO QCD corrections. Moreover, a number of distributions, including the $M_{t\bar{t}}$ and p_T distribution, and their theory errors should be determined more precisely. Furthermore, these improvements will have to be included into Monte Carlo simulation programs. In view of the progress that hadron collider phenomenology has experienced in the recent past, one can be quite confident that at least some of these issues will be resolved in the not too distant future.

Acknowledgements

I am grateful to Martin Beneke, Stefan Berge, Sven Moch, Peter Uwer, Zongguo Si, Wolfgang Wagner, and Peter Zerwas for helpful discussions, to Sven Moch for providing figure 4, and to Alan D. Martin for suggesting to write this review. This work was supported by Deutsche Forschungsgemeinschaft SFB/TR9.

References

[1] F. Abe *et al.* [CDF Collaboration], Phys. Rev. Lett. **74** (1995) 2626 [arXiv:hep-ex/9503002].

[2] S. Abachi *et al.* [D0 Collaboration], Phys. Rev. Lett. **74** (1995) 2632 [arXiv:hep-ex/9503003].

[3] V. M. Abazov *et al.* [D0 Collaboration], Phys. Rev. Lett. **98** (2007) 181802 [arXiv:hep-ex/0612052];
V. M. Abazov *et al.* [D0 Collaboration], "Evidence for production of single top quarks," arXiv:0803.0739 [hep-ex].

[4] `http://www-cdf.fnal.gov/physics/new/top/public_singletop.html`
CDF Collaboration, "Combination of CDF Single Top Quark Searches with 2.2 fb^{-1} of Data," CDF Note 9251 (2008).

[5] M. Beneke *et al.*, "Top quark physics," arXiv:hep-ph/0003033.

[6] D. Chakraborty, J. Konigsberg and D. L. Rainwater, Ann. Rev. Nucl. Part. Sci. **53** (2003) 301 [arXiv:hep-ph/0303092].

[7] W. Wagner, Rept. Prog. Phys. **68** (2005) 2409 [arXiv:hep-ph/0507207].

[8] A. Quadt, Eur. Phys. J. C **48** (2006) 835.

[9] M. Beneke and V. M. Braun, Nucl. Phys. B **426** (1994) 301 [arXiv:hep-ph/9402364].

[10] I. I. Y. Bigi, M. A. Shifman, N. G. Uraltsev and A. I. Vainshtein, Phys. Rev. D **50** (1994) 2234 [arXiv:hep-ph/9402360].

[11] P. Ball, M. Beneke and V. M. Braun, Nucl. Phys. B **452** (1995) 563 [arXiv:hep-ph/9502300].

[12] M. C. Smith and S. S. Willenbrock, Phys. Rev. Lett. **79** (1997) 3825 [arXiv:hep-ph/9612329].

[13] N. Gray, D. J. Broadhurst, W. Grafe and K. Schilcher, Z. Phys. C **48** (1990) 673.

[14] K. G. Chetyrkin and M. Steinhauser, Phys. Rev. Lett. **83** (1999) 4001 [arXiv:hep-ph/9907509].

[15] K. Melnikov and T. v. Ritbergen, Phys. Lett. B **482** (2000) 99 [arXiv:hep-ph/9912391].

[16] T. T. E. Group *et al.* [CDF Collaboration], "A Combination of CDF and D0 Results on the Mass of the Top Quark," arXiv:0803.1683 [hep-ex].

[17] [CDF Collaboration], "A Combination of CDF and D0 results on the mass of the top quark," arXiv:hep-ex/0703034.

[18] J. Alcaraz *et al.* [LEP Collaborations], "Precision Electroweak Measurements and Constraints on the Standard Model," arXiv:0712.0929 [hep-ex].

[19] W. M. Yao *et al.* [Particle Data Group], J. Phys. G **33** (2006) 1.

[20] I. I. Y. Bigi, Y. L. Dokshitzer, V. A. Khoze, J. H. Kühn and P. M. Zerwas, Phys. Lett. B **181** (1986) 157.

[21] J. H. Kühn, Nucl. Phys. B **237** (1984) 77.

[22] F. Hubaut, E. Monnier, P. Pralavorio, K. Smolek and V. Simak, Eur. Phys. J. C **44S2** (2005) 13 [arXiv:hep-ex/0508061].

[23] G. L. Bayatian *et al.* [CMS Collaboration], J. Phys. G **34**, 995 (2007).

[24] E. L. Berger and T. M. P. Tait, "Top spin and experimental tests," arXiv:hep-ph/0002305.

[25] D. Chang, W. F. Chang and E. Ma, Phys. Rev. D **59** (1999) 091503 [arXiv:hep-ph/9810531].

[26] V. M. Abazov *et al.* [D0 Collaboration], Phys. Rev. Lett. **98** (2007) 041801 [arXiv:hep-ex/0608044].

[27] A. Beretvas *et al.* [CDF Collaboration], "Finding the charge of the top quark in the dilepton channel," arXiv:0707.1339 [hep-ex].

[28] S. Leone [CDF Collaboration], "Electroweak and Top Physics at the Tevatron and Indirect Higgs Limits," arXiv:0710.4983 [hep-ex].

[29] V. M. Abazov *et al.* [D0 Collaboration], "Simultaneous measurement of the ratio $B(t \to Wb)/B(t \to Wq)$ and the top quark pair production cross section with the D0 detector at $\sqrt{s}$ =1.96 TeV," arXiv:0801.1326 [hep-ex].

[30] M. Jezabek and J. H. Kühn, Nucl. Phys. B **314** (1989) 1.

[31] A. Denner and T. Sack, Nucl. Phys. B **358** (1991) 46.

[32] G. Eilam, R. R. Mendel, R. Migneron and A. Soni, Phys. Rev. Lett. **66** (1991) 3105.

[33] M. Jezabek and J. H. Kühn, Phys. Rev. D **48** (1993) 1910 [Erratum-ibid. D **49** (1994) 4970] [arXiv:hep-ph/9302295].

[34] A. Czarnecki and K. Melnikov, Nucl. Phys. B **544** (1999) 520 [arXiv:hep-ph/9806244].

[35] K. G. Chetyrkin, R. Harlander, T. Seidensticker and M. Steinhauser, Phys. Rev. D **60** (1999) 114015 [arXiv:hep-ph/9906273].

[36] H. S. Do, S. Groote, J. G. Körner and M. C. Mauser, Phys. Rev. D **67** (2003) 091501 [arXiv:hep-ph/0209185].

[37] M. Fischer, S. Groote, J. G. Körner and M. C. Mauser, Phys. Rev. D **65** (2002) 054036 [arXiv:hep-ph/0101322].

[38] J. A. Aguilar-Saavedra, J. Carvalho, N. Castro, F. Veloso and A. Onofre, Eur. Phys. J. C **50** (2007) 519 [arXiv:hep-ph/0605190].

[39] A. Abulencia *et al.* [CDF II Collaboration], Phys. Rev. D **75** (2007) 052001 [arXiv:hep-ex/0612011].

[40] A. Abulencia *et al.* [CDF Collaboration], Phys. Rev. Lett. **98** (2007) 072001 [arXiv:hep-ex/0608062].

[41] V. M. Abazov *et al.* [D0 Collaboration], Phys. Rev. D **75** (2007) 031102 [arXiv:hep-ex/0609045].

[42] V. M. Abazov *et al.* [D0 Collaboration], "Model-independent measurement of the W boson helicity in top quark decays," arXiv:0711.0032 [hep-ex].

[43] J. A. Aguilar-Saavedra, J. Carvalho, N. Castro, A. Onofre and F. Veloso, arXiv:0705.3041 [hep-ph].

[44] A. Czarnecki, M. Jezabek and J. H. Kühn, Nucl. Phys. B **351** (1991) 70.

[45] A. Brandenburg, Z. G. Si and P. Uwer, Phys. Lett. B **539** (2002) 235 [arXiv:hep-ph/0205023].

[46] M. Fischer, S. Groote, J. G. Körner, M. C. Mauser and B. Lampe, Phys. Lett. B **451** (1999) 406 [arXiv:hep-ph/9811482].

[47] M. Jezabek and J. H. Kühn, Phys. Lett. B **329** (1994) 317 [arXiv:hep-ph/9403366].

[48] W. Bernreuther, M. Fuecker and Y. Umeda, Phys. Lett. B **582** (2004) 32 [arXiv:hep-ph/0308296].

[49] W. Bernreuther, O. Nachtmann, P. Overmann and T. Schröder, Nucl. Phys. B **388** (1992) 53 [Erratum-ibid. B **406** (1993) 516].

[50] J. P. Ma and A. Brandenburg, Z. Phys. C **56** (1992) 97.

[51] G. L. Kane, G. A. Ladinsky and C. P. Yuan, Phys. Rev. D **45** (1992) 124.

[52] K. Fujikawa and A. Yamada, Phys. Rev. D **49** (1994) 5890.

[53] P. L. Cho and M. Misiak, Phys. Rev. D **49** (1994) 5894 [arXiv:hep-ph/9310332].

[54] B. Grzadkowski and M. Misiak, "Anomalous Wtb coupling effects in the weak radiative B-meson decay," arXiv:0802.1413 [hep-ph].

[55] F. Larios, M. A. Perez and C. P. Yuan, Phys. Lett. B **457** (1999) 334 [arXiv:hep-ph/9903394].

[56] G. Burdman, M. C. Gonzalez-Garcia and S. F. Novaes, Phys. Rev. D **61** (2000) 114016 [arXiv:hep-ph/9906329].

[57] A. Brandenburg and M. Maniatis, Phys. Lett. B **545** (2002) 139 [arXiv:hep-ph/0207154].

[58] J. j. Cao, R. J. Oakes, F. Wang and J. M. Yang, Phys. Rev. D **68** (2003) 054019 [arXiv:hep-ph/0306278].

[59] H. J. He, T. Tait and C. P. Yuan, Phys. Rev. D **62** (2000) 011702 [arXiv:hep-ph/9911266].

[60] K. i. Hikasa, K. Whisnant, J. M. Yang and B. L. Young, Phys. Rev. D **58** (1998) 114003 [arXiv:hep-ph/9806401].

[61] E. Boos, L. Dudko and T. Ohl, Eur. Phys. J. C **11** (1999) 473 [arXiv:hep-ph/9903215].

[62] C. R. Chen, F. Larios and C. P. Yuan, Phys. Lett. B **631** (2005) 126 [AIP Conf. Proc. **792** (2005) 591] [arXiv:hep-ph/0503040].

[63] W. Bernreuther and P. Overmann, Z. Phys. C **61** (1994) 599.

[64] C. A. Nelson, B. T. Kress, M. Lopes and T. P. McCauley, Phys. Rev. D **56** (1997) 5928 [arXiv:hep-ph/9707211].

[65] C. A. Nelson and A. M. Cohen, Eur. Phys. J. C **8** (1999) 393 [arXiv:hep-ph/9806373].

[66] C. A. Nelson and L. J. . Adler, Eur. Phys. J. C **17** (2000) 399 [arXiv:hep-ph/0007086].

[67] B. Grzadkowski and Z. Hioki, Phys. Lett. B **476** (2000) 87 [arXiv:hep-ph/9911505].

[68] S. D. Rindani, Pramana **54** (2000) 791 [arXiv:hep-ph/0002006].

[69] R. M. Godbole, S. D. Rindani and R. K. Singh, JHEP **0612** (2006) 021 [arXiv:hep-ph/0605100].

[70] J. F. Gunion, H. E. Haber, G. L. Kane and S. Dawson, "The Higgs Hunter's Guide," Westview Press, Cambridge, Mass. (1990).

[71] P. Gambino and M. Misiak, Nucl. Phys. B **611** (2001) 338 [arXiv:hep-ph/0104034].

[72] C. S. Li and T. C. Yuan, Phys. Rev. D **42** (1990) 3088 [Erratum-ibid. D **47** (1993) 2156].

[73] A. Czarnecki and S. Davidson, Phys. Rev. D **48** (1993) 4183 [arXiv:hep-ph/9301237].

[74] J. A. Coarasa, D. Garcia, J. Guasch, R. A. Jimenez and J. Sola, Eur. Phys. J. C **2** (1998) 373 [arXiv:hep-ph/9607485].

[75] M. S. Carena, D. Garcia, U. Nierste and C. E. M. Wagner, Nucl. Phys. B **577** (2000) 88 [arXiv:hep-ph/9912516].

[76] V. M. Abazov *et al.* [D0 Collaboration], Phys. Rev. Lett. **88** (2002) 151803 [arXiv:hep-ex/0102039].

[77] A. Abulencia *et al.* [CDF Collaboration], Phys. Rev. Lett. **96** (2006) 042003 [arXiv:hep-ex/0510065].

[78] G. Grenier, "Search for supersymmetric charged Higgs bosons at the TeVatron," arXiv:0710.0853 [hep-ex].

[79] "ATLAS detector and physics performance. Technical design report. Vol. 2,", report CERN-LHCC-99-15.

[80] J. G. Körner and M. C. Mauser, "O(alpha(s)) radiative corrections to polarized top decay into a charged Higgs t(pol.) $\to H^+$ + b," arXiv:hep-ph/0211098.

[81] J. R. Ellis and S. Rudaz, Phys. Lett. B **128** (1983) 248.

[82] K. I. Hikasa and M. Kobayashi, Phys. Rev. D **36** (1987) 724.

[83] H. Baer, M. Drees, R. Godbole, J. F. Gunion and X. Tata, Phys. Rev. D **44** (1991) 725.

[84] W. Porod, Phys. Rev. D **59** (1999) 095009 [arXiv:hep-ph/9812230].

[85] C. Boehm, A. Djouadi and Y. Mambrini, Phys. Rev. D **61** (2000) 095006 [arXiv:hep-ph/9907428].

[86] A. A. Affolder *et al.* [CDF Collaboration], Phys. Rev. D **63** (2001) 091101 [arXiv:hep-ex/0011004].

[87] M. Hosch, R. J. Oakes, K. Whisnant, J. M. Yang, B. l. Young and X. Zhang, Phys. Rev. D **58** (1998) 034002 [arXiv:hep-ph/9711234].

[88] D. E. Acosta *et al.* [CDF Collaboration], Phys. Rev. Lett. **90** (2003) 251801 [arXiv:hep-ex/0302009].

[89] V. M. Abazov *et al.* [D0 Collaboration], Phys. Lett. B **659** (2008) 500 [arXiv:0707.2864 [hep-ex]].

[90] V. M. Abazov *et al.* [D0 collaboration], Phys. Lett. B **581** (2004) 147.

[91] V. M. Abazov *et al.* [D0 Collaboration], Phys. Lett. B **645** (2007) 119 [arXiv:hep-ex/0611003].

[92] T. Aaltonen *et al.* [CDF Collaboration], Phys. Rev. D **76** (2007) 072010 [arXiv:0707.2567 [hep-ex]].

[93] A. Duperrin [CDF Collaboration], "Searches for Higgs and BSM at the Tevatron," arXiv:0710.4265 [hep-ex].

[94] M. S. Carena, M. Quiros and C. E. M. Wagner, Nucl. Phys. B **524** (1998) 3 [arXiv:hep-ph/9710401].

[95] S. L. Glashow, J. Iliopoulos and L. Maiani, Phys. Rev. D **2** (1970) 1285.

[96] J. L. Diaz-Cruz, R. Martinez, M. A. Perez and A. Rosado, Phys. Rev. D **41** (1990) 891.

[97] G. Eilam, J. L. Hewett and A. Soni, Phys. Rev. D **44** (1991) 1473 [Erratum-ibid. D **59** (1999) 039901].

[98] B. Mele, S. Petrarca and A. Soddu, Phys. Lett. B **435** (1998) 401 [arXiv:hep-ph/9805498].

[99] J. Carvalho *et al.* [ATLAS Collaboration], Eur. Phys. J. C **52** (2007) 999 [arXiv:0712.1127 [hep-ex]].

[100] C. T. Hill and E. H. Simmons, Phys. Rept. **381** (2003) 235 [Erratum-ibid. **390** (2004) 553] [arXiv:hep-ph/0203079].

[101] C. Valenzuela, Phys. Rev. D **71** (2005) 095014 [arXiv:hep-ph/0503111].

[102] J. A. Aguilar-Saavedra, Acta Phys. Polon. B **35** (2004) 2695 [arXiv:hep-ph/0409342].

[103] M. E. Luke and M. J. Savage, Phys. Lett. B **307** (1993) 387 [arXiv:hep-ph/9303249].

[104] D. Atwood, L. Reina and A. Soni, Phys. Rev. D **55** (1997) 3156 [arXiv:hep-ph/9609279].

[105] J. M. Yang and C. S. Li, Phys. Rev. D **49** (1994) 3412 [Erratum-ibid. D **51** (1995) 3974].

[106] J. Guasch and J. Sola, Nucl. Phys. B **562** (1999) 3 [arXiv:hep-ph/9906268].

[107] D. Delepine and S. Khalil, Phys. Lett. B **599** (2004) 62 [arXiv:hep-ph/0406264].

[108] J. J. Liu, C. S. Li, L. L. Yang and L. G. Jin, Phys. Lett. B **599** (2004) 92 [arXiv:hep-ph/0406155].

[109] J. J. Cao, G. Eilam, M. Frank, K. Hikasa, G. L. Liu, I. Turan and J. M. Yang, Phys. Rev. D **75** (2007) 075021 [arXiv:hep-ph/0702264].

[110] G. Eilam, A. Gemintern, T. Han, J. M. Yang and X. Zhang, Phys. Lett. B **510** (2001) 227 [arXiv:hep-ph/0102037].

[111] K. J. Abraham, K. Whisnant, J. M. Yang and B. L. Young, Phys. Rev. D **63** (2001) 034011 [arXiv:hep-ph/0007280].

[112] G. r. Lu, F. r. Yin, X. l. Wang and L. d. Wan, Phys. Rev. D **68** (2003) 015002 [arXiv:hep-ph/0303122].

[113] J. A. Aguilar-Saavedra, Phys. Rev. D **67** (2003) 035003 [Erratum-ibid. D **69** (2004) 099901] [arXiv:hep-ph/0210112].

[114] S. Bar-Shalom, G. Eilam and A. Soni, Phys. Rev. D **60** (1999) 035007 [arXiv:hep-ph/9812518].

[115] F. Abe *et al.* [CDF Collaboration], Phys. Rev. Lett. **80** (1998) 2525.

[116] P. Achard *et al.* [L3 Collaboration], Phys. Lett. B **549** (2002) 290 [arXiv:hep-ex/0210041].

[117] S. Chekanov *et al.* [ZEUS Collaboration], Phys. Lett. B **559** (2003) 153 [arXiv:hep-ex/0302010].

[118] V. M. Abazov *et al.* [D0 Collaboration], Phys. Rev. Lett. **99** (2007) 191802 [arXiv:0801.2556 [hep-ex]].

[119] CDF Collaboration, "Search for the Flavor Changing Neutral Current Decay $t \to Zq$ in $p\bar{p}$ collisions at $\sqrt{s} = 1.96$ TeV with 1.9 fb^{-1} of CDF-II data," CDF Note 9202 (2008).

[120] I. Borjanovic *et al.*, Eur. Phys. J. C **39S2** (2005) 63 [arXiv:hep-ex/0403021].

[121] J. D'hondt, "Top Quark Physics at the LHC," arXiv:0707.1247 [hep-ph].

[122] P. Nason, S. Dawson and R. K. Ellis, Nucl. Phys. B **303** (1988) 607.

[123] W. Beenakker, H. Kuijf, W. L. van Neerven and J. Smith, Phys. Rev. D **40** (1989) 54.

[124] P. Nason, S. Dawson and R. K. Ellis, Nucl. Phys. B **327** (1989) 49 [Erratum-ibid. B **335** (1990) 260].

[125] W. Beenakker, W. L. van Neerven, R. Meng, G. A. Schuler and J. Smith, Nucl. Phys. B **351** (1991) 507.

[126] M. L. Mangano, P. Nason and G. Ridolfi, Nucl. Phys. B **373** (1992) 295.

[127] S. Frixione, M. L. Mangano, P. Nason and G. Ridolfi, Phys. Lett. B **351** (1995) 555 [arXiv:hep-ph/9503213].

[128] G. Sterman, Nucl. Phys. B **281** (1987) 310.

[129] S. Catani and L. Trentadue, Nucl. Phys. B **327** (1989) 323.

[130] N. Kidonakis and G. Sterman, Nucl. Phys. B **505** (1997) 321 [arXiv:hep-ph/9705234].

[131] R. Bonciani, S. Catani, M. L. Mangano and P. Nason, Nucl. Phys. B **529** (1998) 424 [arXiv:hep-ph/9801375].

[132] N. Kidonakis, E. Laenen, S. Moch and R. Vogt, Phys. Rev. D **64** (2001) 114001 [arXiv:hep-ph/0105041].

[133] N. Kidonakis and R. Vogt, Phys. Rev. D **68** (2003) 114014 [arXiv:hep-ph/0308222].

[134] A. Banfi and E. Laenen, Phys. Rev. D **71** (2005) 034003 [arXiv:hep-ph/0411241].

[135] W. Beenakker, A. Denner, W. Hollik, R. Mertig, T. Sack and D. Wackeroth, Nucl. Phys. B **411** (1994) 343.

[136] W. Bernreuther, M. Fuecker and Z. G. Si, Phys. Lett. B **633** (2006) 54 [arXiv:hep-ph/0508091].

[137] J. H. Kühn, A. Scharf and P. Uwer, Eur. Phys. J. C **45** (2006) 139 [arXiv:hep-ph/0508092].

[138] W. Bernreuther, M. Fuecker and Z. G. Si, Phys. Rev. D **74** (2006) 113005 [arXiv:hep-ph/0610334].

[139] W. Bernreuther, M. Fuecker and Z. G. Si, "Weak interaction corrections to hadronic top quark pair production: contributions from quark-gluon and $b\bar{b}$ induced reactions," arXiv:0804.1237 [hep-ph].

[140] J. H. Kühn, A. Scharf and P. Uwer, Eur. Phys. J. C **51** (2007) 37 [arXiv:hep-ph/0610335].

[141] S. Moretti, M. R. Nolten and D. A. Ross, Phys. Lett. B **639** (2006) 513 [Erratum-ibid. B **660** (2008) 607] [arXiv:hep-ph/0603083].

[142] W. Hollik and M. Kollar, Phys. Rev. D **77** (2008) 014008 [arXiv:0708.1697 [hep-ph]].

[143] S. Dittmaier, P. Uwer and S. Weinzierl, Phys. Rev. Lett. **98** (2007) 262002 [arXiv:hep-ph/0703120].

[144] W. Bernreuther, A. Brandenburg, Z. G. Si and P. Uwer, Phys. Rev. Lett. **87** (2001) 242002 [arXiv:hep-ph/0107086].

[145] W. Bernreuther, A. Brandenburg, Z. G. Si and P. Uwer, Nucl. Phys. B **690** (2004) 81 [arXiv:hep-ph/0403035].

[146] W. Beenakker, F. A. Berends and A. P. Chapovsky, Phys. Lett. B **454** (1999) 129 [arXiv:hep-ph/9902304].

[147] L. Meyer, diploma thesis, RWTH Aachen (2005).

[148] M. Czakon, A. Mitov and S. Moch, Phys. Lett. B **651** (2007) 147 [arXiv:0705.1975 [hep-ph]].

[149] M. Czakon, A. Mitov and S. Moch, "Heavy-quark production in gluon fusion at two loops in QCD," arXiv:0707.4139 [hep-ph].

[150] M. Czakon, "Mass effects and four-particle amplitudes at the two-loop level in QCD," arXiv:0803.1414 [hep-ph].

[151] J. G. Körner, Z. Merebashvili and M. Rogal, "NNLO $O(\alpha_s^4)$ results for heavy quark pair production in quark–antiquark collisions: The one-loop squared contributions," arXiv:0802.0106 [hep-ph].

[152] V. S. Fadin, V. A. Khoze and A. D. Martin, Phys. Rev. D **49** (1994) 2247.

[153] K. Melnikov and O. I. Yakovlev, Phys. Lett. B **324** (1994) 217 [arXiv:hep-ph/9302311].

[154] N. Kauer and D. Zeppenfeld, Phys. Rev. D **65** (2002) 014021 [arXiv:hep-ph/0107181].

[155] N. Kauer, Phys. Rev. D **67** (2003) 054013 [arXiv:hep-ph/0212091].

[156] M. L. Mangano and T. J. Stelzer, Ann. Rev. Nucl. Part. Sci. **55** (2005) 555.

[157] T. Sjostrand, L. Lonnblad, S. Mrenna and P. Skands, "PYTHIA 6.3: Physics and manual," arXiv:hep-ph/0308153.

[158] T. Sjostrand, S. Mrenna and P. Skands, "A Brief Introduction to PYTHIA 8.1," arXiv:0710.3820 [hep-ph].

[159] G. Corcella *et al.*, "HERWIG 6.5 release note," arXiv:hep-ph/0210213.

[160] M. Bahr *et al.*, "Herwig++ Physics and Manual," arXiv:0803.0883 [hep-ph].

[161] CEDAR: `http:/www.cedar.ac.uk/hepcode/`

[162] S. R. Slabospitsky and L. Sonnenschein, Comput. Phys. Commun. **148** (2002) 87 [arXiv:hep-ph/0201292].

[163] M. L. Mangano, M. Moretti, F. Piccinini, R. Pittau and A. D. Polosa, JHEP **0307** (2003) 001 [arXiv:hep-ph/0206293].

[164] F. Maltoni and T. Stelzer, JHEP **0302** (2003) 027 [arXiv:hep-ph/0208156].

[165] S. Tsuno, T. Kaneko, Y. Kurihara, S. Odaka and K. Kato, Comput. Phys. Commun. **175** (2006) 665 [arXiv:hep-ph/0602213].

[166] S. Frixione and B. R. Webber, "The MC@NLO 3.3 event generator," arXiv:hep-ph/0612272.

[167] J. Campbell, R. K. Ellis, "MCFM - Monte Carlo for FeMtobarn processes", `http://mcfm.fnal.gov/`

[168] R. K. Ellis, Nucl. Phys. Proc. Suppl. **160** (2006) 170.

[169] S. Frixione, P. Nason and G. Ridolfi, JHEP **0709** (2007) 126 [arXiv:0707.3088 [hep-ph]].

[170] S. Frixione, P. Nason and G. Ridolfi, arXiv:0707.3081 [hep-ph].

[171] E. E. Boos, V. E. Bunichev, L. V. Dudko, V. I. Savrin and A. V. Sherstnev, Phys. Atom. Nucl. **69** (2006) 1317 [Yad. Fiz. **69** (2006) 1352].

[172] J. Pumplin, D. R. Stump, J. Huston, H. L. Lai, P. Nadolsky and W. K. Tung, JHEP **0207** (2002) 012 [arXiv:hep-ph/0201195].

[173] A. D. Martin, R. G. Roberts, W. J. Stirling and R. S. Thorne, Eur. Phys. J. C **28** (2003) 455 [arXiv:hep-ph/0211080].

[174] A. D. Martin, R. G. Roberts, W. J. Stirling and R. S. Thorne, Eur. Phys. J. C **35** (2004) 325 [arXiv:hep-ph/0308087].

[175] S. Moch and P. Uwer, "Theoretical status and prospects for top-quark pair production at hadron colliders," arXiv:0804.1476 [hep-ph].

[176] M. Cacciari, S. Frixione, M. M. Mangano, P. Nason and G. Ridolfi, "Updated predictions for the total production cross sections of top and of heavier quark pairs at the Tevatron and at the LHC," arXiv:0804.2800 [hep-ph].

[177] M. Cacciari, S. Frixione, M. L. Mangano, P. Nason and G. Ridolfi, JHEP **0404** (2004) 068 [arXiv:hep-ph/0303085].

[178] S. Catani, M. L. Mangano, P. Nason and L. Trentadue, Phys. Lett. B **378** (1996) 329 [arXiv:hep-ph/9602208].

[179] W. K. Tung, H. L. Lai, A. Belyaev, J. Pumplin, D. Stump and C. P. Yuan, JHEP **0702** (2007) 053 [arXiv:hep-ph/0611254].

[180] A. D. Martin, W. J. Stirling, R. S. Thorne and G. Watt, Phys. Lett. B **652** (2007) 292 [arXiv:0706.0459 [hep-ph]].

[181] A. Abulencia *et al.* [CDF Collaboration], Phys. Rev. Lett. **97** (2006) 082004 [arXiv:hep-ex/0606017].

[182] T. Aaltonen *et al.* [CDF Collaboration], Phys. Rev. D **76** (2007) 072009 [arXiv:0706.3790 [hep-ex]].

[183] P. M. Nadolsky *et al.*, "Implications of CTEQ global analysis for collider observables," arXiv:0802.0007 [hep-ph].

[184] T. Aaltonen *et al.* [CDF Collaboration], Phys. Rev. Lett. **100** (2008) 062005 [arXiv:0710.4037 [hep-ex]].

[185] J. A. Aguilar-Saavedra *et al.* [ECFA/DESY LC Physics Working Group], "TESLA Technical Design Report Part III: Physics at an e+e- Linear Collider," arXiv:hep-ph/0106315.

[186] A. H. Hoang *et al.*, Eur. Phys. J. direct C **2** (2000) 1 [arXiv:hep-ph/0001286].

[187] S. Fleming, A. H. Hoang, S. Mantry and I. W. Stewart, "Jets from Massive Unstable Particles: Top-Mass Determination," arXiv:hep-ph/0703207.

[188] T. Aaltonen *et al.* [CDF Collaboration], Phys. Rev. D **75** (2007) 111103 [arXiv:0705.1594 [hep-ex]].

[189] V. M. Abazov *et al.* [D0 Collaboration], Phys. Rev. D **75**, 092001 (2007) [arXiv:hep-ex/0702018].

[190] P. Skands and D. Wicke, Eur. Phys. J. C **52** (2007) 133 [arXiv:hep-ph/0703081].

[191] A. Kharchilava, Phys. Lett. B **476** (2000) 73 [arXiv:hep-ph/9912320].

[192] C. S. Hill, J. R. Incandela and J. M. Lamb, Phys. Rev. D **71** (2005) 054029 [arXiv:hep-ex/0501043].

[193] R. Frederix and F. Maltoni, "Top pair invariant mass distribution: a window on new physics," arXiv:0712.2355 [hep-ph].

[194] K. Hagiwara, Y. Sumino and H. Yokoya, "Bound-state Effects on Top Quark Production at Hadron Colliders," arXiv:0804.1014 [hep-ph].

[195] U. Baur and L. H. Orr, Phys. Rev. D **76** (2007) 094012 [arXiv:0707.2066 [hep-ph]].

[196] F. Halzen, P. Hoyer and C. S. Kim, Phys. Lett. B **195** (1987) 74.

[197] J. H. Kühn and G. Rodrigo, Phys. Rev. D **59** (1999) 054017 [arXiv:hep-ph/9807420].

[198] M. T. Bowen, S. D. Ellis and D. Rainwater, Phys. Rev. D **73** (2006) 014008 [arXiv:hep-ph/0509267].

[199] O. Antunano, J. H. Kühn and G. V. Rodrigo, Phys. Rev. D **77** (2008) 014003 [arXiv:0709.1652 [hep-ph]].

[200] D. Atwood, S. Bar-Shalom, G. Eilam and A. Soni, Phys. Rept. **347** (2001) 1 [arXiv:hep-ph/0006032].

[201] *et al.* [D0 Collaboration], "First measurement of the forward-backward charge asymmetry in top quark pair production," arXiv:0712.0851 [hep-ex].

[202] CDF Collaboration, "Measurement of the Charge Asymmetry in Top Pair Production using 1.9 fb^{-1}," CDF Note 9156 (2007); "Measurement of the Forward Backward Asymmetry in Top Pair Production," CDF Note 9169 (2007).

[203] L. M. Sehgal and M. Wanninger, Phys. Lett. B **200** (1988) 211.

[204] W. Bernreuther, A. Brandenburg and P. Uwer, Phys. Lett. B **368** (1996) 153 [arXiv:hep-ph/9510300].

[205] W. G. D. Dharmaratna and G. R. Goldstein, Phys. Rev. D **53** (1996) 1073.

[206] V. D. Barger, J. Ohnemus and R. J. N. Phillips, Int. J. Mod. Phys. A **4** (1989) 617.

[207] T. Arens and L. M. Sehgal, Phys. Lett. B **302** (1993) 501.

[208] T. Stelzer and S. Willenbrock, Phys. Lett. B **374** (1996) 169 [arXiv:hep-ph/9512292].

[209] A. Brandenburg, Phys. Lett. B **388** (1996) 626 [arXiv:hep-ph/9603333].

[210] D. Chang, S. C. Lee and A. Sumarokov, Phys. Rev. Lett. **77** (1996) 1218 [arXiv:hep-ph/9512417].

[211] G. Mahlon and S. J. Parke, Phys. Rev. D **53** (1996) 4886 [arXiv:hep-ph/9512264].

[212] G. Mahlon and S. J. Parke, Phys. Lett. B **411** (1997) 173 [arXiv:hep-ph/9706304].

[213] P. Uwer, Phys. Lett. B **609** (2005) 271 [arXiv:hep-ph/0412097].

[214] C. A. Nelson, E. G. Barbagiovanni, J. J. Berger, E. K. Pueschel and J. R. Wickman, Eur. Phys. J. C **45** (2006) 121 [arXiv:hep-ph/0506240].

[215] C. A. Nelson, J. J. Berger and J. R. Wickman, Eur. Phys. J. C **46** (2006) 385 [arXiv:hep-ph/0510348].

[216] U. Baur, A. Juste, L. H. Orr and D. Rainwater, Phys. Rev. D **71** (2005) 054013 [arXiv:hep-ph/0412021].

[217] W. Bernreuther, R. Bonciani, T. Gehrmann, R. Heinesch, T. Leineweber, P. Mastrolia and E. Remiddi, Phys. Rev. Lett. **95** (2005) 261802 [arXiv:hep-ph/0509341].

[218] W. F. L. Hollik, Fortsch. Phys. **38** (1990) 165.

[219] C. F. Berger, M. Perelstein and F. Petriello, "Top quark properties in little Higgs models," arXiv:hep-ph/0512053.

[220] W. Bernreuther, T. Schröder and T. N. Pham, Phys. Lett. B **279** (1992) 389.

[221] U. Baur, M. Buice and L. H. Orr, Phys. Rev. D **64** (2001) 094019 [arXiv:hep-ph/0106341].

[222] U. Baur, A. Juste, D. Rainwater and L. H. Orr, Phys. Rev. D **73** (2006) 034016 [arXiv:hep-ph/0512262].

[223] W. Beenakker, S. Dittmaier, M. Krämer, B. Plümper, M. Spira and P. M. Zerwas, Phys. Rev. Lett. **87** (2001) 201805 [arXiv:hep-ph/0107081].

[224] W. Beenakker, S. Dittmaier, M. Krämer, B. Plümper, M. Spira and P. M. Zerwas, Nucl. Phys. B **653** (2003) 151 [arXiv:hep-ph/0211352].

[225] S. Dawson, L. H. Orr, L. Reina and D. Wackeroth, Phys. Rev. D **67** (2003) 071503 [arXiv:hep-ph/0211438].

[226] S. Dawson, C. Jackson, L. H. Orr, L. Reina and D. Wackeroth, Phys. Rev. D **68** (2003) 034022 [arXiv:hep-ph/0305087].

[227] A. Stange and S. Willenbrock, Phys. Rev. D **48** (1993) 2054 [arXiv:hep-ph/9302291].

[228] H. Y. Zhou, C. S. Li and Y. P. Kuang, Phys. Rev. D **55** (1997) 4412 [arXiv:hep-ph/9603435].

[229] W. Hollik, W. M. Mösle and D. Wackeroth, Nucl. Phys. B **516** (1998) 29 [arXiv:hep-ph/9706218].

[230] C. Kao and D. Wackeroth, Phys. Rev. D **61** (2000) 055009 [arXiv:hep-ph/9902202].

[231] S. Berge, W. Hollik, W. M. Mösle and D. Wackeroth, Phys. Rev. D **76** (2007) 034016 [arXiv:hep-ph/0703016].

[232] S. Alam, K. Hagiwara, S. Matsumoto, K. Hagiwara and S. Matsumoto, Phys. Rev. D **55** (1997) 1307 [arXiv:hep-ph/9607466].

[233] Z. Sullivan, Phys. Rev. D **56** (1997) 451 [arXiv:hep-ph/9611302].

[234] J. Kim, J. L. Lopez, D. V. Nanopoulos and R. Rangarajan, Phys. Rev. D **54** (1996) 4364 [arXiv:hep-ph/9605419].

[235] J. M. Yang and C. S. Li, Phys. Rev. D **54** (1996) 4380 [arXiv:hep-ph/9603442].

[236] D. A. Ross and M. Wiebusch, JHEP **0711** (2007) 041 [arXiv:0707.4402 [hep-ph]].

[237] A. Pilaftsis, Phys. Lett. B **435** (1998) 88 [arXiv:hep-ph/9805373].

[238] C. R. Schmidt and M. E. Peskin, Phys. Rev. Lett. **69** (1992) 410.

[239] W. Bernreuther and A. Brandenburg, Phys. Lett. B **314** (1993) 104.

[240] W. Bernreuther and A. Brandenburg, Phys. Rev. D **49** (1994) 4481 [arXiv:hep-ph/9312210].

[241] H. Y. Zhou, Phys. Rev. D **58** (1998) 114002 [arXiv:hep-ph/9805358].

[242] W. Khater and P. Osland, Nucl. Phys. B **661** (2003) 209 [arXiv:hep-ph/0302004].

[243] C. R. Schmidt, Phys. Lett. B **293** (1992) 111.

[244] D. Atwood, A. Kagan and T. G. Rizzo, Phys. Rev. D **52** (1995) 6264 [arXiv:hep-ph/9407408].

[245] P. Haberl, O. Nachtmann and A. Wilch, Phys. Rev. D **53** (1996) 4875 [arXiv:hep-ph/9505409].

[246] K. m. Cheung, Phys. Rev. D **55** (1997) 4430 [arXiv:hep-ph/9610368].

[247] D. Atwood, A. Aeppli and A. Soni, Phys. Rev. Lett. **69** (1992) 2754.

[248] A. Brandenburg and J. P. Ma, Phys. Lett. B **298** (1993) 211.

[249] S. Y. Choi, C. S. Kim and J. Lee, Phys. Lett. B **415** (1997) 67 [arXiv:hep-ph/9706379].

[250] B. Grzadkowski, B. Lampe and K. J. Abraham, Phys. Lett. B **415** (1997) 193 [arXiv:hep-ph/9706489].

[251] D. Eriksson, G. Ingelman, J. Rathsman and O. Stal, JHEP **0801** (2008) 024 [arXiv:0710.5906 [hep-ph]].

[252] C. T. Hill, Phys. Lett. B **266** (1991) 419.

[253] C. T. Hill and S. J. Parke, Phys. Rev. D **49** (1994) 4454 [arXiv:hep-ph/9312324].

[254] N. Arkani-Hamed, A. G. Cohen and H. Georgi, Phys. Lett. B **513** (2001) 232 [arXiv:hep-ph/0105239].

[255] M. Schmaltz and D. Tucker-Smith, Ann. Rev. Nucl. Part. Sci. **55** (2005) 229 [arXiv:hep-ph/0502182].

[256] I. Antoniadis, Phys. Lett. B **246** (1990) 377.

[257] N. Arkani-Hamed, S. Dimopoulos and G. R. Dvali, Phys. Lett. B **429** (1998) 263 [arXiv:hep-ph/9803315].

[258] L. Randall and R. Sundrum, Phys. Rev. Lett. **83** (1999) 4690 [arXiv:hep-th/9906064].

[259] K. Agashe, A. Delgado, M. J. May and R. Sundrum, JHEP **0308** (2003) 050 [arXiv:hep-ph/0308036].

[260] A. L. Fitzpatrick, J. Kaplan, L. Randall and L. T. Wang, JHEP **0709** (2007) 013 [arXiv:hep-ph/0701150].

[261] B. Lillie, L. Randall and L. T. Wang, JHEP **0709** (2007) 074 [arXiv:hep-ph/0701166].

[262] A. Djouadi, G. Moreau and R. K. Singh, "Kaluza–Klein excitations of gauge bosons at the LHC," arXiv:0706.4191 [hep-ph].

[263] B. Lillie, J. Shu and T. M. P. Tait, Phys. Rev. D **76** (2007) 115016 [arXiv:0706.3960 [hep-ph]].

[264] K. J. F. Gaemers and F. Hoogeveen, Phys. Lett. B **146** (1984) 347.

[265] D. Dicus, A. Stange and S. Willenbrock, Phys. Lett. B **333** (1994) 126.

[266] W. Bernreuther, M. Flesch and P. Haberl, Phys. Rev. D **58** (1998) 114031 [arXiv:hep-ph/9709284].

[267] E. Eichten and K. D. Lane, Phys. Lett. B **327** (1994) 129 [arXiv:hep-ph/9401236].

[268] D. Choudhury, R. M. Godbole, R. K. Singh and K. Wagh, Phys. Lett. B **657** (2007) 69 [arXiv:0705.1499 [hep-ph]].

[269] M. Arai, N. Okada, K. Smolek and V. Simak, Phys. Rev. D **70** (2004) 115015 [hep-ph/0409273].

[270] M. Arai, N. Okada, K. Smolek and V. Simak, Phys. Rev. D **75** (2007) 095008 [arXiv:hep-ph/0701155].

[271] I. Antoniadis, K. Benakli and M. Quiros, Phys. Lett. B **460** (1999) 176 [arXiv:hep-ph/9905311].

[272] K. Agashe *et al.*, Phys. Rev. D **76** (2007) 115015 [arXiv:0709.0007 [hep-ph]].

[273] G. Burdman, B. A. Dobrescu and E. Ponton, Phys. Rev. D **74** (2006) 075008 [arXiv:hep-ph/0601186].

[274] U. Baur and L. H. Orr, "Searching for $t\bar{t}$ Resonances at the Large Hadron Collider," arXiv:0803.1160 [hep-ph].

[275] V. Barger, T. Han and D. G. E. Walker, Phys. Rev. Lett. **100** (2008) 031801 [arXiv:hep-ph/0612016].

[276] T. Han, G. Valencia and Y. Wang, Phys. Rev. D **70** (2004) 034002 [arXiv:hep-ph/0405055].

[277] C. Schwinn, Phys. Rev. D **71** (2005) 113005 [arXiv:hep-ph/0504240].

[278] B. Lillie, J. Shu and T. M. P. Tait, "Top Compositeness at the Tevatron and LHC," arXiv:0712.3057 [hep-ph].

[279] C. Schwanenberger [CDF and D0 Collaboration], PoS **HEP2005** (2006) 349 [arXiv:hep-ex/0602048].

[280] S. Cabrera [CDF collaboration], "Looking for signals of New Physics in the Top quark samples with the CDF detector," arXiv:0709.2264 [hep-ex].

[281] J. C. Collins and D. E. Soper, Phys. Rev. D **16** (1977) 2219.

[282] W. Bernreuther, A. Brandenburg and M. Flesch, "Effects of Higgs sector CP violation in top-quark pair production at the LHC," arXiv:hep-ph/9812387.

[283] A. G. Cohen, D. B. Kaplan and A. E. Nelson, Ann. Rev. Nucl. Part. Sci. **43** (1993) 27 [arXiv:hep-ph/9302210].

[284] E. Accomando *et al.*, "Workshop on CP studies and non-standard Higgs physics," arXiv:hep-ph/0608079.

[285] M. A. G. Aivazis, J. C. Collins, F. I. Olness and W. K. Tung, Phys. Rev. D **50**, 3102 (1994) [arXiv:hep-ph/9312319].

[286] G. Bordes and B. van Eijk, Nucl. Phys. B **435** (1995) 23.

[287] T. Stelzer, Z. Sullivan and S. Willenbrock, Phys. Rev. D **56** (1997) 5919 [arXiv:hep-ph/9705398].

[288] T. Stelzer, Z. Sullivan and S. Willenbrock, Phys. Rev. D **58** (1998) 094021 [arXiv:hep-ph/9807340].

[289] B. W. Harris, E. Laenen, L. Phaf, Z. Sullivan and S. Weinzierl, Phys. Rev. D **66** (2002) 054024 [arXiv:hep-ph/0207055].

[290] Z. Sullivan, Phys. Rev. D **70** (2004) 114012 [arXiv:hep-ph/0408049].

[291] Z. Sullivan, Phys. Rev. D **72** (2005) 094034 [arXiv:hep-ph/0510224].

[292] J. Campbell, R. K. Ellis and F. Tramontano, Phys. Rev. D **70** (2004) 094012 [arXiv:hep-ph/0408158].

[293] Q. H. Cao and C. P. Yuan, Phys. Rev. D **71** (2005) 054022 [arXiv:hep-ph/0408180].

[294] Q. H. Cao, R. Schwienhorst, J. A. Benitez, R. Brock and C. P. Yuan, Phys. Rev. D **72** (2005) 094027 [arXiv:hep-ph/0504230].

[295] S. Frixione, E. Laenen, P. Motylinski and B. R. Webber, JHEP **0603** (2006) 092 [arXiv:hep-ph/0512250].

[296] M. Beccaria et al., "A complete one-loop calculation of electroweak supersymmetric effects in t-channel single top production at LHC," arXiv:0802.1994 [hep-ph].

[297] M. Beccaria, G. Macorini, F. M. Renard and C. Verzegnassi, Phys. Rev. D **74** (2006) 013008 [arXiv:hep-ph/0605108].

[298] N. Kidonakis, Phys. Rev. D **74** (2006) 114012 [arXiv:hep-ph/0609287].

[299] N. Kidonakis, Phys. Rev. D **75** (2007) 071501 [arXiv:hep-ph/0701080].

[300] M. C. Smith and S. Willenbrock, Phys. Rev. D **54** (1996) 6696 [arXiv:hep-ph/9604223].

[301] Q. H. Cao, R. Schwienhorst and C. P. Yuan, Phys. Rev. D **71** (2005) 054023 [arXiv:hep-ph/0409040].

[302] S. Mrenna and C. P. Yuan, Phys. Lett. B **416** (1998) 200 [arXiv:hep-ph/9703224].

[303] A. S. Belyaev, E. E. Boos and L. V. Dudko, Phys. Rev. D **59** (1999) 075001 [arXiv:hep-ph/9806332].

[304] A. Belyaev and E. Boos, Phys. Rev. D **63** (2001) 034012 [arXiv:hep-ph/0003260].

[305] T. M. P. Tait, Phys. Rev. D **61** (2000) 034001 [arXiv:hep-ph/9909352].

[306] J. Campbell and F. Tramontano, Nucl. Phys. B **726** (2005) 109 [arXiv:hep-ph/0506289].

[307] W. T. Giele, S. Keller and E. Laenen, Phys. Lett. B **372** (1996) 141 [arXiv:hep-ph/9511449].

[308] S. Zhu, Phys. Lett. B **524** (2002) 283 [Erratum-ibid. B **537** (2002) 351].

[309] G. Mahlon and S. J. Parke, Phys. Rev. D **55** (1997) 7249 [arXiv:hep-ph/9611367].

[310] G. Mahlon and S. J. Parke, Phys. Lett. B **476** (2000) 323 [arXiv:hep-ph/9912458].

[311] E. E. Boos and A. V. Sherstnev, Phys. Lett. B **534** (2002) 97 [arXiv:hep-ph/0201271].

[312] J. A. Aguilar-Saavedra, "Single top quark production at LHC with anomalous Wtb couplings," arXiv:0803.3810 [hep-ph].

[313] C. X. Yue, L. Zhou and S. Yang, Eur. Phys. J. C **48** (2006) 243 [arXiv:hep-ph/0604001].

[314] Q. H. Cao, J. Wudka and C. P. Yuan, Phys. Lett. B **658**, 50 (2007) [arXiv:0704.2809 [hep-ph]].

[315] J. J. Zhang, C. S. Li, Z. Li and L. L. Yang, Phys. Rev. D **75** (2007) 014020 [arXiv:hep-ph/0610087].

[316] M. Beccaria et al., Eur. Phys. J. C **53** (2008) 257 [arXiv:0705.3101 [hep-ph]].

[317] J. C. Pati and A. Salam, Phys. Rev. D **10** (1974) 275 [Erratum-ibid. D **11** (1975) 703].

[318] R. N. Mohapatra and J. C. Pati, Phys. Rev. D **11** (1975) 566.

[319] R. N. Mohapatra and J. C. Pati, Phys. Rev. D **11** (1975) 2558.

[320] E. H. Simmons, Phys. Rev. D **55** (1997) 5494 [arXiv:hep-ph/9612402].

[321] H. J. He and C. P. Yuan, Phys. Rev. Lett. **83** (1999) 28 [arXiv:hep-ph/9810367].

[322] T. Tait and C. P. Yuan, Phys. Rev. D **63** (2001) 014018 [arXiv:hep-ph/0007298].

[323] E. Boos, V. Bunichev, L. Dudko and M. Perfilov, Phys. Lett. B **655** (2007) 245 [arXiv:hep-ph/0610080].

[324] C. M. Magass, "Search for new heavy charged gauge bosons," doctoral thesis, RWTH Aachen (2007).

[325] F. Maltoni, K. Paul, T. Stelzer and S. Willenbrock, Phys. Rev. D **64** (2001) 094023 [arXiv:hep-ph/0106293].

[326] T. Han, R. D. Peccei and X. Zhang, Nucl. Phys. B **454** (1995) 527 [arXiv:hep-ph/9506461].

[327] T. Han, M. Hosch, K. Whisnant, B. L. Young and X. Zhang, Phys. Rev. D **58** (1998) 073008 [arXiv:hep-ph/9806486].

[328] F. Larios and F. Penunuri, J. Phys. G **30** (2004) 895 [arXiv:hep-ph/0311056].

[329] J. J. Liu, C. S. Li, L. L. Yang and L. G. Jin, Phys. Rev. D **72** (2005) 074018 [arXiv:hep-ph/0508016].

[330] J. J. Liu, C. S. Li, L. L. Yang and L. G. Jin, Nucl. Phys. B **705** (2005) 3 [arXiv:hep-ph/0404099].

[331] D. Lopez-Val, J. Guasch and J. Sola, JHEP **0712** (2007) 054 [arXiv:0710.0587 [hep-ph]].

[332] J. j. Cao, G. l. Liu, J. M. Yang and H. j. Zhang, Phys. Rev. D **76** (2007) 014004 [arXiv:hep-ph/0703308].

[333] Yu. P. Gouz and S. R. Slabospitsky, Phys. Lett. B **457** (1999) 177 [arXiv:hep-ph/9811330].